

USING THE PAST AS THE KEY TO THE PRESENT: INFORMING COASTAL
RESOURCE MANAGEMENT WITH GEOLOGIC RECORDS

A Dissertation Presented

by

Benjamin David DeJong

to

The Faculty of the Graduate College

of

The University of Vermont

In Partial Fulfillment of the Requirements
for the Degree of Doctor of Philosophy
Specializing in Natural Resources

May, 2015

Defense Date: February 19, 2015
Dissertation Examination Committee:

Paul R. Bierman, Ph.D., Advisor

Andrea Lini, Ph.D., Chairperson

Donna M. Rizzo, Ph.D.

Carol Adair, Ph.D.

Cynthia J. Forehand, Ph.D., Dean of the Graduate College

ABSTRACT

Rising sea levels present an ongoing threat to communities and resources around the Chesapeake Bay, east coast, USA, where tide gauges indicate that the relative rise of sea level is approximately twice the rate of average, eustatic sea-level rise. This has significantly compromised the health and viability of salt marsh habitat on the Eastern Shore during the 20th century, and the biologists who are charged with managing coastal resources in the coming decades need to understand the nature and causes of high rates of regional sea-level rise to develop suitable adaptation plans.

Dated geologic deposits and geophysical models suggest that sea-level rise is relatively high on mid-Atlantic coastlines because the land surface is subsiding due to a collapsing glacial forebulge following the Last Glacial Maximum (LGM). To fully understand this process, past sea-level indicators such as dated shoreline deposits are needed to reconstruct regional sea-level behavior in the past, but rigorous age control on geologic deposits is largely restricted to the Holocene and to marine isotope stage (MIS) 5, so the rates and timescales over which these processes operate remain unknown.

This research provides long-term paleoenvironmental records from ancient environments under east-central Chesapeake Bay to place the current sea-level threats into the context of a long geologic history of sea-level fluctuations. First, the Pleistocene geologic framework of the region is reconstructed through borehole drilling. Sediments from boreholes provided material for interpreting depositional environments, and for establishing age control for deposits, so that the entire stratigraphy was constrained both in space and time.

The geologic framework and ages indicate that Chesapeake Bay alternated between a deeply incised fluvial system and a filled estuary repeatedly in response to major climate fluctuations since at least the early Pleistocene, ~2 Ma. The ages and sedimentology indicate that the field area was submerged intermittently in a shallow estuary until nearly the end of marine isotope stage 3. Because global sea-level proxies suggest that sea level was ~40-80 meters lower than present at that time, these ages suggest that the penultimate glacial forebulge must have remained significantly lowered for nearly 100 ky following the retreat of ice. The implication of this time lag is that mid-Atlantic coastlines are still in a relatively early state of forebulge collapse, and subsidence following retreat of ice from the Last Glacial Maximum will likely continue for the foreseeable future. Ongoing subsidence will continue to exacerbate projected eustatic sea-level rise due to changing global climate, and coastal adaptation plans must remain focused on encouraging the migration of vital habitat toward higher elevations in the landscape.

CITATIONS

Material from this dissertation has been accepted for publication in *GSA TODAY* on January 15, 2015 in the following form:

DeJong, B.D., Bierman, P.R., Newell, W.L., Rittenour, T.M., Mahan, S.A., Balco, G., Rood, D.H.. Pleistocene relative sea levels in the Chesapeake Bay region and their implications for the next century, *GSA TODAY*.

AND

Material from this dissertation has been submitted for publication in *Nuclear Instruments and Methods in Physics Research Section B: Beam Interactions with Materials and Atoms* on December 15, 2014 in the following form:

DeJong, B.D., Hidy, A.J., Bierman, P.R., Optimizing cosmogenic burial isochrons using muon-inclusive simple burial dating, *Instruments and Methods in Physics Research Section B: Beam Interactions with Materials and Atoms*.

ACKNOWLEDGEMENTS

There are many individuals and institutions that deserve my appreciation for supporting me during my PhD. First and foremost, I thank U.S.G.S. colleagues for training me as a scientist and for financially backing this research. I especially thank Art Schultz, David Powars, Bryan Landacre, Chris Bernhardt, Lucy Edwards and Jean Self-Trail for their unwavering support both in the field and over countless hours of phone conversations focused around piecing this story together. I also thank the Geology Department at the University of Vermont for teaching assistantships and laboratory support; while Andrea consistently referred to me as a spy from Natural Resources, their hospitality shined through. Geology and NR graduate students made the whole experience enjoyable, and I thank them one and all. I am also very thankful to my committee, Dr. Andrea Lini, Dr. Donna Rizzo, and Dr. Carol Adair, for providing crucial feedback and constant availability.

I offer my utmost thanks to Eugene (“G”) Cobbs III and Jeffrey (“Jeffee”) B. Grey, who drilled well over 1.25 km of coastal plain stratigraphy for this project. This research is literally impossible without their expertise, and the drill bit on my desk is a constant reminder of the long hours we spent sweating in the hot Delmarva sun (and March snow storms). They went way above and beyond.

I offer my deepest gratitude to Dr. Wayne Newell and Dr. Paul Bierman. Wayne

inspired the majority of this work; he is a rare breed of renaissance man that taught me how to tap into my curiosity, to see patterns, and let my observations guide me. Paul opened my eyes to the bigger picture; he has a brilliant way of showing the forest for the trees. I have yet to meet an individual who can juggle so many responsibilities at once, and little did I know when coming to Vermont that I was to be mentored by the guy who literally “wrote the book”. His can-do attitude quells all anxieties, especially when commitments feel particularly heavy both in the office and in a growing family.

Finally, I thank my family and friends. My grandmother Millie DeJong, parents Pete and Anne DeJong, my sister Kim and her husband Kirk, my brother Jim and his wife Jodi, and my nephews Isaac, Will, Owen, Jed, and Max provide unwavering support, love, and grounding. Kurt, Deb, Elise, Carlo, Jeff, and Grandma are a constant breath of fresh air. Kristin Wolf is my life and my inspiration, and Wyatt is my motivation to get it done and go home every day.

TABLE OF CONTENTS

	Page
ACKNOWLEDGEMENTS	iii
LIST OF TABLES	ix
LIST OF FIGURES	ix
CHAPTER 1: INTRODUCTION	1
1.1. Study area and research objectives	5
1.1.1. Setting and geology	5
1.1.2. Research objectives	9
1.2. Geologic framework studies	10
1.2.1. Accessing the subsurface: Drilling methods used in this research	10
1.3. Constraining depositional ages of geologic units	12
1.3.1. Optically stimulated luminescence	12
1.3.2. Cosmogenic radionuclides	16
1.4. Structure of dissertation	19
CHAPTER 2: PLEISTOCENE RELATIVE SEA LEVELS IN THE CHESAPEAKE BAY REGION AND THEIR IMPLICATIONS FOR THE NEXT CENTURY .	22
2.1. Abstract	23
2.2. Introduction	24
2.3. Study Site and Methods	27

2.4. Results and Interpretations	27
2.5. Discussion.....	30
2.6. Acknowledgements.....	34
2.7. References.....	35
2.8. Figure Captions.....	42
2.9. Supplemental Data.....	49
 CHAPTER 3: OPTIMIZING COSMOGENIC BURIAL ISOCHRONS USING MUON- INCLUSIVE SIMPLE BURIAL DATING	 76
3.1. Abstract.....	77
3.2. Introduction.....	78
3.3. Methods	81
3.4. Results.....	83
3.5. Discussion.....	85
3.6. Acknowledgements.....	87
3.7. References.....	87
3.8. Figure Captions.....	90
 CHAPTER 4: ESTUARINE RESPONSE TO QUATERNARY GLACIAL- INTERGLACIAL CYCLING	 96
4.1. Introductory paragraph	97

4.2. Article text	97
4.3. Results.....	101
4.4 Methods	105
4.5. Acknowledgements.....	106
4.6. Author contributions.....	107
4.7. References.....	107
4.8. Figure Captions.....	112
4.9. Supplemental information	115
CHAPTER 5: QUATERNARY GEOLOGIC EVOLUTION OF EAST-CENTRAL CHESAPEAKE BAY	124
5.1. Abstract.....	125
5.2. Introduction.....	126
5.3. Setting.....	130
5.4. Methods	131
5.5. Results.....	132
5.5.1. Geomorphology	132
5.5.2. Stratigraphy, lithology, and age.....	133
5.5.3. Paleoclimate.....	137
5.6. Discussion.....	138
5.6.1. Early-Mid Pleistocene paleovalley cutting and filling	138

5.6.2. Marine isotope stage 5: Recognition of mid-Atlantic sea-level anomalies ..	139
5.6.3. Marine isotope stage 3: Expansion of the “80 ka problem”	141
5.6.4. Marine isotope stage 2: Low sea levels and a frozen landscape.....	143
5.6.3. Marine isotope stage 1: Marsh establishment, growth, and submersion	144
5.7. Conclusions.....	145
5.8. Acknowledgements.....	146
5.9. References.....	146
5.10. Figure captions.....	155
5.9. Supplemental data.....	163
CHAPTER 6: CONCLUSIONS AND FUTURE RESEARCH	171
6.1. Summary of findings	171
6.2. Suggestions for future work.....	176
COMPREHENSIVE BIBLIOGRAPHY	183

LIST OF TABLES

Table 2-1 (SD1) Cosmogenic nuclide burial age data	66
Table 2-2 (SD2) Optically stimulated luminescence ages produced for the BNWR stratigraphy	68
Table 2-3 (SD3) Radiocarbon ages produced for the Holocene stratigraphy of the BNWR	70
Table 3-1 Cosmogenic radionuclide data and burial age estimates	95
Table 4-1 (SI1) Cosmogenic nuclide data table associated with isochron and simple burial ages	117
Table 4-2 (SI2) Amino acid racemization sample details	119
Table 4-3 (SI3) ^{10}Be data and erosion rate estimates associated with non-glaciated Susquehanna basins	121
Table 5-1 (SD1) All age data associated with Quaternary deposits at the BNWR.....	166
Table 5-2 (SD2) Dinoflagellate species list for Miocene units under BNWR	167

LIST OF FIGURES

Figure 1-1 Time series of the Blackwater River valley	6
Figure 2-1 Map showing Atlantic coast of the United States with population density by county (U.S. Census Bureau, 2011) placed alongside Late Holocene and 20th century RSL rise curves (2-sigma errors; Engelhart et al., 2010).....	46
Figure 2-2 Land and sea-level elevations through time	47
Figure 2-3 Time series of the Blackwater River valley	48
Figure 2-4 LiDAR imagery and geomorphology of the study area	49
Figure 2-5 Cross-section showing the Pleistocene deposits that underlie the BNWR	50
Figure 2-6 (SD1) The three platforms used for drilling the BNWR substrate and examples of sediments retrieved from these methods.....	53
Figure 2-7 (SD2) OSL field sampling setup	54
Figure 2-8 (SD3) Locations of all boreholes with Figure 3 line of section for reference.	55
Figure 2-9 (SD4) Sediment core from KD (eastern end of Figure 5).	56
Figure 2-10 (SD5) Examples of MIS 3 deposits cored and sampled in this study	57
Figure 2-11 (SD6) Flow chart showing full processing steps used in the University of Vermont Cosmogenic Radionuclide Laboratory to purify quartz and extract ²⁶ Al and ¹⁰ Be from quartz	60

Figure 2-12 (SD7) Isochrons produced for gravels at the base of the Pleistocene stratigraphy at the BNWR (ages in Ma)	64
Figure 2-13 (SD8) Variability in surface elevations of MIS 3 deposits dated using both OSL and ¹⁴ C dating	69
Figure 3-1 Map showing location of study area	92
Figure 3-2 The simple burial plot explained	93
Figure 3-3 Isochron and simple burial plots for samples analyzed in this study	94
Figure 4-1 Study area showing Chesapeake Bay and the contributing area of the Susquehanna River watershed	114
Figure 4-2 Isochron ages shown in cross-section	115
Figure 4-3 Cosmogenic ages and concentrations through time	116
Figure 4-4 (SI1) Isochron and simple burial plots	118
Figure 4-5 (SI2) Amino acid D-L values associated with amino acid racemization samples	120
Figure 5-1 Map of the mid-Atlantic region	158
Figure 5-2 LIDAR imagery, geology, and geomorphology of the BNWR	159
Figure 5-3 Cross-section with age proxies	160

Figure 5-4 Transect across the Blackwater River valley showing the Holocene stratigraphy overlapping sediments of MIS3-2 age	161
Figure 5-5 Cross-sectional diagram of pollen data indicating paleo-environmental change.....	162
Figure 5-6 (SD1) Correlation chart of Middle to Late Pleistocene stratigraphic units across the Coastal Plain of Virginia, Maryland and Delaware	163
Figure 5-7 (SD2) North-south tracks of major paleochannels encountered under the field area.....	164
Figure 5-8 (SD3) Chronostratigraphic and biostratigraphic context of the Miocene units under the BNWR.....	165

CHAPTER 1: INTRODUCTION

In order to develop effective strategies for managing coastal resources that are threatened by rising sea levels, land managers must have a comprehensive understanding of the complex, interactive processes and rates of change operative on the landscape. For coastal marshes and wetlands, the strategies for remediating habitat loss are commonly informed only by short-term (decadal) instrumental data collected from tide gauges (Barbosa and Silva, 2009), high-resolution GPS (Sella et al., 2007), or surface elevation tables that measure differential subsidence of marsh sediments and their substrate (Cahoon et al., 2002). Data from these sources help measure regional rates of water and land surface elevation change and are necessary for understanding the distribution and magnitude of landscape change. But, these short-period records fail to address *why* or *how* the changes are proceeding and they fail to place present challenges into a longer context of rates and processes. Research over the past decades in the mid-Atlantic coastal plain of the Eastern U.S., shows that longer-term geologic records are necessary to address these questions.

Our understanding of sea level processes in the mid-Atlantic coastal region is increasingly being shaped by geologic investigation. In the 1980's, radiocarbon dates on peat beds that were deposited along the Eastern seaboard were used to reconstruct the history of the Holocene sea level transgression that persists today (Peltier, 1986). Spatial trends in this record indicated that vertical motion of the land surface, or land subsidence, had variably impacted the timing of coastal inundation (Peltier et al., 1996). By

considering this record along with nearby tide gauge data, present-day subsidence values ranging from $\sim 0.8 - 1.7$ mm/yr were calculated over the this area, with the highest measured rate centered on the Delmarva (DELaware, MARYland, and VirginiA) Peninsula, the landmass that separates Chesapeake Bay from the Atlantic Ocean (Engelhart et al., 2009). This suggests rate consistency over both centennial and millennial timescales. And while rates of global sea level rise have been estimated at $\sim 1.5-2.0$ mm/yr over the last century (Miller and Douglas, 2004), the added effect of land subsidence effectively doubles this rate for the Chesapeake Bay region. This area is home to the largest protected expanse of tidal marshland in the northeast United States, including the Blackwater National Wildlife Refuge (BNWR); 5,000 acres of tidal wetlands were converted to open water in the BNWR between 1938 and 2006 (Scott et al., 2009). I focus on landscape evolution of the BNWR over a range of timescales to better understand these challenges.

Today is not the first time sea level has risen in the Chesapeake Bay region; the Chesapeake Bay and the Delmarva Peninsula evolved to their present form over the course of several major sea-level fluctuations (Hobbs, 2004). The Delmarva Peninsula grew as a southward-propagating spit through coastal, marine, and fluvial processes in response to major cycles of sea level rise and fall beginning in the Pliocene ($\sim 5.0-2.6$ Ma) and continuing through the Quaternary (~ 2.6 Ma to present). When sea levels were lower during glacial lowstands, the ancient Susquehanna and Hudson-Delaware River systems and their tributaries responded by incising as deeply as 50 m into their valleys (Colman et

al., 1990). These deep river valleys were later filled with complex assemblages of river, estuary, and open-bay sediment as sea level rose into subsequent interglacial periods (e.g. Flemming et al., 2011). With each cycle of cutting and filling, the Susquehanna River system migrated in an overall southwesterly direction, leaving behind a well-preserved record of at least 3 ancestral Chesapeake Bays (Colman et al., 1990). This southwesterly migration has been attributed to the southward expansion of Delmarva as a major barrier spit (Colman et al., 1990), but the timescales over which this evolution proceeded are poorly known largely due to the paucity of methods available for directly dating channel gravels.

The surficial deposits and landforms of the BNWR contain rich details about past sea level rise and coastal inundation. The most recent geologic map of this region defines most of the landforms as having origins at the bottom of a shallow estuary (Owens and Denny, 1986). More recent LiDAR (Light Detection And Ranging) data and my own sediment cores support this interpretation, but preliminary ages I produced for them (~45 ka) suggested they were deposited at a time when sea level was far too low for estuarine deposition based on global sea-level curves (Siddall et al., 2008). Understanding the origin and character of these features become increasingly important to managers, as these subtle landforms represent the locations where marsh is expected to migrate in response to sea-level rise in the coming decades. I quickly recognized that the geomorphology and geologic framework of the BNWR could provide insight into past relative sea-level change that could help understand sea-level challenges in the coming

decades and centuries.

By reconstructing the Pleistocene geologic framework under the BNWR, I was able to provide a spatially and temporally constrained, >2 Ma record of landscape evolution that includes process information that is germane to understanding and planning for high rates of relative sea-level rise in the coming decades. The well-known axiom put forth by uniformitarian geologists of the 18th century and popularized during the 19th century that “the present is the key to the past” provided a powerful new perspective for interpreting the antiquity and processes inferred from the rock record. In the context of understanding high rates of relative sea-level rise in mid-Atlantic estuaries and marshes, the reverse is equally relevant: the past behavior of these coast-proximal features best informs their future behavior. With over 40 million people residing in coastal areas between New York City and Washington D.C. (US Census Bureau, 2013), the value of the ecosystem services provided by healthy salt marshes cannot be overstated, particularly with the ongoing threat of high rates of sea level rise (Silliman et al., 2008). My research in the Chesapeake Bay landscape serves as a useful reference for estuaries and their fringing salt marshes worldwide, as all of these geologically young features have their origins in the sea level rise that characterized the last glacial retreat.

1.1 Study area and research objectives

1.1.1. Setting and geology

The BNWR is located in Dorchester County, MD and includes ~110 km² of predominantly tidal wetlands and brackish open water. Along with neighboring protected lands, it represents one of the largest protected complexes of tidal marshland in the Eastern United States and was designated a wetland of international importance under the Ramsar Convention in 1987. The Refuge was established in 1933 to provide a safe stop-over for ducks and geese along the Atlantic Flyway, a major migratory corridor for birds on the eastern seaboard. The marshes serve many additional functions such as conserving biodiversity, providing nursing grounds for commercially viable fish and shellfish, buffering against storms, and offering destinations for tourism and recreation. Because most of the water flowing through the Blackwater River and to the Chesapeake Bay runs off of farmland in the Blackwater River watershed, the marsh also performs the important ecosystem service of filtering nutrient pollution (Stevenson et al., 2002).

In recent decades, tidal inundation at BNWR has progressively diminished the wetland area and limited the future viability of the marsh for which this refuge was established. Healthy marshes are resilient features; biomass accretion and mineral sediment trapping generally keep pace with rising sea levels (Allen, 2000). However sediment inputs to the BNWR are low, and RSL rise is outpacing accretionary processes (Cahoon et al., 2010; Kirwan and Guntenspergen, 2012; Stevenson et al., 2002; Stevenson et al., 1985). Topographic maps, produced by the US Geological Survey in

1904 (Figure 1-1a), show a well-delineated Blackwater River channel flowing through intact marsh within the footprint of BNWR. Between 1904 and 1938, channel

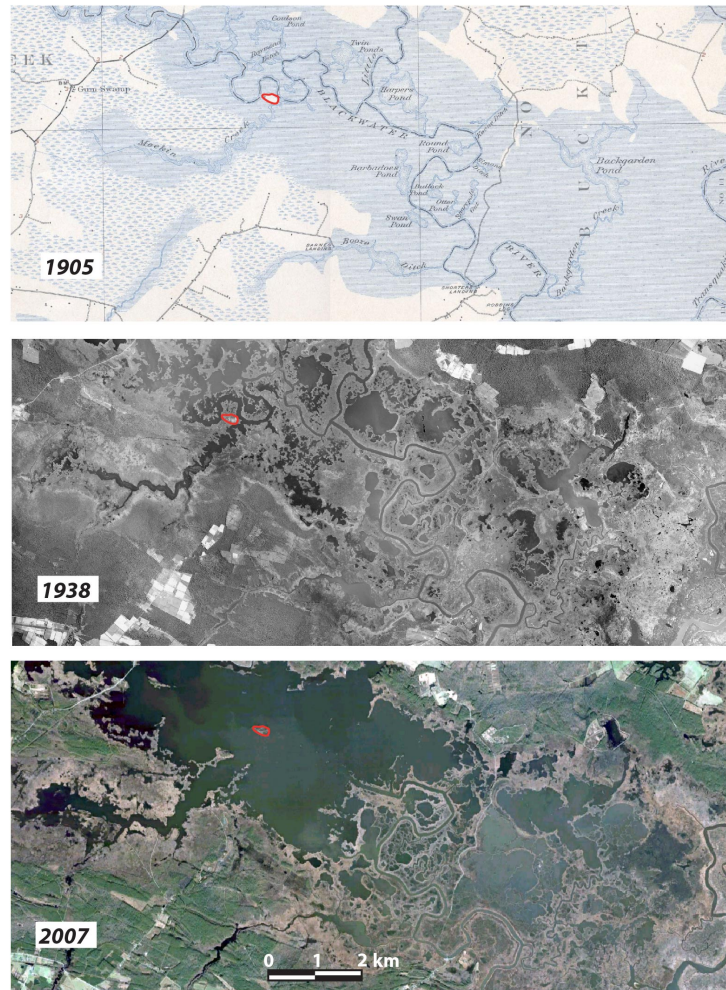


Figure 1-1 Time series of the Blackwater River valley. A. Intact marsh surveyed from 1902-1904 and presented in a 7.5" USGS topographic map from 1905 (USGS, 1905); dark blue hatching around the Blackwater valley is tidal marsh, light blue pattern is freshwater swamp, B. Initiation of major ponding seen in an aerial photograph from 1938 (<http://www.esrgc.org/>), and C. Coalesced ponds forming the informal "Lake Blackwater" in satellite imagery from 2007 (<http://www.bing.com/maps/>). Wetlands are converting to open water at a rate of 50-150 ha/yr in the field area (Cahoon et al., 2010). Image locations are identified in Figure 2-4. Red outline shows location of unnamed island for reference.

morphologies generally remained intact along the Blackwater River, but large ponds had opened up in the marsh, particularly near the confluence of the Blackwater and Little Blackwater Rivers (Figure 1-1b). From 1938 to the present, these ponds grew in size and coalesced to form larger bodies of water (Figure 1-1c). The progressive erosion of adjacent wetlands has increased the area of open water to the degree that the Blackwater River is now colloquially referred to as Lake Blackwater. Portions of the main Blackwater River levees still exist and support high marsh, but they are not accreting rapidly enough to keep pace with water level rise (Cahoon et al., 2010). High winds enhance coastal erosion by pushing large volumes of water along the newly elongated fetch of Lake Blackwater, eroding down-wind shorelines, particularly during heavy storms and storm surges.

In looking at the geologic architecture of Chesapeake Bay, the metastable and relatively short-lived nature of the estuary and its fringing marsh is readily apparent. The modern Chesapeake Bay occupies a drowned valley carved by the Susquehanna River prior to the beginning of the last ice age (Colman et al., 2002; Reusser et al., 2004). Drilling into the Chesapeake Bay sediments that have accumulated in that valley yields a sequence of material from basal Susquehanna River gravels overlain by deltaic river sands, and covered with Holocene estuarine muds that accumulated as sea levels rose to present levels (Baucom et al., 2000). This sequence of valley incision followed by valley aggradation was repeated through the Pleistocene in cyclic fashion, and the Chesapeake Bay represents the most recent iteration. With each erosion-deposition cycle, the trunk

stream of the paleo-Susquehanna River migrated in an overall southwesterly fashion, providing a well-preserved record of this long history (Colman et al., 1990). At least one, and possibly two paleochannels of the Susquehanna River were predicted to track north to south under the western portion of the study area based on both offshore and onshore seismic profiling (Colman et al., 1990; Genau et al., 1994). These paleochannels were observed in boreholes over the course of this research, but a much greater distribution of deep channels was also observed in geographic association with the present-day Blackwater and Choptank Rivers, making for a far more complex Pleistocene stratigraphy under the BNWR than anticipated.

The ~500 km² region surrounding the footprint of the BNWR is the ideal location for this study because 1) the Refuge is currently drafting an adaptation plan to respond to current and future rising sea levels that includes limited subsurface information; 2) the response of this landscape to previous Pleistocene sea level fluctuations is well preserved in the substrate; 3) access is greatly facilitated by a partnership between the U.S. Geological Survey and the BNWR managers in the U.S. Fish and Wildlife Service. Understanding the response of this landscape to several previous cycles of sea level fluctuation will provide the proper backdrop for assessing adaptation strategies for sea level rise in the coming decades.

1.1.2. Research objectives

The primary objective of my research is to use the geologic record of the BNWR to help inform adaptation plans that are being drafted by a consortium of resource managers, headed by the U.S. Fish and Wildlife Service, who are working to maintain marsh habitat in light of ongoing sea level rise. Because this overarching objective is germane to a range of timescales and methods, there are several derivative objectives in this research:

I. To develop a detailed framework for the surface and shallow subsurface landforms of the BNWR and surroundings to better understand the origin of this low-relief landscape. Although the surficial geology of the Delmarva Peninsula has been studied for decades, new tools including LiDAR and optically stimulated luminescence (OSL) dating allow for interrogation of the landscape in new ways that help test previous models of landscape evolution.

II. To present to the mid-Atlantic coastal plain research community a new analytical method for developing age control for the Plio-Pleistocene stratigraphy in the region. Cosmogenic nuclide isochron burial dating offers significantly improved chronostratigraphic control of Plio-Pleistocene sand and gravel units that represent a significant portion of the geologic history of the region and an important part of the geologic framework of the Delmarva Peninsula itself.

III. To reconstruct the distribution of Holocene sediments that form a continuum with actively accumulating marsh today that is a major focus of preservation efforts.

Using a recently developed hovercraft with a mounted vibrocore drill, I access submerged portions of the refuge that have been inaccessible for decades to better understand the transgression that persists today, with particular focus on marsh formation, accretion, and ultimately inundation.

1.2. Geologic framework studies

Contextualizing the processes and challenges related to relative sea-level rise in Chesapeake Bay over geologic timescales requires that ancient environments preserved in the subsurface be observed, analyzed, and interpreted. For the first half of the 20th century, the tools to accomplish this were lacking, and so the complexity of Pleistocene deposits and processes remained underappreciated (e.g. Cooke, 1958). Detailed stratigraphic studies showed that the landscape response to Pleistocene glacial-interglacial climate cycling resulted in complex stratigraphic relationships, and understanding these relationships correctly requires placement of depositional units into a subsurface framework constrained in space and time (Oaks and Coch, 1963).

1.2.1. Accessing the subsurface: Drilling equipment used in this research

Land surface elevations within the study area rarely exceed 2 m above mean sea level, and exposures of surficial deposits and underlying substrate are uncommon, ephemeral, and usually related to land-use practices. Therefore any exploration into the subsurface in this landscape requires access via either drilling or geophysical logging and

profiling. Three drilling platforms and one ground penetrating radar instrument were made available from the USGS for subsurface studies at the BNWR.

Hollow-stem Augering: Cores from the BNWR were collected using a hollow-stem auger continuous sampling system Central Mine Equipment (CME)-75. Sediment cores are collected in 7.6 cm (3 in) diameter plastic liners in an inner core barrel that was straight-pushed inside ~21 cm (8.25 in) diameter augers. Lacking any rotational motion, the resulting sediment cores provide exquisite sedimentary details. These cores were used for collection of pollen and OSL samples and to provide detailed sedimentologic information about the surface units in and around the BNWR.

Flight Augering: Flight augering with the CME-45 drill was used for a majority of locations on land. With this rig, we drilled an 11.4 cm (4.5 in) diameter solid-stem auger into the ground with one rotation per auger flight, so as to minimally disturb sediments, and then straight-pulled them to analyze the sediments on the auger flights. This provided accurate depths to contacts as well as samples for sedimentology, geochronology (cosmogenic nuclide), and palynology. While not as ideal as sediment cores, carefully drilled flight auger boreholes can preserve sedimentary structures intact and provide the most cost-effective means of accessing the subsurface. I used flight augering to locate optimal locations for coring with hollow-stem augers.

Vibracoring: Accessing the subsurface in water-locked areas like the interior of the Blackwater River valley proves difficult due to the challenges associated mobilizing large machinery into saturated areas. There are no roads within the footprint of “Lake

Blackwater”, and it is too shallow for barges or boats large enough for mounted drill rigs. The USGS responded to this need by developing a drill-mounted hovercraft in hopes that by merely skimming the water, researchers could gain access to these remote locations and provide crucial information that was not previously attainable. The result was the Hoverprobe 2000 (HP2000), a hovercraft-mounted, hydraulically powered sonic core (vibracore) drill (Newell and Queen, 2000). The HP2000 proved capable of capturing up to 15 m of 6.35 cm (2.5 in) diameter core in ~1.5 m (5 ft) sections in Holocene sediments in the BNWR.

1.3. Constraining depositional ages of geologic units

Most of the significant findings of this dissertation hinge on producing robust ages for geologic deposits in order to contextualize deposits in space and time. In this dissertation, I used amino acid racemization and radiocarbon dating, which have already been extensively applied in the mid-Atlantic coastal plain (ie. Colman et al., 2002; Wehmiller, 2013, respectively), and optically stimulated luminescence and cosmogenic nuclides, which are relatively new methods used in the region. A brief introduction of optically stimulated luminescence and cosmogenic nuclides follows to provide additional information on the methods prior to showing their application.

1.3.1. Optically stimulated luminescence

OSL geochronology measures ionizing radiation accumulated in quartz sand to

indicate the time elapsed since buried sediment grains were last exposed to sunlight, typically up to ~200 ka (Aitken, 1998). Once buried, sediments are exposed to ambient radiation produced by the decay of naturally occurring radionuclides (U, Th, and K) within surrounding sediments, and also to cosmic rays in the case of shallow burial (Aitken, 1998). This low-level radiation produces free electrons that become trapped in crystal lattice defects near the surface of (in my case) quartz grains, and they continue to accumulate so long as the sediments remain shielded from light. The accumulated radiation, or the “equivalent dose” can be measured by exposing the sediments to light in a controlled laboratory environment. This excites the electrons, and they are emitted to produce a measurable luminescence signal, the brightness of which reflects the accumulated ionized radiation. The rate at which the sediments are irradiated during burial, or “dose rate”, can be calculated from the concentration of radionuclides in the surrounding material. Age calculations are then made possible by a straightforward calculation:

$$\text{Age (ky)} = \text{Equivalent dose (Gy)} / \text{Dose rate (Gy/ky)}$$

The analytical procedures used in optical dating vary extensively, and choosing the appropriate procedure depends upon the nature of the sediment. The method utilized for the BNWR samples was the single-aliquot regenerative-dose (SAR) protocol described by Murray and Wintle (2000). This protocol has been shown to be the best available method for luminescence dating of fluvial deposits and has been successfully and

extensively used (review in Rittenour, 2008).

Difficulties commonly arise when applying OSL dating to river and estuarine deposits (Aitken, 1998; Wallinga, 2002). The main goal in OSL geochronology is to sample material that was fully exposed to sunlight during transport prior to burial so that any luminescence signal remaining from previous episodes of burial is erased (or “bleached”). In full sunlight, this signal is reduced by a factor of 10 in just seconds-to-minutes (Godfrey-Smith et al., 1988). The samples that yield the best luminescence signal are those that experienced multiple episodes of transport over long distances and are composed of well-sorted, medium-grained quartz sand (Aiken, 1998). Eolian sediments, thus, prove to be the ideal material for OSL dating. But the transport mechanisms associated with fluvio-estuarine processes active in Chesapeake Bay clearly do not ensure such ideal bleaching conditions. Sediment transport may proceed under several meters of water, and in some instances the water may be turbid. These conditions have the potential to greatly reduce light intensity and/or restrict the spectrum of the light reaching the sediment, which may only permit partial bleaching of sand grains (Aitken, 1998; Wallinga, 2002). This situation has the potential to cause age overestimates by incorporating sand grains with high residual, or inherited, luminescence signals at deposition.

Additionally, calculating an accurate radiation dose rate for BNWR sands poses challenges. For the most accurate dose rate calculation, samples should be surrounded by a radius of at least 30 cm of homogeneous sediment and should not have undergone

significant water-content variations during burial (Aitken, 1998; Forman et al., 2000); alluvial sands in BNWR do not guarantee either. OSL samples from BNWR were collected from 2.5 ft (0.76 m) length sections of core and I did not always have the option of ensuring a 30 cm buffer of sediment from nearby contacts. Additionally, depending on the antiquity of sample material and the depths from which samples are collected, they potentially have significant variability in the degree of water saturation during burial. This variability reduces the accuracy of dose-rates measured in the lab, thereby increasing the error reported with ages.

Despite such obstacles, optical dating has been successfully employed to develop chronologies for fluvial-to-estuarine deposits (Mallinson et al., 2008; review in Rittenour, 2008), and it worked well in the BNWR. I carefully selected my OSL samples by first flight-augering sample locations to target material that minimized complications, and any uncertainties related to complications are included in the errors reported with ages. Results are consistent between both the Utah State University Luminescence Laboratory and the USGS Luminescence Laboratory. Two pilot samples from fluvio-estuarine sands typical of the BNWR stratigraphy were run prior to the major sampling campaign, and they produced ages that are consistent within their respective uncertainties as well as with other OSL ages produced regionally (USU-265 and USU-266, Table 2-2 (SD2); Mallinson et al., 2008; Pavich et al., 2006; Scott et al., 2010). The vast majority of OSL ages produced in this study, collected from below estuarine landforms, date to MIS 3. Taking these ages in consideration alongside accepted eustatic sea-level curves implies a

unique relative sea-level history of the field area caused by glacio-isostatic adjustment of the land surface.

1.3.2. Cosmogenic Nuclides

Cosmogenic nuclide burial dating uses the measurement of the rare isotopes ^{26}Al and ^{10}Be that are produced on Earth's surface by nuclear reactions between cosmic rays and quartz-bearing rocks (Gosse and Phillips, 2001). As high-energy cosmic rays enter Earth's atmosphere, they collide with atmospheric gases to produce a variety of secondary particles including neutrons and muons (Lal and Peters, 1967). It is the high-energy collision of neutrons and muons with quartz-bearing material in the upper meters of rock and soil that produces ^{26}Al and ^{10}Be at a fixed and well-known ratio (nominally 6.75:1 for spallogenic production at sea level [Nishiizumi et al., 1986, 2007] but note recent suggestions that the ratio may be 5% higher and altitude-dependent [Argento et al. 2013; Lifton et al., 2014]). The half lives of ^{26}Al and ^{10}Be , 0.705 Myr and 1.36 Myr respectively, allow burial dating of deposits ranging from 0.2 to 4 Ma [these figures are based on the ^{26}Al decay constant of $9.83 \pm 0.25 \times 10^{-7} \text{ yr}^{-1}$ (from the reference standards of Nishiizumi, 2004) and the ^{10}Be decay constant of $5.10 \pm 0.26 \times 10^{-7} \text{ yr}^{-1}$ (from the reference standards of Nishiizumi et al., 2007)], a time interval just beyond the utility of OSL methods that includes many major fluctuations of sea level rise and fall in the MACP.

The simple ^{26}Al - ^{10}Be burial dating method requires 1) quartz material that

contains no cosmogenic radionuclides prior to exposure, and is then exposed in one event during which ^{26}Al and ^{10}Be accumulate at the surface production ratio, and 2) the quartz material is then buried deeply enough to shield it from further cosmic ray flux (Granger and Muzikar, 2001). Upon burial, the ratio between these two radionuclides diverges from the production ratio because of differential radioactive decay at a predictable rate that can be used as a burial clock. This method is ideal for dating river sediments deposited in caves (Granger et al., 1997) or in deep lakes (Balco et al., 2013). But many geologic settings, including those represented within the BNWR stratigraphy, do not conform to this simple, two-stage history (single period of exposure followed by instantaneous, deep burial).

An alternative burial dating method has recently been developed to deal with more complex exposure and burial histories. The isochron method enables dating of quartz-bearing material with unknown inherited ^{26}Al and ^{10}Be concentrations and unknown burial histories (Balco and Rovey, 2008; Granger, 2014). Originally developed to date till-paleosol sequences with samples collected from different depths, a variant of this method involves sampling several (≥ 3) clasts and/or grain size separates from sand fractions that are derived from different settings within the watershed, and thus subject to different exposure histories, but have identical post-burial nuclide production (e.g. they were buried together simultaneously). The ^{26}Al and ^{10}Be concentrations from all clasts and grain size separates form a linear relationship, or an isochron, in $^{26}\text{Al} - ^{10}\text{Be}$ space. The slope of this isochron depends on the $^{26}\text{Al} / ^{10}\text{Be}$ production ratio, the ^{26}Al and ^{10}Be

decay constants, and on the burial time, but it is independent of the production of nuclides during burial. Provided clasts are buried with a wide range of isotope concentrations, the slope of the isochron drawn through ^{26}Al and ^{10}Be concentrations can indicate a burial age for the deposit (see section 2.9 for governing equations).

The isochron method is appropriate for dating Pleistocene gravels in the BNWR. The coarse-grained fluvial deposits that were deposited in discrete stratigraphic horizons during glacial maxima derive from a variety of settings within the Susquehanna basin and were buried by sequences of interglacial bay-fill material of variable thickness at unknown rates. ^{10}Be measurements in contemporary sediments from sub-basins in the Susquehanna watershed at a variety of spatial scales indicate erosion rates that are high enough that radioactive decay does not alter the initial $^{26}\text{Al} - ^{10}\text{Be}$ ratios of gravels (Reuter, 2005). Additionally, unpublished amino acid racemization dating on several mollusks recovered in bay fill material overlying gravels in BNWR confirm previous findings (Genau et al., 1994) that the age of the channel gravels on the western Delmarva are within the age range datable by the isochron burial dating method (John Wehmiller, personal communication March, 2012). By dating gravel deposits under the BNWR with isochrons, I produced the first-ever, quantified ages for gravel deposits that extend known timescales for Pleistocene cut-fill processes by a magnitude of 4x.

1.4. Structure of dissertation

Chapter 1 is an introduction that provides an overview of the importance of placing processes governing present-day environmental threats into a longer geologic context from which they are derived. This includes a short discussion on the need for a well-defined geologic framework for contextualizing results of analyses accomplished from borehole sediments, and the methods I used to erect such a framework for the BNWR. The dating methods that I used for my dissertation research are briefly introduced as well as the geographic and geologic setting of the field area.

Chapter 2 is a manuscript accepted for publication (August 2015) in the journal *GSA TODAY*. This manuscript presents the optically stimulated luminescence ages that I produced for the BNWR stratigraphy and discusses the implications of those ages to coastal populations and resources in the Chesapeake Bay region. Specifically, the age-elevation relationships of estuarine deposits that mantle the BNWR surface suggest that the land surface is out of isostatic equilibrium, resulting in ongoing subsidence that will continue for the foreseeable future and exacerbate sea-level rise from changing global climates.

Chapter 3 is a manuscript that has been submitted to the journal *Nuclear Instruments and Methods in Physics Research Section B: Beam Interactions with Materials and Atoms*. This manuscript introduces the methodology by which I interpreted cosmogenic nuclides to develop age control on the older Blackwater NWR stratigraphy. Conceived with co-author Alan Hidy at the Accelerator Mass Spectrometry

13 conference in Barcelonnette, France in August 2014, this manuscript provides an additional perspective by which to evaluate cosmogenic nuclide burial isochron ages, and is ultimately intended to provide criteria for acceptance and/or rejection of data points in isochron datasets.

Chapter 4 is a manuscript prepared for submission to the journal *Nature Geoscience*. This manuscript shows my application of cosmogenic nuclide geochronology to the stratigraphy of the BNWR. There were two motivations for this work: To develop ages for channel deposits in order to gain a better sense of the timescales over which the Delmarva Peninsula took shape and evolved, and to use those ages to compare processes in the Susquehanna River watershed at the basin scale over the length of the Pleistocene. Data in this chapter show that cut-fill processes were active over the majority of the Pleistocene, and that apparent erosion rates increased by an order of 50% from the Pliocene to the Pleistocene.

Chapter 5 is a working draft intended for submission to *Geosphere*, a fully online publication of the Geological Society of America. This manuscript functions as a synthesis paper that draws from the results of chapters 2 and 4 to present the full Pleistocene geologic framework and interpreted geologic history of the BNWR. The overall purpose of this manuscript is to communicate the observations and geologic mapping philosophies that I have developed over the past 7 years working with the US Geological Survey to assist those that continue to study the surficial geology in the Delmarva setting.

Chapter 6 presents a brief overview of the most significant findings of this work and provides suggestions for future work. This chapter is followed by a comprehensive bibliography for this dissertation.

**CHAPTER 2: PLEISTOCENE RELATIVE SEA LEVELS IN THE
CHESAPEAKE BAY REGION AND THEIR IMPLICATIONS FOR THE NEXT
CENTURY**

Accepted for publication in GSA TODAY

Benjamin D. DeJong, U.S. Geological Survey, Reston, VA, 20192, and
Rubenstein School of the Environment and Natural Resources, University of Vermont,
Burlington, VT 05405, bdejong@usgs.gov, 435-760-5440

Paul R. Bierman, Geology Department and Rubenstein School of the Environment and
Natural Resources, University of Vermont, Burlington, VT 05405, pbierman@uvm.edu,
802-238-6826

Wayne L. Newell, U.S. Geological Survey, Reston, VA, 20192, wnewell@usgs.gov,
703-648-6991

Tammy M. Rittenour, Utah State University, Logan, UT, 84322,
tammy.rittenour@usu.edu, 435-213-5756

Shannon A. Mahan, U.S. Geological Survey, Lakewood, CO 80225
smahan@usgs.gov, 303-236-7928

Greg Balco, Berkeley Geochronology Center, Berkeley, CA, 94709, balcs@bgc.org,
510-644-9201

Dylan H. Rood, Scottish Universities Environmental Research Centre (SUERC),
University of Glasgow, East Kilbride G750QF, Scotland, UK; now at Department of
Earth Science and Engineering, Imperial College London, South Kensington Campus,
London SW7 2AZ, UK, d.rood@imperial.ac.uk, +44 (0)20 7594 7333

2.1. Abstract

Today, relative sea-level rise (3.4 mm/yr) is faster in the Chesapeake Bay region than any other location on the Atlantic coast of North America, and twice the global average eustatic rate (1.7 mm/yr). Dated, interglacial deposits suggest that relative sea levels in the Chesapeake Bay region deviate from global trends over a range of timescales. Glacioisostatic adjustment of the land surface from loading and unloading of continental ice is likely responsible for these deviations, but our understanding of the scale and timeframe over which isostatic response operates in this region remain incomplete because dated sea-level proxies are mostly limited to the Holocene and to deposits >80 ka.

To understand better glacioisostatic control over past and present relative sea level, we applied a suite of dating methods to the stratigraphy of the Blackwater National Wildlife Refuge, one of the most rapidly subsiding and lowest-elevation surfaces bordering Chesapeake Bay. Data indicate that the region was submerged over most of marine isotope stage 3 (~60-30 ka), although multiple proxies suggest global sea level then was 40-80 m lower than present. Today marine isotope stage 3 deposits are above sea level because they were raised by the last glacial forebulge, but decay of that same forebulge is causing ongoing subsidence. These results suggest that glacioisostasy controls relative sea level in the mid-Atlantic region for tens of thousands of years following retreat of the Laurentide Ice Sheet. Thus, isostatically-driven subsidence of the Chesapeake Bay region will continue for millennia, exacerbating the effects of global

sea-level rise and impacting the region's large population centers and valuable coastal natural resources.

2.2. Introduction

The sea level for any location at a given point in time represents a sum of factors including the volume of ocean water, steric (thermal) effects, tectonic activity, and crustal deformation in response to glacio-hydro-isostatic adjustment (GIA) from loading and unloading of continental ice and water masses (Church, 2010). GIA can be a dominant driver of relative sea level (RSL) near ice margins, where the weight of ice displaces the mantle beneath glaciated regions, uplifting a “forebulge” in the peripheral, non-glaciated region (Peltier, 1986). With ice retreat, the forebulge progressively subsides at rates dependent on mantle rheology and lithosphere thickness (Peltier 1996).

GIA plays a role in RSL near the Chesapeake Bay region (CBR) of the United States (Figure 2-1) for many millennia after the ice melts away (Peltier, 2009). GIA effects were first recognized in the CBR when shoreline deposits ~3-5 m above present sea level, long assumed to be ~125 ka (marine isotope stage [MIS] 5e; MIS designations from Lisiecki and Raymo, 2005), were found to have ~80 ka ages (MIS 5a; Cronin, 1981). During this time, global average sea level was up to 20 m below its present level (Figure 2-2). While flexural isostatic uplift and subsidence have been documented in the CBR (i.e. Pazzaglia and Gardner, 1993), the rates (~0.006 mm/yr) associated with them are insufficient to account for the age-elevation relationships of these shorelines.

The presence of MIS 5a shorelines 3-5 m above present sea level indicates that the land surface within the CBR was significantly lower during the formation of these shorelines due to regional land subsidence from the collapse of the MIS 6 forebulge, and that the CBR region experienced renewed forebulge uplift during the MIS 2 to raise these shorelines above present sea level (Potter and Lambeck, 2003; Wehmiller et al., 2004). The Holocene stratigraphic record in the CBR helps understand forebulge dynamics; differential subsidence from the collapse of the MIS 2 forebulge caused variable timing and rates of inundation along the eastern seaboard during the Holocene transgression (Peltier, 1996). These differential rates have been exploited to reconstruct the form of the forebulge (Engelhart et al., 2009) and to constrain GIA models (Figure 2-1; Davis and Mitrovica; 1996; Peltier, 1996).

Recent studies employing optically stimulated luminescence (OSL) dating suggest that the lowest elevation, emerged estuarine deposits within the mid-Atlantic were deposited during MIS 3, significantly extending the inferred duration and magnitude of land subsidence due to collapse of the MIS 6 forebulge. Shoreline landforms near sea level (<8 m above mean sea level [asl]) on the western shore of central Chesapeake Bay, (Figure 2-1; Pavich et al., 2006), at the mouth of Chesapeake Bay (Scott et al., 2010), and on the North Carolina coast (Mallinson et al., 2008; Parham et al., 2013) indicate estuarine deposition throughout MIS 3 (67 to 32 ka). Eustatic sea level during this time was highly variable but always ~40-80 m lower than present (Figure 2-2; Siddall et al., 2008). These new data challenge the long-held implication that locations within the

CBR, and specifically the Delmarva Peninsula, was never submerged after MIS 5 (e.g. Ramsey, 2010). The presence of MIS 3 deposits near present sea level suggests an alternative sea-level history for the region, and one which implies forebulge uplift of at least 40 meters since the time of deposition. This uplift has been attributed to growth of the last glacial maximum (LGM; MIS 2) forebulge (Pavich et al., 2006; Mallinson et al., 2008; Scott et al., 2010; Parham et al., 2013) that remains uplifted out of isostatic equilibrium (Potter and Lambeck, 2003).

This paper uses multiple methods to date deposits within the zone of greatest subsidence in the CBR (Figure 2-1) and place today's rapid relative sea-level rise into the context of a several-million-year geologic framework. We used a LIght Detection And Ranging (LiDAR) digital elevation model (DEM) to analyze low-relief landforms and did extensive drilling to constrain the Pleistocene stratigraphic framework. Our data show that regional subsidence related to collapse of the MIS 6 glacio-isostatic forebulge impacted the mid-Atlantic region well into MIS 3, tens of thousands of years after MIS 5 deglaciation. Long-lasting subsidence associated with collapse of the MIS 6 forebulge suggests present-day subsidence related to the collapse of the MIS 2 forebulge will continue for the foreseeable future. We conclude that ongoing subsidence adds to the impacts of sea-level rise driven by warming climate and melting ice sheets and should be considered in coastal sea level risk assessments.

2.3. Study site and methods

To reconstruct the sea-level history in Chesapeake Bay, we focused on the Blackwater National Wildlife Refuge (BNWR, $\sim 110 \text{ km}^2$; red-bordered rectangle on Figure 2-1), which experienced major inundation and transformation of wetlands to open water in the 20th century (Figure 2-3). Sediment from seventy boreholes was described, analyzed, and sampled. The DEM (Figure 2-4) was used to characterize the geomorphology. We constrained the oldest erosional event preserved directly above the underlying Miocene strata using cosmogenic nuclide isochron burial dating (Balco and Rovey, 2008). We dated 28 samples using optically stimulated luminescence (OSL) dating. The OSL ages allow us to develop a geochronology for the BNWR landforms and estuarine sediments to a depth of $\sim 9 \text{ m}$ (Figure 2-5). Eight radiocarbon dates constrain the timing of Holocene inundation and the beginning of marsh accretion. Detailed methods are provided in supplemental data.

2.4. Results and interpretations

The BNWR is underlain by Pleistocene deposits that vary in thickness from $\sim 3\text{-}55 \text{ m}$ (Figure 2-5). Glacial-interglacial climate fluctuations induced major cycles of localized river incision and aggradation in the CBR (Colman et al., 1990), and the subsurface BNWR stratigraphy includes cut-fill deposits associated with at least three paleochannel systems (Figure 2-5). Isochron ages at the base of the Pleistocene section are $1.72 \pm 0.75 \text{ Ma}$ for a Susquehanna River paleochannel and $2.06 \pm 0.07 \text{ Ma}$ for a local

paleochannel system (1s; Figure 2-5 and SD Table 1). The older age indicates that major cutting and filling commenced in the study area shortly after the onset of Northern Hemisphere continental glaciation (2.4 Ma, Balco and Rovey, 2010). These ages are significantly older than previous age estimates for paleochannels of the Chesapeake Bay (~18 - 450 ka; Colman et al., 1990). The complex Pleistocene stratigraphic record and age-range of material overlying these dated deposits suggest that cut-fill processes dominated landscape evolution over glacial-interglacial timescales in the field area (Figure 2-5).

LiDAR allows us to identify a variety of landforms on the BNWR surface that form a continuum with the shallow stratigraphy (<12 m; Figures 2-4, 2-5). A regressive, wave-cut scarp with multiple bifurcations (beach ridges; Figure 2-4B) separates upland areas to the north and east from the lower terrain in the south and west that is occupied by an expansive tidal marsh. These shoreline features consist of an ~3 m fining upward sequence of burrowed, silty fine sand to massive, medium sand (Figure SD 5) with an age range of 53-40 ka (n=6; see Figure 2-5 and SD Table 2). Below the scarp, large subaqueous bars (Figure 2-4B) that roughly parallel the paleo-shoreline dominate the geomorphology. The bars consist of facies ranging from horizontally bedded, alternating sand and silt to moderately sorted fine to medium sand interpreted as intermittently wave-sorted tidal channel deposits and wave-built bars within tidal tributaries or bays. OSL ages for surficial landforms below the scarp range from 69-35 ka (n=15). The morphology, lithology, and ages of these features indicate estuarine conditions prevailed

during most of MIS 3, with active bar migration continuing during regression. Locally, unconformities separate multiple, stacked MIS 3 deposits and in some locations MIS 3 deposits cut older estuarine units that were dated to both MIS 5a and MIS 5e (Figures 2-5, SD 4, SD 5).

The MIS 3 estuarine surface is truncated by a north-south trending, meandering channel with scroll bars as well as elliptical depressions interpreted as ephemeral basins (Figure 2-4B). The rims of basins are composed of laminated silty fine to medium sand with ages 30-26 ka (n=3). The channel must be younger than the ~35 ka sand bars it cuts. The basins and channel are likely relict from periglacial processes that were dominant in this landscape beginning ~30 ka and continuing through the LGM (Denny et al., 1979; Newell and Clark, 2008; French et al., 2009; Markewich et al., 2009; Newell and DeJong, 2011; Gao, 2014).

Sediments from the Holocene transgression (yellow, Figure 2-5) overlap MIS 3 estuarine deposits within incised valleys of the Blackwater River and its tributaries. They consist of a lower silt (~3-4 m) with locally abundant organic material that transitions gradually to an upper, dense, organic peat (~3-4 m). A radiocarbon (^{14}C) age from woody material near the base of the silt (-8.5 m) suggests initial Holocene transgression into the Blackwater River valley by 5310-5570 cal yr B.P. Woody material within the silt, just below the peat boundary, is 690-910 cal yr B.P. and sets a maximum age for marsh accretion. Radiocarbon samples collected above this boundary and within the peat have modern ages (SD Table 3).

2.5. Discussion

Fluctuating sea levels, resulting from changes in eustatic sea level, and crustal deformation (uplift and subsidence) related to GIA, define the Pleistocene history of the BNWR and the greater CBR. The Pleistocene record and cosmogenic ages suggest that the onset of Northern Hemisphere glaciation at the Plio-Pleistocene boundary initiated repeated cycles of incision and deposition. The paleo-Susquehanna River and its tributaries responded to repeated ~50-100 m sea-level fluctuations (Lisiecki and Raymo, 2005), with deep incision of river valleys during glacial lowstands and fluvio-estuarine deposition during transgressions. Estuarine conditions prevailed during MIS 3, when global proxies indicate eustatic sea level was ~40-80 m below present, suggesting prolonged relaxation of a MIS 6 forebulge during MIS 3.

Temperatures and sea levels plunged at ~30 ka, from their already low MIS 3 levels (Figure 2-2). As the Laurentide Ice Sheet grew, so did the forebulge that uplifted the CBR through the LGM, likely contributing to rapid incision documented along the Susquehanna and Potomac Rivers (Reusser et al., 2004), as the CBR was transformed into a periglacial landscape. During the Holocene, the forebulge progressively subsided, as indicated by differential timing of Holocene inundation and variable rates of sea-level rise along the US Atlantic coast (Engelhart et al., 2009). The Blackwater River valley was inundated by ~5 ka, initiating deposition of bay bottom silt. Widespread marshes were established sometime within the last millennium and accreted, keeping pace with sea-level rise. At the turn of the 20th century, RSL rise accelerated (Engelhart et al.,

2009), resulting in inundation, erosion, and ponding in the BNWR as sea-level rise outpaced marsh accretionary processes (Figure 2-3; Stevenson et al., 2002).

The presence of MIS 3 estuarine deposits near today's sea level confirms the effects of GIA over long timescales for the BNWR and supports similar interpretations within the greater CBR. The elevations of MIS 3 estuarine deposits generally decrease from the Central Delmarva Peninsula southward to North Carolina (Scott et al., 2010); no dated, emerged MIS 3 estuarine deposits south of North Carolina have been reported in the literature. While the maximum elevations of MIS 3 deposits vary (Figure SD 8), decreasing elevations to the south are consistent with the shape of the forebulge based on subsidence rates (Engelhart et al., 2009). High precision GPS data, though limited by short time series, also indicate the highest rates of subsidence on the Atlantic coast are centered on the CBR (Sella et al., 2007; Snay et al., 2007).

Our data support the hypothesis that subsidence in the CBR is caused by the continued collapse of the MIS 2 forebulge (Potter and Lambeck, 2003). While subsidence rates vary within the CBR (Figure 2-1; Engelhart et al., 2009), potentially due to local groundwater withdrawal for commercial use (Eggleston and Pope, 2013), the central Delmarva Peninsula has the highest rates of subsidence in the mid-Atlantic (~1.3 - 1.7 mm/yr; Engelhart et al., 2009). Parsing GIA-driven subsidence from other RSL drivers is uncertain (e.g. Cronin, 2012), but the agreement of 20th century subsidence values calculated from tide gauge records where effects of seasonal and decadal variability are removed (~1.6 mm/yr, Boon et al., 2010) and from dated Holocene deposits (~1.3 mm/yr;

Engelhart et al., 2009) from the same location near our study area implies consistency of rates over millennial timescales. Subsidence is thus primarily driven by GIA in the CBR, which makes RSL rise in the Chesapeake Bay-Washington, D.C. area twice the 20th century, global average rate of sea-level rise (1.7 mm/yr; IPCC, 2013). If timescales of MIS 6 forebulge subsidence are used for comparison, subsidence from the LGM forebulge collapse will continue for many more millennia.

Ongoing, GIA-driven subsidence in the CBR challenges a region already threatened by sea-level rise. At the BNWR, we use rate consistency to predict ~0.16 m of subsidence for the region in the 21st century (using 20th century values from Boon and others [2010] that presumably include the effects of groundwater withdrawal). The likely range of average global sea-level rise for the 21st century is 0.33-0.82 m based on a non-aggressive climate mitigation policy (IPCC, 2013). Superimposing this sea-level rise estimate over 0.16 m of subsidence yields a total predicted RSL rise of 0.49-0.98 m for the BNWR by AD 2100.

These are minimum estimates; several lines of evidence suggest that sea levels will rise more quickly in the CBR. Recent tide gauge analyses indicate the acceleration of sea-level rise in the North Atlantic in recent decades, possibly due to dynamic ocean circulation processes (Yin et al., 2010; Boon, 2012; Ezer and Corlett, 2012; Sallenger et al., 2012). If this acceleration continues, it could induce an additional rise of 15 cm for Chesapeake Bay and Washington D.C. by AD 2100 (Yin et al., 2010). Recent evidence also confirms the instability of glaciers in West Antarctica, which has the potential to

raise global sea levels significantly, particularly beyond AD 2100 (Joughin et al., 2014; Rignot et al., 2014). As global sea levels rise and the CBR subsides, storm surges are projected to increase both in frequency (IPCC, 2013) and magnitude (Tebaldi et al., 2012). Superimposing Hurricane Isabel water levels on the range of RSLs we predict for the CWB would cause a storm tide of ~3.8-4.6 m in Washington D.C., and ~2.8-3.5 m for Chesapeake Bay (NOAA, 2003). Given the location of the CBR along the path of storms tracking up the Atlantic coast (Figure 2-1), increasing RSL rise will further exacerbate already high costs of storm damage such as the \$65 billion price tag associated with Hurricane Sandy (NOAA, 2013).

Even the most conservative estimate of projected RSL rise poses significant threats to the CBR. Bridges, military facilities, national monuments, and portions of the rapid transit system would be flooded in Washington D.C. and ~70,000 residents impacted by a 0.4 m rise in sea level (Ayyub et al., 2012). Island communities in Chesapeake Bay are particularly vulnerable to RSL rise. The last 2 inhabited islands in Chesapeake Bay are ≤ 1 m above sea level; they occupy the same geomorphic surface as the western portion of our field area, and will experience similar rates of subsidence. In the BNWR, a LiDAR-based inundation study using a conservative model for sea-level rise shows that the majority of tidal marsh will be inundated by AD 2050 (Larsen et al., 2004).

The elevated risk of flooding in the CBR is already triggering a social response. At the BNWR, managers are designing corridors for the landward migration of habitat

through easements and land acquisition to ensure the persistence of tidal marsh beyond AD 2100. Similar options are increasingly limited on other coastlines, where continued development and site modification for housing severely limits potential for inland migration of habitat, and wetland loss significantly reduces natural buffers to storms in these regions (Titus et al., 2009). Island communities have limited options; Chesapeake Bay islands have been abandoned due to sea-level rise in the past century (e.g. Gibbons and Nicholls, 2006).

For Washington, D.C. and other coastal cities, risk assessment and adaptation planning based on the full range of possible RSL rise scenarios is critical. The analysis by Ayyub et al. (2012) indicates significant losses for Washington D.C. with a rise of 0.4 m, well below minimum predicted rise of sea level for AD 2100 of 0.49 to 0.98 m. Such an analysis under-predicts the most likely RSL rise over the next century, in part because it does not explicitly consider that GIA will drive increased RSL independent of climate change. We conclude that risk assessments and adaptation planning for sea-level rise should consider the full range of sea-level estimates (e.g., Miller et al., 2013) and take local subsidence values into consideration, particularly for high-density population centers like Washington, D.C.

2.6. Acknowledgements

Research supported by the USGS. M. Whitbeck (USFWS) granted access to the Blackwater NWR. USGS drillers E. Cobbs, J. Grey made this work possible. We thank

M. Nelson, A. Bentham, I. Clark, H. Pierce, J. McGeehin, D. Powars, S. Zimmerman, and J. Smoot, and D. Granger. M. Pavich reviewed this manuscript.

2.7. References

- Ayyub, B. M., Braileanu, H. G., and Qureshi, N., 2012, Prediction and impact of sea level rise on properties and infrastructure of Washington, D.C.: *Risk Anal*, v. 32, no. 11, p. 1901-1918.
- Balco, G., and Rovey, C. W., 2008, An isochron method for cosmogenic-nuclide dating of buried soils and sediments: *American Journal of Science*, v. 308, no. 10, p. 1083-1114.
- Balco, G., and Rovey, C. W., 2010, Absolute chronology for major Pleistocene advances of the Laurentide Ice Sheet: *Geology*, v. 38, no. 9, p. 795-798.
- Boon, J. D., 2012, Evidence of sea level acceleration at U.S. and Canadian tide stations, Atlantic coast, North America: *Journal of Coastal Research*, v. 285, p. 1437-1445.
- Boon, J. D., Brubaker, J. M., and Forrest, D. R., 2010, Chesapeake Bay land subsidence and sea level change: An evaluation of past and present trends and future outlook, A Report to the Army Corps of Engineers. Virginia Institute of Marine Science Special Report No. 425 in *Applied Marine Science and Ocean Engineering*, 35 pp.
- Cahoon, D. R., Guntnerspergen, G., Baird, S., Nagel, J., Hensel, P., Lynch, J., Bishara, D., Brennand, P., Jones, J., and Otto, C., 2010, Do annual prescribed fires

enhance or slow the loss of coastal marsh habitat at Blackwater National Wildlife Refuge? Final Project Report to Joint Fire Science Program, http://www.firescience.gov/projects/06-2-1-35/project/06-2-1-35_blackwater_burn_final_report_mar_31_2010.pdf.

Church, J. A., Woodworth, P. L., Aarup, T., and Wildon, W. S., 2010, Understanding Sea-Level Rise and Variability, UK, Wiley-Blackwell., 456 pp.

Colman, S. M., Halka, J. P., Hobbs III, C. H., Mixon, R. B., and Foster, D. S., 1990, Ancient channels of the Susquehanna River beneath Chesapeake Bay and the Delmarva Peninsula: Geological Society of America Bulletin, v. 102, p. 1268-1279.

Cronin, T. M., 1981, Rates and possible causes of neotectonic vertical crustal movements of the emerged southeastern United States Atlantic Coastal Plain: Geological Society of America Bulletin, v. 92, no. 11, p. 812-833.

Cronin, T.M., 2012, Rapid sea-level rise: Quaternary Science Reviews, v. 56, p. 11-30.

Davis, J. L., and Mitrovica, J. X., 1996, Glacial isostatic adjustment and the anomalous tide gauge record of eastern North America: Nature, v. 379, p. 331-333.

Denny, C. S., Owens, J. P., Sirkin, L. A., and Rubin, M., 1979, The Parsonsburg Sand in the Central Delmarva Peninsula, Maryland and Delaware, USGS Professional Paper 1067-B, p. B1-B16.

Dyke, A. S., Andrews, J. T., Clark, P. U., England, J. H., Miller, G. H., Shaw, J., and Veillette, J. J., 2002, The Laurentide and Innuitian ice sheets during the Last

- Glacial Maximum: *Quaternary Science Reviews*, v. 21, p. 9-31.
- Eggleston, J. E., and Pope, J., 2013, Land Subsidence and Relative Sea-Level Rise in the Southern Chesapeake Bay Region, USGS Circular 1392, 30 pp.
- Engelhart, S. E., Horton, B. P., Douglas, B. C., Peltier, W. R., and Tornqvist, T. E., 2009, Spatial variability of late Holocene and 20th century sea-level rise along the Atlantic coast of the United States: *Geology*, v. 37, no. 12, p. 1115-1118.
- Ezer, T., and Corlett, W. B., 2012, Is sea level rise accelerating in the Chesapeake Bay? A demonstration of a novel new approach for analyzing sea level data: *Geophysical Research Letters*, v. 39, no. 19, p. 1-6.
- French, H., Demitroff, M., and Newell, W. L., 2009, Past permafrost on the mid-Atlantic coastal plain, eastern United States: *Permafrost and Periglacial Processes*, v. 20, p. 285-294.
- Gao, C., 2014, Relict Thermal-contraction-crack polygons and past permafrost south of the Late Wisconsinan glacial limit in the mid-Atlantic coastal plain, USA: *Permafrost and Periglacial Processes*, p. 144-149.
- Gibbons, S. J. A., and Nicholls, R. J., 2006, Island abandonment and sea-level rise: An historical analog from the Chesapeake Bay, USA: *Global Environmental Change*, v. 16, no. 1, p. 40-47.
- IPCC, 2013, *Climate change 2013: The physical science basis. Contribution of the Working Group 1 to the Fifth Assessment report of the Intergovernmental Panel on Climate Change.*, Cambridge, UK, Cambridge Univ. Press, 2216 pp.

- Joughin, I., Smith, B. E., and Medley, B., 2014, Marine ice sheet collapse potentially under way for the Thwaites Glacier Basin, West Antarctica: *Science*, v. 344, no. 6185, p. 735-738.
- Larsen, C., Clark, I., Guntenspergen, G. R., Cahoon, D. R., Caruso, V., Hupp, C., and Yanosky, T., 2004, The Blackwater NWR Inundation Model: Rising Sea Level on a Low-lying Coast: USGS Open File Report 04-1302.
- Lisiecki, L. E., and Raymo, M. E., 2005, A Pliocene-Pleistocene stack of 57 globally distributed benthic $\delta^{18}\text{O}$ records: *Paleoceanography*, v. 20, no. 1, p. 1-17.
- Mallinson, D., Burdette, K., Mahan, S., and Brook, G., 2008, Optically stimulated luminescence age controls on late Pleistocene and Holocene coastal lithosomes, North Carolina, USA: *Quaternary Research*, v. 69, no. 1, p. 97-109.
- Markewich, H. W., Litwin, R. J., Pavich, M. J., and Brook, G. A., 2009, Late Pleistocene eolian features in southeastern Maryland and Chesapeake Bay region indicate strong WNW–NW winds accompanied growth of the Laurentide Ice Sheet: *Quaternary Research*, v. 71, no. 3, p. 409-425.
- Miller, K. G., Kopp, R. E., Horton, B. P., Browning, J. V., and Kemp, A. C., 2013, A geological perspective on sea-level rise and its impacts along the U.S. mid-Atlantic coast: *Earth's Future*, v. 1, no. 1, p. 3-18.
- Newell, W. L., and Clark, I., 2008, Geomorphic map of Worcester County, Maryland, interpreted from a LiDAR-based digital elevation model, USGS Open File Report 2008-1005, 34 pp.

- Newell, W. L., and DeJong, B. D., 2011, Cold-climate slope deposits and landscape modifications of the Mid-Atlantic Coastal Plain, Eastern USA: Geological Society, London, Special Publications, v. 354, no. 1, p. 259-276.
- NOAA, 2003, Storm Data and Unusual Weather Phenomena, <http://www.weather.gov/media/lwx/stormdata/storm0903.pdf>
- NOAA, 2013, National Climatic Data Center; <http://www.ncdc.noaa.gov/billions/events>
- Parham, P. R., Riggs, S. R., Culver, S. J., Mallinson, D. J., Jack Rink, W., and Burdette, K., 2013, Quaternary coastal lithofacies, sequence development and stratigraphy in a passive margin setting, North Carolina and Virginia, USA: Sedimentology, v. 60, no. 2, p. 503-547.
- Pavich, M. J., and Markewich, H. W., Brook, G.A., 2006, Significance of Kent Island Formation to geomorphic history of the Mid-Atlantic region, Geological Society of America, Abstracts with programs 38, p. 226.
- Pazzaglia, F. J., and Gardner, A. S., 1993, Fluvial terraces of the lower Susquehanna River: Geomorphology, v. 8, p. 83-113.
- Peltier, W. R., 1986, Deglaciation induced vertical motion of the North American continent and transient lower mantle rheology: Journal of Geophysical Research, v. 91, no. B8, p. 9099-9123.
- Peltier, W. R., 1996, Global sea level rise and glacial isostatic adjustment: An analysis of data from the east coast of North America: Geophysical Research Letters, v. 23, no. 7, p. 717-720.

- Peltier, W. R., 2009, Closure of the budget of global sea level rise over the GRACE era: the importance of magnitudes of the required corrections for global glacial isostatic adjustment: *Quaternary Science Reviews*, v. 28, p. 1658-1674.
- Potter, E.-K., and Lambeck, K., 2003, Reconciliation of sea-level observations in the Western North Atlantic during the last glacial cycle: *Earth and Planetary Science Letters*, v. 217, no. 1-2, p. 171-181.
- Ramsey, K. W., 2010, Stratigraphy, correlation, and depositional environments of the middle to late Pleistocene interglacial deposits of southern Delaware, Delaware Geologic Survey Report of Investigations 76, 43 pp.
- Reusser, L. J., Bierman, P. R., Pavich, M. J., Zen, E.-a., Larsen, J., and Finkel, R. C., 2004, Rapid Late Pleistocene incision of Atlantic passive-margin river gorges: *Science*, v. 305, p. 499-502.
- Rignot, E., Mouginot, J., Morlighem, M., Seroussi, H., and Scheuchl, B., 2014, Widespread, rapid grounding line retreat of Pine Island, Thwaites, Smith, and Kohler glaciers, West Antarctica, from 1992 to 2011: *Geophysical Research Letters*, p. 1-8.
- Sallenger, A. H., Doran, K. S., and Howd, P. A., 2012, Hotspot of accelerated sea-level rise on the Atlantic coast of North America: *Nature Climate Change*, v. 2, p. 884-888.
- Scott, T. W., Swift, D. J. P., Whittecar, G. R., and Brook, G. A., 2010, Glacioisostatic influences on Virginia's late Pleistocene coastal plain deposits: *Geomorphology*,

v. 116, no. 1-2, p. 175-188.

Sella, G. F., Stein, S., Dixon, T. H., Craymer, M., James, T. S., Mazzotti, S., and Dokka, R., 2007, Observation of glacial isostatic adjustment in “stable” North America with GPS: *Geophysical Research Letters*, v. 34.

Snay, R., Cline, M., Dillinger, W., Foote, R., Hilla, S., W., K., Ray, J., Rohde, J., Sella, G., and Soler, T., 2007, Using global positioning system-derived crustal velocities to estimate rates of absolute sea level change from North American tide gauge records: *Journal of Geophysical Research*, v. 112, no. B4.

Siddall, M., Rohling, E. J., Thompson, W. G., and Waelbroeck, C., 2008, Marine isotope stage 3 sea level fluctuations: Data synthesis and new outlook: *Reviews of Geophysics*, v. 46, no. 4., 29 pp.

Stevenson, J. C., Kearney, M. S., and Koch, E. W., 2002, Impacts of sea level rise on tidal wetlands and shallow water habitats: A case study from Chesapeake Bay: *American Fisheries Society Symposium*, v. 32, p. 23-26.

Tebaldi, C., Strauss, B. H., and Zervas, C. E., 2012, Modelling sea level rise impacts on storm surges along US coasts: *Environmental Research Letters*, v. 7, no. 1, p. 1-11.

Thompson, W. G., and Goldstein, S. L., 2006, A radiometric calibration of the SPECMAP timescale: *Quaternary Science Reviews*, v. 25, no. 23-24, p. 3207-3215.

Titus, J. G., Hudgens, D. E., Trescott, D. L., Craghan, M., Nuckols, W. H., Hershner, C.

H., Kassakian, J. M., Linn, C. J., Merritt, P. G., McCue, T. M., O'Connell, J. F., Tanski, J., and Wang, J., 2009, State and local governments plan for development of most land vulnerable to rising sea level along the US Atlantic coast: Environmental Research Letters, v. 4, no. 4, p. 1-7.

U.S. Census Bureau American FactFinder, 2014, U.S., 2010 Census Redistricting Data Summary File (https://www.census.gov/geo/maps-data/maps/pdfs/thematic/us_popdensity_2010map.pdf)

U.S. Geological Survey, Crapo Quadrangle, Maryland [map], 1:50,000, 15 Minute Series, Washington D.C., 1905.

Wehmiller, J. F., Simmons, K. R., Cheng, H., Lawrence Edwards, R., Martin-McNaughton, J., York, L. L., Krantz, D. E., and Shen, C.-C., 2004, Uranium-series coral ages from the US Atlantic Coastal Plain—the “80ka problem” revisited: Quaternary International, v. 120, no. 1, p. 3-14.

Yin, J., Griffies, S. M., and Stouffer, R. J., 2010, Spatial variability of sea-level rise in twenty-first century projections: Journal of Climate, v. 23, no. 17, p. 4585-4607.

2.8. Figure captions

Figure 2-1. Map showing Atlantic coast of the United States with population density by county (U.S. Census Bureau, 2011) placed alongside Late Holocene and 20th century RSL rise curves (2-sigma errors; Engelhart et al., 2010). RSL rise predicted from GIA modeling is from the M2 viscosity model (Peltier, 1996). Yellow shaded region brackets

area of highest RSL rise on the Atlantic coast; dotted line indicates maximum extent of the LIS (Dyke et al., 2002). P, S, MP: Locations of OSL ages indicating MIS 3 coastal deposits near Washington, D.C. (37 ka, n=1; Pavich et al., 2006; n=1) in southern Virginia (50-33 ka, n=2; Scott et al., 2010) and North Carolina (59-28 ka, n=15; Mallinson et al., 2008, Parham et al., 2013), respectively. A-A' shows location of Figure 2A.

Figure 2-2. Land and sea-level elevations through time. A. Schematic cross-section showing land surface to relative sea level relations at specific times in glacial cycles as a function of distance from the Laurentide ice sheet (LIS). Adapted by permission from D. Krantz and C. Hobbs (pers. communication). B. Oxygen isotope and sea-level curves for the last 150 ky from Lisiecki and Raymo (2005) and Thompson and Goldstein (2006), respectively. The glacioisostatic (land surface) curve (after Scott et al., 2010) is based on ages produced for shoreline deposits in the mid-Atlantic region and illustrates how land-surface elevation change induced by GIA can account for submergence of the CBR when eustatic sea level was much lower than present.

Figure 2-3. Time series of the Blackwater River valley showing A. Intact marsh surveyed from 1902-1904 and presented in a 7.5" USGS topographic map from 1905 (USGS, 1905); dark blue hatching around the Blackwater valley is tidal marsh, light blue pattern is freshwater swamp, B. Initiation of major ponding seen in an aerial photograph

from 1938 (<http://www.esrgc.org/>), and C. Coalesced ponds forming the informal “Lake Blackwater” in satellite imagery from 2007 (<http://www.bing.com/maps/>). Wetlands are converting to open water at a rate of 50-150 ha/yr in the field area (Cahoon et al., 2010). Image locations are identified in Figure 4B. Red outline shows location of unnamed island for reference.

Figure 2-4 LiDAR imagery and geomorphology of the study area. A. LiDAR-derived DEM of the BNWR projected in UTM Zone 18N with the NAD83 datum (from H. Pierce, USGS). Cell size is 2.5 by 2.5 m; graduated elevation scale indicated to the left of the image exaggerates subtle features in the lowest elevation ranges. White outline indicates boundary of the BNWR. B. Same LiDAR DEM as A) in gray-scale with geomorphic features referenced in the text superimposed. 1905 channel margins were digitized from the topographic map seen in Figure 3A.

Figure 2-5. A. Cross-section showing the Pleistocene deposits that underlie the BNWR. All ages are in thousands of years (ka). *Italicized* ages are cosmogenic burial isochrons, underlined ages are radiocarbon ages, all others are OSL ages. The top-most tan unit is a silt cap in which soils are formed over the majority of the field area. Yellow shading represents Holocene deposits; green shading represents MIS 5 and MIS 3 deposits; red, orange, and blue shading indicates three distinct paleochannel systems, with depths of western channels inferred from boreholes drilled off the line of section; gray substrate is

the Miocene Chesapeake Group. Note break in vertical scale. See Figures SD 4 and SD 5 for more detail on sedimentology.

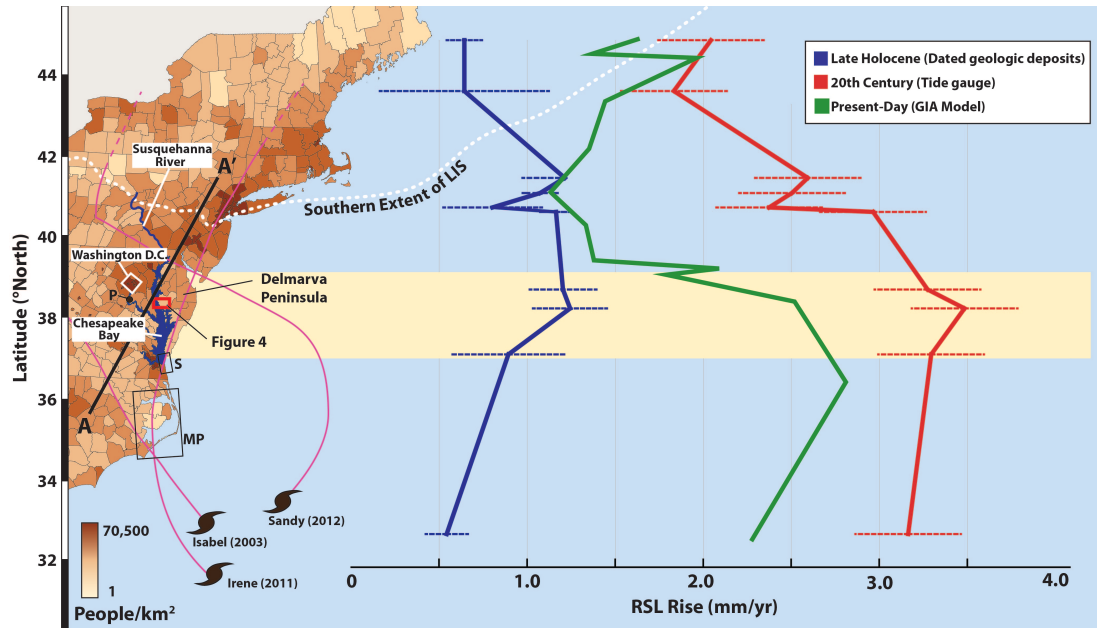


Figure 2-1 Map showing Atlantic coast of the United States with population density by county (U.S. Census Bureau, 2011) placed alongside Late Holocene and 20th century RSL rise curves (2-sigma errors; Engelhart et al., 2010)

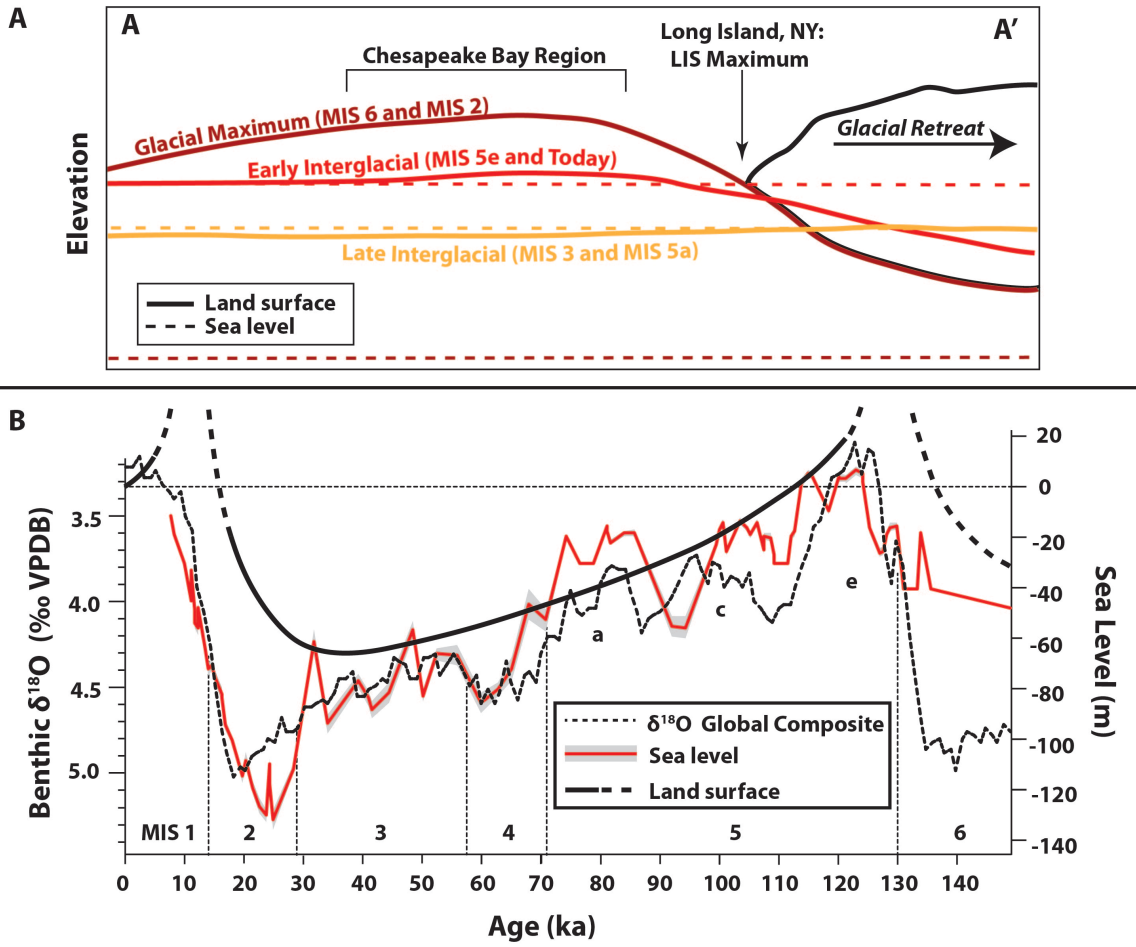


Figure 2-2 Land and sea-level elevations through time.

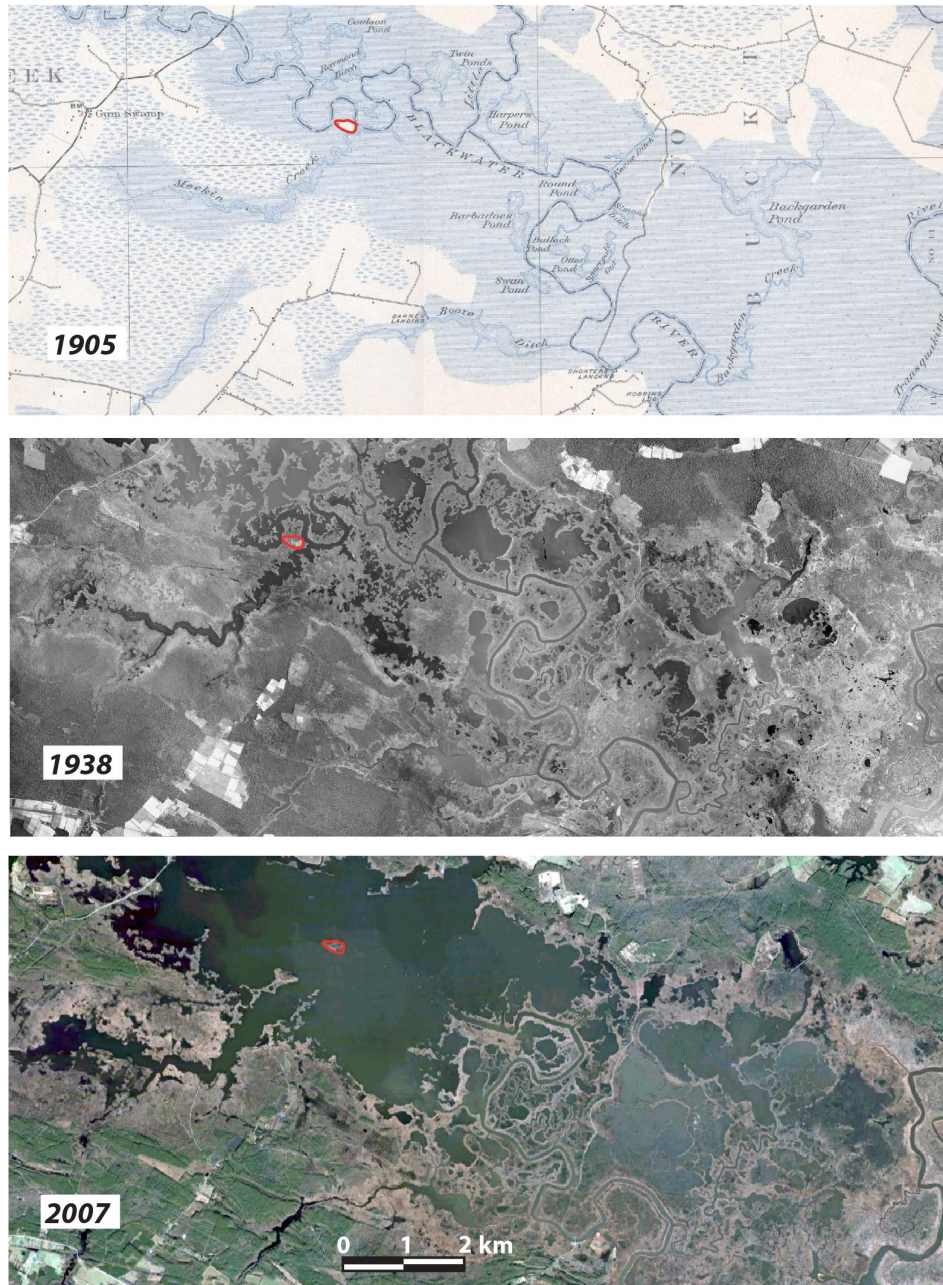


Figure 2-3 Time series of the Blackwater River valley

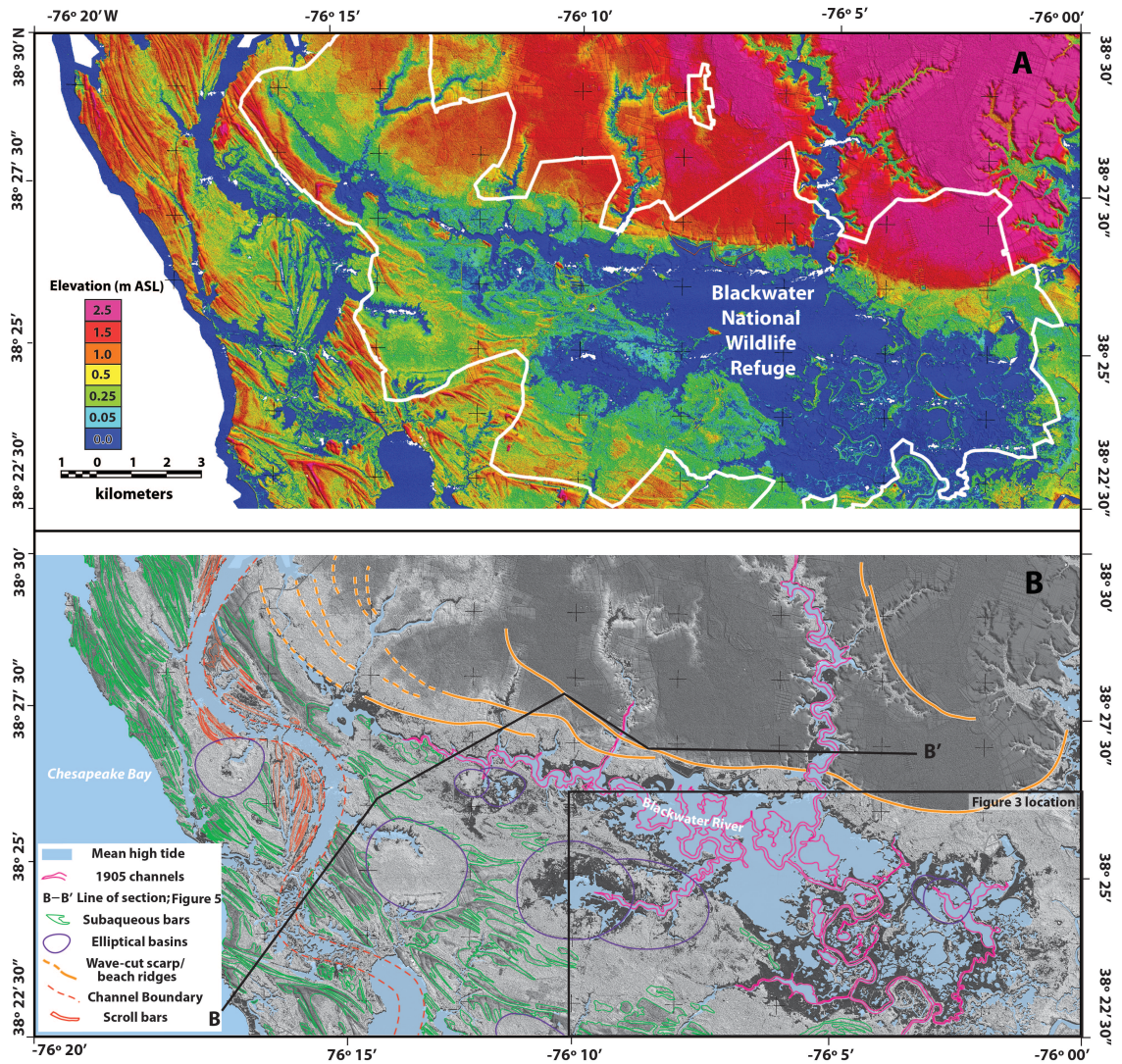


Figure 2-4 LiDAR imagery and geomorphology of the study area.

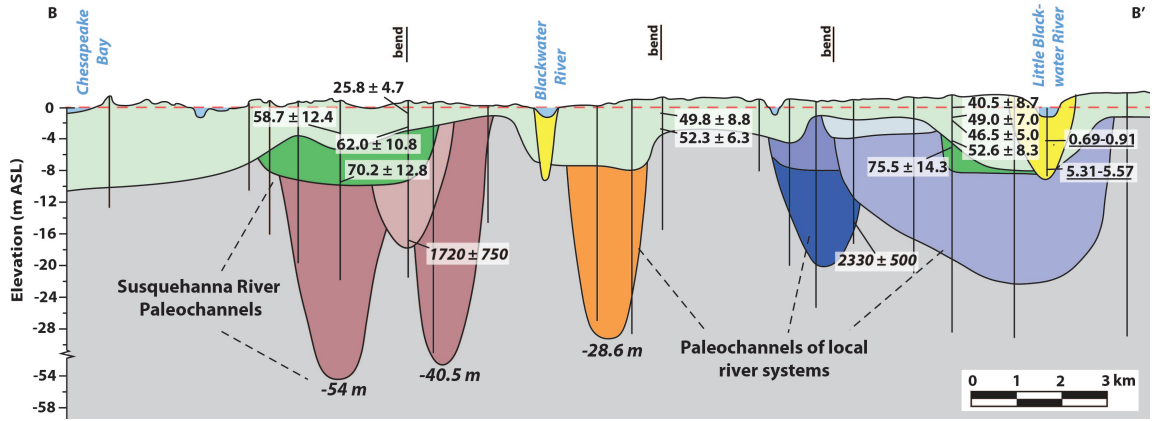


Figure 2-5 Cross-section showing the Pleistocene deposits that underlie the BNWR.

2.9. Supplemental data

Detailed Methods and Data Tables

Drilling and sample collection

The altitude within the study area rarely exceeds 2 m asl, and exposures of surficial deposits and underlying substrate are uncommon, ephemeral, and usually related to land-use practices. Therefore any detailed subsurface exploration requires drilling. Three drilling platforms were used:

Hollow-stem auger system: The cores from the BNWR were collected using a hollow-stem auger continuous sampling system (Figure SD 1A). Sediment cores were collected in 7.6 cm (3 in) diameter plastic liners in an inner core barrel that is straight-pushed inside ~21 cm (8.25 in) diameter augers. These cores were used to collect OSL samples and to provide detailed sedimentologic information about the surface units in and around the BNWR. Sands for OSL were first identified via flight augering and cored inside painted (black) core liners using the hollow-stem coring system. The core liners were carefully extracted from the inner steel core barrel under the tarp, wrapped in black plastic, and placed in a box to ensure the sand was not exposed to light during sampling (Figure SD 2).

Flight Augering: Flight augering (Figure SD 1B) was used for a majority of locations, as

this is by far the most cost-effective means of accessing the subsurface. An 11.4 cm (4.5 in) diameter solid-stem auger was drilled into the ground with 1 rotation per auger flight to minimize sediment disturbance and then straight-pulled to the surface for sample collection and analysis. This provided accurate depths to contacts as well as samples for sedimentology and cosmogenic nuclide geochronology (gravel deposits).

Vibracoring: Reconstructing the history of marsh deposits in the Blackwater River valley required drilling from a floating vessel. To accomplish this, we used a hovercraft-mounted, hydraulically powered sonic core (vibracore) drill (Figure SD 1C). This system yielded 6.35 cm (2.5 in) diameter continuous core drilled in 1.52 m (5 ft) sections. The vibracore system was used to collect all samples for sedimentology and radiocarbon geochronology of the Holocene stratigraphy in the Blackwater River valley as well as 2 OSL samples (USU-265, USU-266) directly underlying this stratigraphy.

All drilling locations used in establishing stratigraphic control for this study are indicated in Figure SD 3. Locations with associated geochronology data are labeled and keyed to Tables SD 1-3.

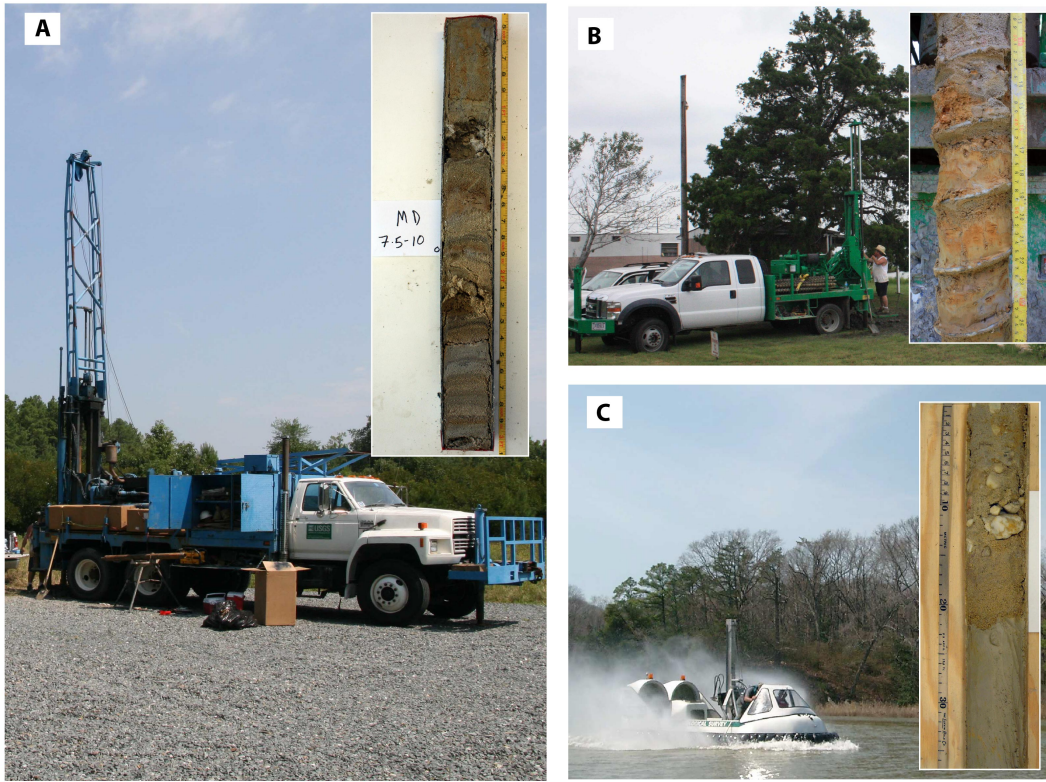


Figure 2-6 (SD1) The three platforms used for drilling the BNWR substrate and examples of sediments retrieved from these methods: A) Truck-mounted hollow-stem auger system; B) truck-mounted solid-stem auger system; C) hovercraft-mounted vibracore system.



Figure 2-7 (SD2) OSL field sampling setup. Painted core liner is shown inside split inner core barrel. Sediment cores were collected and packaged under the tarp for transport to the laboratory without being exposed to light.

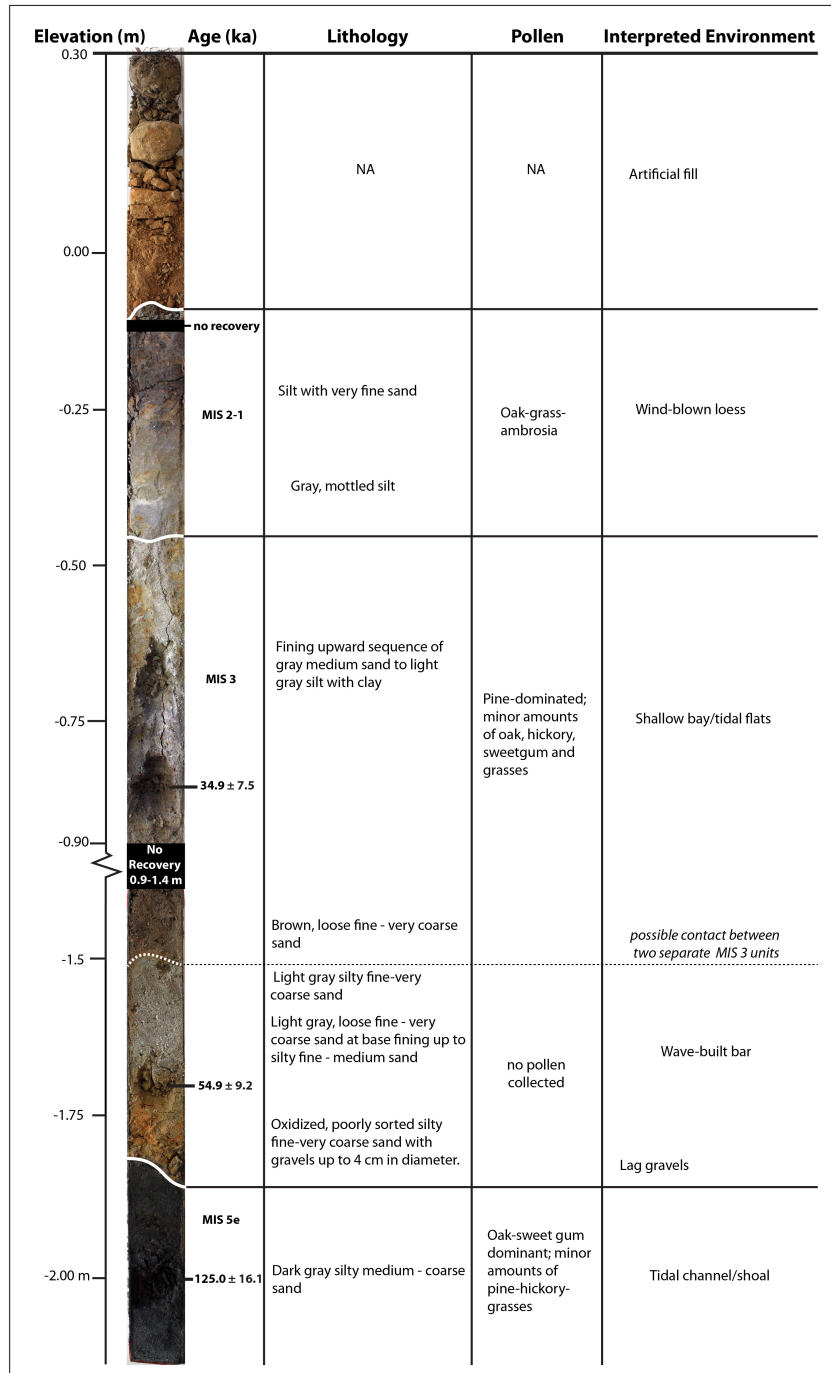


Figure 2-9 (SD4) Sediment core from KD (eastern end of Figure 5).
Note condensed MIS 3 units truncating MIS 5e unit.

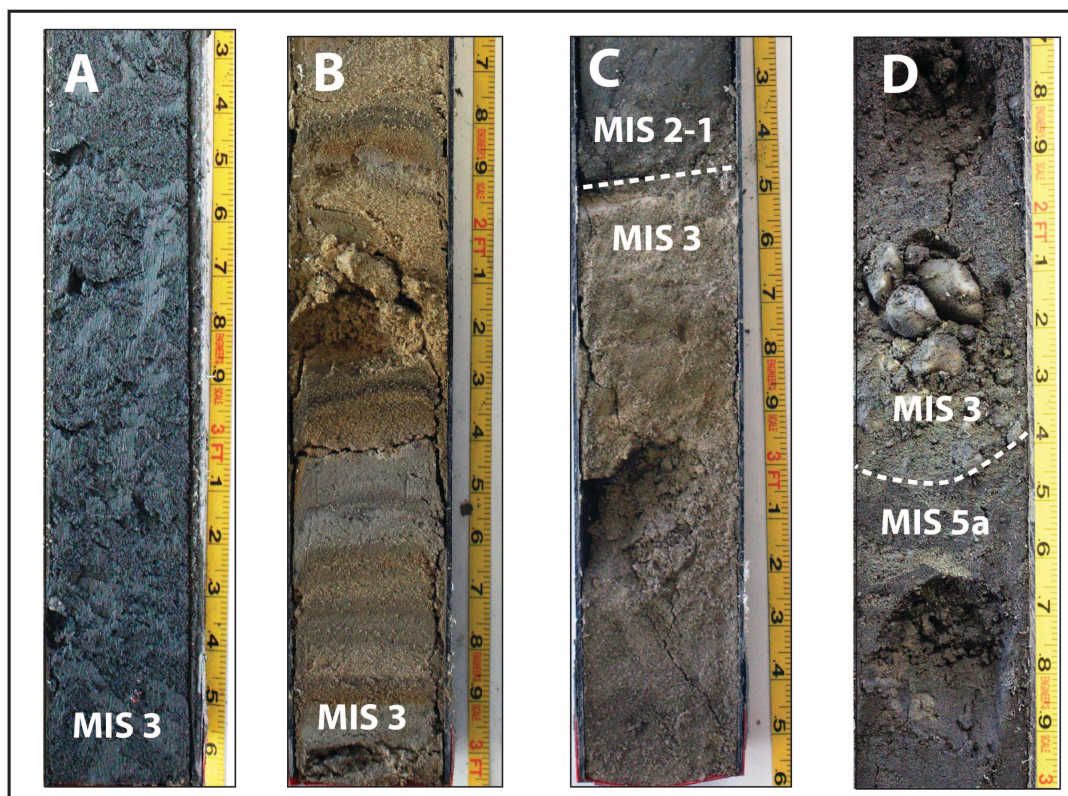


Figure 2-10 (SD5) Examples of MIS 3 deposits cored and sampled in this study.

- A) Heavily burrowed estuarine mud and sand bracketed to MIS 3 by underlying sand at the RS location; B) Sand lenses, mud drapes, and heavy mineral laminae from sand bar feature at the MD location; C) massive, shoreline sand from the top of the scarp at the BNN location; D) MIS 3 shoreline sands truncating MIS 5a estuarine sand with a gravelly contact between at the KEN location.

Cosmogenic radionuclide isochron burial dating

Sample Processing

Sample processing for cosmogenic radionuclide isochron burial dating was completed at the Cosmogenic Radionuclide Laboratory at the University of Vermont according to their standard protocols (Figure SD 6). Individual clasts were sub-sampled from core and auger samples, crushed in a jaw crusher, and ground in a plate grinder to the 90-500 μm fraction. Samples then underwent several acid immersion baths according to Kohl and Nishiizumi (1992) including two 24-hour, 6N HCl baths followed by three 24 hour baths in 0.5% HF, 0.5% HNO₃ solution. The remaining opaque and heavy minerals were removed from the grain size separates (non-clasts) using LST heavy liquid, as these samples tended to be less pure than pulverized clasts. The samples were then dried and tested for purity on an inductively coupled plasma (ICP) optical emission spectrometer. If a sample failed this test, it was treated with one more weak, extended HF-HNO₃ bath.

Once pure, the samples were transferred to the cosmogenic laboratory where they were spiked with ⁹Be, dissolved completely in concentrated HF, and run through cation and anion columns for isolation of Be and Al. The Be and Al fractions were then precipitated as hydroxides, dried off to form small pellets, and packed into targets with Nb or Ag for measurement at either the Lawrence Livermore National Laboratory (¹⁰Be; Rood et al., 2010, 2013) or the Scottish Universities Environmental Research Centre (SUERC) (²⁶Al; Xu et al., 2010, 2014) accelerator mass spectrometers.

DeJong and Bierman were present for Be analyses, and Bierman was present for all Al analyses. Be data were normalized to 07KNSTD3110 with a reported ratio of 2.85×10^{-12} (Nishiizumi et al., 2007). Al data were normalized to the Z92-0222 standard with defined ratio of 4.11×10^{-11} (Xu et al., 2014, 2010).

A blank (Al and Be carrier added with no sample) and an internal standard were processed with each batch. The blanks include the same amount of carrier as samples, so the average measured blank isotopic ratio for all batches in which BNWR samples were processed was subtracted from the measured isotopic ratios of samples (Table SD 2). The long-term average for Be included 4 measurements and yielded an average $^{10}\text{Be}/^9\text{Be}$ ratio of $7.54 \times 10^{-16} \pm 2.11 \times 10^{-16}$. Five measurements for Al yielded an average $^{26}\text{Al}/^{27}\text{Al}$ ratio of $1.60 \times 10^{-15} \pm 9.97 \times 10^{-16}$. The “standard N” of Jull and others (in press) was also run with each batch for inter- and intra-laboratory comparison (Table SD 2).

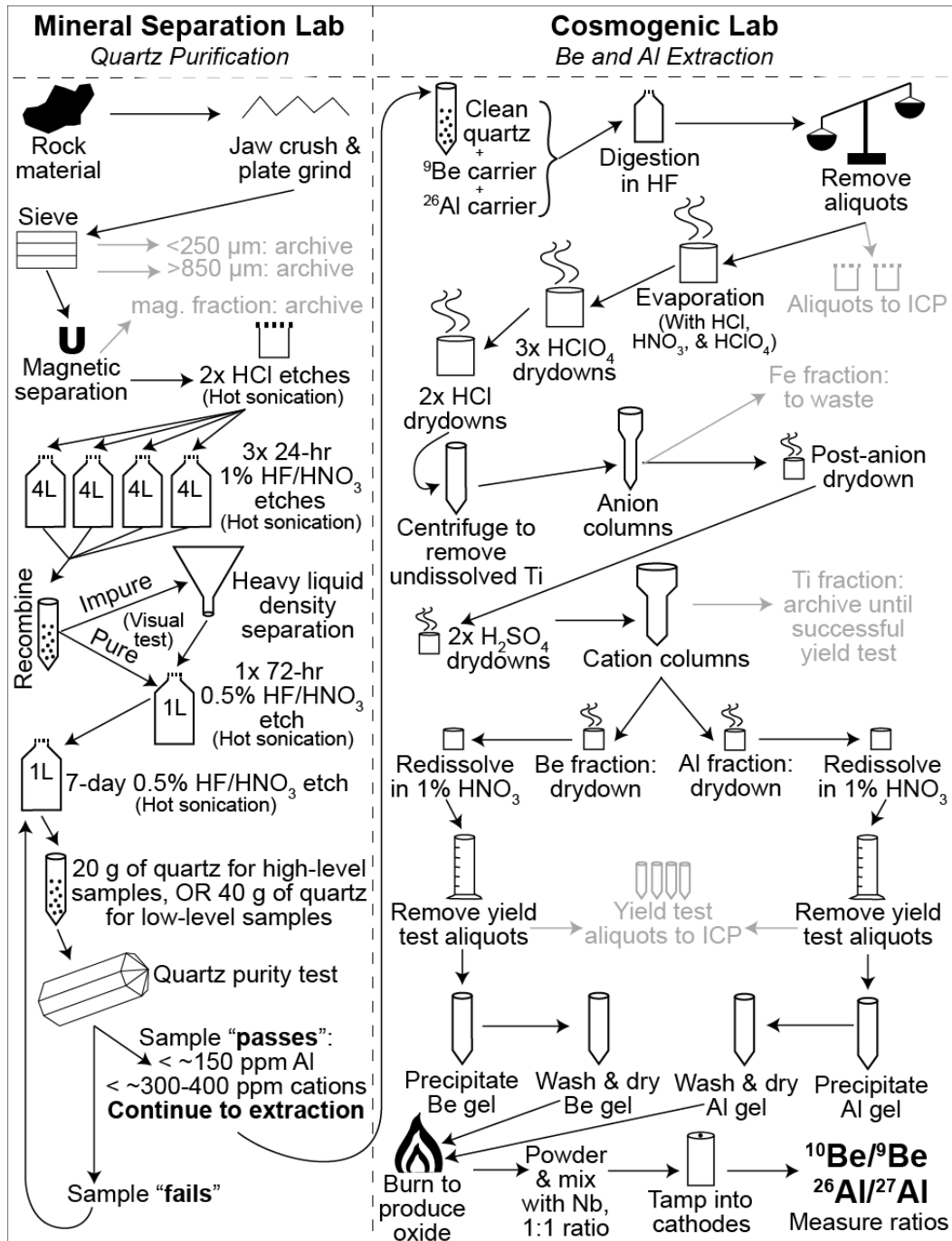


Figure 2-11 (SD6) Flow chart showing full processing steps used in the University of Vermont Cosmogenic Radionuclide Laboratory to purify quartz and extract ²⁶Al and ¹⁰Be from quartz. Grayed steps include tested (spent) or archived material.

Data Reduction

The isochron method enables dating of quartz-bearing material with unknown inherited ^{26}Al and ^{10}Be concentrations and unknown burial histories (Balco and Rovey, 2008). Originally developed to date till-paleosol sequences with samples collected from different depths, a variant of this method involves sampling several (≥ 3) clasts and/or grain size separates from sand fractions that are derived from different settings within the watershed, and thus subject to different exposure histories, but have identical post-burial nuclide production (e.g. they were buried together simultaneously). The ^{26}Al and ^{10}Be concentrations from all clasts and grain size separates form a linear relationship, or an isochron, in $^{26}\text{Al} - ^{10}\text{Be}$ space (Figure SD 6). The slope of this isochron depends on the $^{26}\text{Al} / ^{10}\text{Be}$ production ratio, the ^{26}Al and ^{10}Be decay constants, and on the burial time, but it is independent of the production of nuclides during burial. So if clasts are derived from a wide range of sites with diverse erosion rates, and erosion rates in the watershed are high enough (greater than a few meters per million years) that radioactive decay during transport can be disregarded, the slope of the isochron drawn through ^{26}Al and ^{10}Be concentrations can indicate a burial age for the deposit (Figure SD 7).

The isochron method is appropriate for dating Pleistocene gravels in the BNWR setting. The coarse-grained fluvial deposits that were deposited in discrete stratigraphic horizons derive from a variety of settings within the Susquehanna basin and were buried by sequences of interglacial bay-fill material of variable thickness at unknown rates.

Erosion rates quantified for sub-basins in the Susquehanna watershed at a variety of spatial scales indicate rates that are high enough (4-54 m/My; Reuter, 2005) that radioactive decay does not alter the initial ^{26}Al - ^{10}Be ratios of gravels. Additionally, unpublished amino acid racemization dating on several mollusks recovered in bay fill material overlying gravels in BNWR confirm previous findings (Genau et al., 1994) that the age of the channel gravels on the western Delmarva are within the age range datable by the isochron burial dating method (John Wehmiller, personal communication March, 2012).

The measured ^{26}Al and ^{10}Be concentrations ($N_{10,m}$ and $N_{m,i}$; atoms g^{-1}) in each individual clast or sand fraction are:

$$N_{10,m} = \frac{P_{10}(0)\Lambda}{\varepsilon} e^{-t_b\lambda_{10}} + N_{10,pb} \quad (1)$$

$$(2) \quad N_{26,m} = \frac{P_{26}(0)\Lambda}{\varepsilon} e^{-t_b\lambda_{26}} + N_{26,pb}$$

where $P_i(0)$ is the surface production rate of the nuclide i (atoms $\text{g}^{-1} \text{yr}^{-1}$), Λ is the attenuation length for spallogenic production (generally assumed to be $160 \text{ g}\cdot\text{cm}^{-2}$), ε is the erosion rate ($\text{g}\cdot\text{cm}^{-2}\text{yr}^{-1}$) where the clast originated, λ_i is the decay constant for nuclide i , t_b is the duration of burial (yr), and $N_{26,pb}$ and $N_{10,pb}$ are the post-burial ^{26}Al and ^{10}Be concentrations (atoms g^{-1}) in that clast. Because the upstream erosion rate for any

particular clast is unknown, ε can be eliminated by solving (1) for Λ/ε and substituting into equation (2). The result is a relationship between the measured ^{26}Al and ^{10}Be concentrations for a set of clasts or grain size fractions of sand:

$$N_{26,m} = \frac{P_{26}(0)}{P_{10}(0)} e^{-(\lambda_{26}-\lambda_{10})t_b} N_{10,m} - \frac{P_{26}(0)}{P_{10}(0)} e^{-(\lambda_{26}-\lambda_{10})t_b} N_{10,pb} + N_{26,pb} \quad (3)$$

Equation (3) is the key to the isochron burial dating method because it yields a linear relationship between measured ^{26}Al and ^{10}Be concentrations from clasts that originated from sites with a range of erosion rates, and the slope of the regression line can determine an age of burial independent of assumptions related to subsurface nuclide production rates or the burial history of the clasts (Figure SD 7).

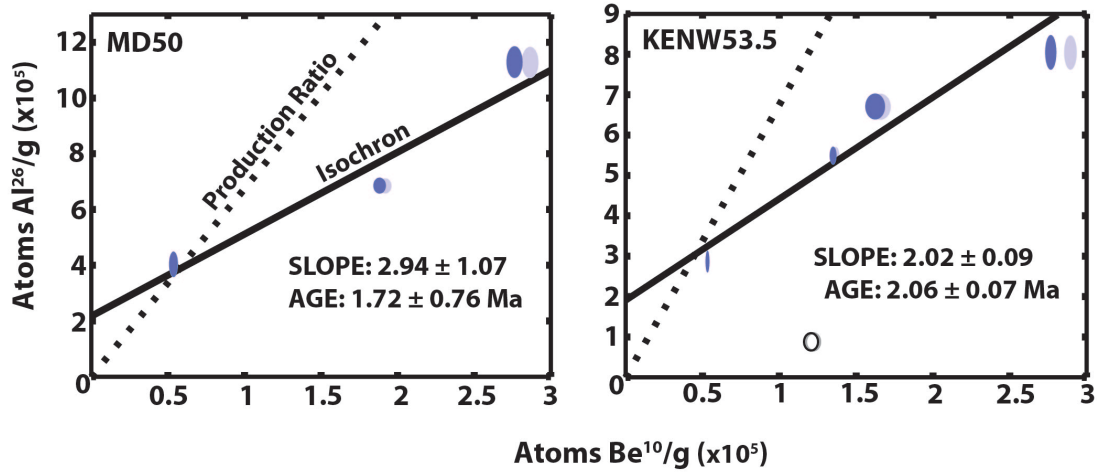


Figure 2-12 (SD7) Isochrons produced for gravels at the base of the Pleistocene stratigraphy at the BNWR (ages in Ma).

Ellipses indicate 68% confidence regions; light ellipses indicate raw data, dark ellipses indicate linearized data (after Granger, 2014). Errors exclude decay constant uncertainties. The gray ellipse in KENW 53.5 indicates prior episode(s) of burial and was not used in age regression.

Table 2-1 (SD1) Cosmogenic nuclide burial age data

Isochron	Location	Depth in core (m)	Sample ID (UVM ID)	Sample Type	¹⁰ Be Concentration ^a (atoms/g)	²⁶ Al Concentration ^b (atoms/g)	²⁶ Al/ ¹⁰ Be	Burial Age ^c (Ma)
MD50	38°26'0.33"N 76°13'45.90"W	15.2	B513BL35	Clast	5.47E+04 ± 2.82E+03	4.03E+05 ± 4.60E+04	7.36 ± 0.92	
			B517BL36	Clast	2.86E+05 ± 5.44E+03	1.13E+06 ± 5.54E+04	3.95 ± 0.21	1.72 ± 0.75
			B525BL37A	Sand (500-850 um)	1.92E+05 ± 4.14E+03	6.86E+05 ± 2.72E+04	3.57 ± 0.16	
KENW53.5	38°26'52.97"N 76°7'26.47"W	16.3	B513BL18	Clast	5.34E+04 ± 1.24E+03	2.88E+05 ± 2.77E+04	5.39 ± 0.53	
			B513BL19	Clast	1.37E+05 ± 2.30E+03	5.52E+05 ± 2.19E+04	4.03 ± 0.17	
			B513BL20	Clast	2.90E+05 ± 4.08E+03	8.09E+05 ± 4.31E+04	2.79 ± 0.15	2.06 ± 0.07
			B556BL41	Clast	1.66E+05 ± 6.82E+03	6.74E+05 ± 3.22E+04	4.05 ± 0.25	
			<i>B517BL21</i>	<i>Clast</i>	<i>1.22E+05 ± 3.28E+03</i>	<i>7.80E+04 ± 1.58E+04</i>	<i>0.64 ± 0.13</i>	
Data associated with background correction								
			Sample ID (UVM ID)		¹⁰ Be/ ²⁷ Al			
			B513BLANK		5.76E-16 ± 1.34E-16	1.56E-15 ± 6.38E-16		
			B517BLANK		5.75E-16 ± 2.52E-16	6.07E-16 ± 4.30E-16		
			B518BLANK		9.87E-16 ± 1.68E-16	3.13E-15 ± 8.68E-16		
			B525BLANK		8.77E-16 ± 1.52E-16	1.89E-15 ± 7.71E-16		
			B521BLANK		NM	NM		
						8.38E-16 ± 4.19E-16		
			Average^d		7.54E-16 ± 2.11E-16	1.60E-15 ± 9.97E-16		
CRONUS Standard^e								
Sample ID (UVM ID)	Quartz (g)	⁹ Be (ug)	²⁷ Al (ug)	¹⁰ Be (atoms/g)	²⁶ Al (atoms/g)	¹⁰ Be/ ²⁶ Al	²⁶ Al/ ²⁷ Al	
B513STAN N	9.57	254.6	3243	2.39E+05 ± 3.73E+03	1.01E+06 ± 3.80E+04	4.25 ± 0.17	1.34E-13 ± 2.10E-15	1.34E-13 ± 5.03E-15
B517STAN N	10.30	253.6	3640	2.26E+05 ± 3.37E+03	1.10E+06 ± 5.75E+04	4.85 ± 0.26	1.37E-13 ± 2.05E-15	1.39E-13 ± 7.29E-15
B518STAN N	11.02	253.6	4016	2.21E+05 ± 3.17E+03	1.07E+06 ± 4.45E+04	4.83 ± 0.21	1.44E-13 ± 2.06E-15	1.31E-13 ± 5.47E-15
^d Measured at the Lawrence Livermore National Laboratory and normalized to the "07KNSTD" standard with an assumed ratio of 2.85 x 10 ⁻¹² . See Nishiizumi and others (2007) ^e Measured at the Scottish Universities Environmental Research Centre and normalized to the Z92-0222 standard with defined ratio of 4.11 x 10 ⁻¹¹ . See Xu and others (2010, 2014) ^f All ages reported to 1 sigma uncertainty ^g Long-term average used in background correction ^h "Standard N" of the CRONUS project. See Jull and others (2013) Italicized sample experienced prior burial and is not included in age calculation NM = not measured								

Optically Stimulated Luminescence

Sample Processing

All samples were opened and processed at the Utah State University Luminescence Laboratory under dim amber safelight conditions. Sample processing followed standard procedures involving sieving, gravity separation and acid treatments with HCl and HF to isolate the quartz component of a narrow grain-size range. We used the coarsest grained sand fractions possible (250-180 μm , except for USU-1211), as suggested for samples deposited subaqueously (Olley et al., 1998). We tested the sensitivity of quartz by ramping stimulating LED's and measuring various components of the OSL signal; the fast component was always $>10\times$ higher than the medium and the slow components, indicating that quartz is appropriate for OSL (Stauch et al., 2012). Several samples exhibit high overdispersion values, but the skew is small enough that partial bleaching is not suspected. The purity of the samples was checked by measurement with infra-red stimulation to detect the presence of feldspar. Sample processing procedures followed those outlined in Aitken (1998) and described in Rittenour et al. (2003, 2005).

Data Reduction

The USU and USGS Luminescence Laboratories follow the latest single-aliquot regenerative-dose (SAR) procedures for dating quartz sand (Murray and Wintle, 2000, 2003; Wintle and Murray, 2006). The SAR protocol includes tests for sensitivity

correction and brackets the equivalent dose (D_e) the sample received during burial by irradiating the sample at five different doses (below, at, and above the D_e , plus a zero dose and a repeated dose to check for recuperation of the signal and sensitivity correction). The resultant data were fit with a saturating exponential curve from which the D_e was calculated from the Central Age Model (CAM) or the Minimum Age Model (MAM) of Galbraith et al. (1999), depending on the distribution of D_e results. In cases where the samples have significant positive skew, ages were calculated based on a MAM (e.g. USU-1211, USU-1222, USU-1226). OSL age is reported at 2σ standard error and is calculated by dividing the D_e (in grays, gy) by the environmental dose rate (gy/ka) that the sample has been exposed to during burial.

Dose-rate calculations were determined by chemical analysis of the U, Th, K and Rb content using ICP-MS and ICP-AES techniques at ALS Chemex, Elko NV and at the USGS Luminescence Laboratory and from conversion factors from Guerin et al. (2011). The contribution of cosmic radiation to the dose rate was calculated using sample depth, elevation, and latitude/longitude following Prescott and Hutton (1994). Dose rates are calculated based on water content, sediment chemistry, and cosmic contribution (Aitken, 1998).

Table 2-2 (SD2) Optically stimulated luminescence ages produced for the BNWR stratigraphy

TABLE SD2. Optically stimulated luminescence ages produced for the BNWR stratigraphy

Sample ID (core depth in meters)	Location	% Water content ^a	K (%) ^b	U (ppm) ^b	Th (ppm) ^b	Cosmic dose (Gy/ka) ^c	Total Dose Rate (Gy/ka)	Equivalent Dose (Gy)	n ^d	Scatter ^e	Age ^f (ka)	Correlation ^h	Description
BELOW SCARP													
<i>Tubman (TD)</i>													
USU-1201 (2.59-2.62)	38°25'5.32"N, 76°11'55.96"W	20 (42)	0.51 ± 0.02	1.60 ± 0.08	6.50 ± 0.33	0.15 ± 0.01	1.19 ± 0.16	36.2 ± 5.56	22 (38)	44.3	30.4 ± 3.4	MIS 2	Basin rim
USU-1202 (2.83-2.87)		13 (36)	0.50 ± 0.02	0.90 ± 0.05	3.00 ± 0.15	0.14 ± 0.01	0.88 ± 0.12	25.9 ± 4.88	14 (20)	46.9	29.4 ± 3.5	MIS 2	Basin rim
USU-1203 (3.35-3.38)		21 (34)	0.60 ± 0.02	0.40 ± 0.10	1.30 ± 0.20	0.14 ± 0.02	0.72 ± 0.10	66.6 ± 7.34	21 (35)	22.6	92.5 ± 14.2	MIS 5a/c	Estuarine sand
<i>Russel Swamp (RS)</i>													
USU-1204 (4.39-4.42)	38°25'10.21"N,	21 (28)	0.65 ± 0.02	0.70 ± 0.08	2.40 ± 0.22	0.12 ± 0.01	0.88 ± 0.12	51.7 ± 9.53	24 (38)	41.2	58.7 ± 12.4	MIS 3	Base of bar sand
USU-1205 (8.56-8.59)	76°14'14.48"W	16 (27)	0.63 ± 0.02	1.10 ± 0.06	2.60 ± 0.13	0.07 ± 0.01	0.97 ± 0.04	39.5 ± 3.79	12 (27)	55.8	40.7 ± 4.2	MIS 3	Base of middle unit
USU-1206 (8.90-8.93)		18 (40)	0.46 ± 0.01	0.40 ± 0.02	1.10 ± 0.06	0.07 ± 0.01	0.59 ± 0.03	41.4 ± 7.29	20 (24)	60.8	70.2 ± 12.8	MIS 2	Top lower unit
<i>Moneystamp (MD)</i>													
USU-1207 (2.50-2.53)	38°26'0.33"N,	14 (26)	0.59 ± 0.02	0.9 ± 0.05	3.45 ± 0.17	0.15 ± 0.01	1.04 ± 0.07	26.9 ± 4.57	12 (20)	44.0	25.8 ± 4.7	MIS 2	Basin rim
USU-1208 (2.77-2.80)	76°13'45.90"W	9 (27)	0.38 ± 0.1	0.7 ± 0.04	1.60 ± 0.08	0.15 ± 0.01	0.65 ± 0.08	40.1 ± 5.68	23 (42)	28.7	62.0 ± 10.8	Early MIS 3	Bar sand
<i>Parsons (PD)</i>													
USU-1209 (2.68-2.71)	38°28'5.60"N,	10 (36)	0.96 ± 0.03	1.40 ± 0.07	4.90 ± 0.25	0.15 ± 0.01	1.04 ± 0.14	46.3 ± 6.63	20 (43)	27.4	44.7 ± 7.9	MIS 3	Top bar sand
USU-1210 (4.42-4.36)	76°15'46.91"W	21 (38)	0.63 ± 0.03	1.10 ± 0.06	2.35 ± 0.12	0.12 ± 0.01	0.94 ± 0.06	42.8 ± 5.56	14 (20)	34.2	45.5 ± 6.5	MIS 3	Bottom bar sand
<i>Reber (RD)</i>													
USU-1211 (1.46-1.50)	38°22'56.65"N,	15 (27)	1.26 ± 0.03	2.8 ± 0.20	10.1 ± 0.90	0.17 ± 0.02	2.33 ± 0.38	83.92 ± 12.38	18 (60)*	18.7	36.0 ± 6.8	Late MIS 3	Top bar sand
USU-1212 (2.47-2.50)	76°14'27.74"W	18 (27)	0.79 ± 0.04	1.65 ± 0.09	6.20 ± 0.31	0.15 ± 0.01	1.52 ± 0.10	57.6 ± 8.87	9 (15)	25.9	37.9 ± 6.4	Late MIS 3	Bottom bar sand
USU-1213 (8.66-8.67)		17 (26)	0.54 ± 0.01	1.1 ± 0.10	1.70 ± 0.20	0.08 ± 0.01	0.81 ± 0.12	36.27 ± 7.81	19 (43)	40.4	44.8 ± 10.9	MIS 3	Estuarine sand
<i>Robbins (ROB)</i>													
USU-1221 (280-2.83)	38°22'45.64"N, 76°4'35.72"W	14 (25)	0.51 ± 0.02	1.30 ± 0.07	3.65 ± 0.18	0.15 ± 0.01	0.97 ± 0.14	66.7 ± 12.7	20 (37)	37.2	68.7 ± 15.2	MIS 5a/3	Bar sand
<i>Maple Dam Road (MDRN)</i>													
USU-1215 (1.65-1.68)	38°25'0.24"N,	14 (19)	0.32 ± 0.01	0.5 ± 0.03	1.5 ± 0.08	0.17 ± 0.01	0.65 ± 0.04	24.2 ± 3.42	11 (15)	24.9	37.4 ± 5.6	Late MIS 3	Bar sand
USU-1216 (2.04-2.07)	76°3'14.22"W	17 (22)	0.35 ± 0.01	0.2 ± 0.10	0.60 ± 0.20	0.16 ± 0.02	0.50 ± 0.08	27.6 ± 2.81	20 (29)	15.3	55.1 ± 8.6	MIS 3	Bar sand
<i>Kuehnle (KD)</i>													
USU-1218 (1.13-1.16)	38°25'41.57"N,	10 (34)	0.20 ± 0.1	0.6 ± 0.03	2.15 ± 0.11	0.18 ± 0.01	0.58 ± 0.04	20.2 ± 4.04	6 (10)	26.7	34.9 ± 7.5	Late MIS 3	Bar sand
USU-1219 (1.98-2.01)	76°2'41.53"W	14 (24)	0.51 ± 0.01	0.80 ± 0.10	2.20 ± 0.20	0.16 ± 0.02	0.84 ± 0.10	45.82 ± 6.24	21 (50)	25.7	54.9 ± 9.2	MIS 3	Bar sand
USU-1220 (2.32-2.35)		20 (28)	0.42 ± 0.01	1.2 ± 0.06	2.4 ± 0.12	0.15 ± 0.01	0.88 ± 0.05	110 ± 12.5	15 (24)	51.5	125.0 ± 16.1	MIS 5e	Estuarine sand
<i>Harpers C (HC)</i>													
USU-266 (4.29-4.31)	38°24'54.63"N,	27.3 ^f	0.28±0.01	0.6±0.1	3.2±0.3	0.12±0.01	0.65 ± 0.06	27.9 ± 1.9	25 (34)	12.7	43.2 ± 5.9	MIS 3	Estuarine sand
USU-265 (4.59-5.61)	76°4'57.31"W	27.3 ^f	0.28±0.01	0.6±0.1	2.7±0.2	0.12±0.01	0.61 ± 0.05	28.3 ± 2.5	25 (32)	17.1	46.1 ± 6.8	MIS 3	Estuarine sand
ABOVE SCARP													
<i>Kentuck (KEN)</i>													
USU-1222 (1.92-1.95)		14 (25)	0.27 ± 0.01	0.90 ± 0.10	2.7 ± 0.20	0.16 ± 0.02	0.70 ± 0.08	28.4 ± 5.38	21 (44)*	22.6	40.5 ± 8.7	MIS 3	Shoreline sand
USU-1228 (3.22-3.23)		15 (34)	0.73 ± 0.02	1.90 ± 0.10	5.3 ± 0.27	0.14 ± 0.01	1.40 ± 0.09	68.6 ± 8.92	22 (35)	30.8	49.0 ± 7.0	MIS 3	Shoreline sand
USU-1223 (3.29-3.32)	38°27'18.03"N,	15 (34)	0.89 ± 0.03	2.35 ± 0.12	6.45 ± 0.32	0.14 ± 0.01	1.67 ± 0.11	77.7 ± 6.39	11 (20)	32.8	46.5 ± 5.0	MIS 3	Shoreline sand
USU-1224 (5.43-5.46)	76°6'19.98"W	18 (27)	0.43 ± 0.01	0.80 ± 0.04	2.0 ± 0.10	0.10 ± 0.01	0.74 ± 0.05	38.9 ± 5.52	9 (10)	11.7	52.6 ± 8.3	MIS 3	Base transgression
USU-1225 (5.70-5.73)		20 (28)	0.5 ± 0.10	1.0 ± 0.10	2.7 ± 0.20	0.10 ± 0.01	0.89 ± 0.14	64.0 ± 9.97	24 (52)	30.7	75.5 ± 14.3	MIS 5a	Estuarine sand
<i>Buttons Neck (BNN)</i>													
USU-1226 (1.22-1.25)	38°27'52.42"N,	7 (25)	0.24 ± 0.01	0.50 ± 0.10	1.8 ± 0.20	0.18 ± 0.02	0.54 ± 0.12	26.93 ± 3.04	35 (46)*	16.4	49.8 ± 8.8	MIS 3	Shoreline sand
USU-1227 (2.35-2.38)	76°10'20.37"W	15 (51)	0.29 ± 0.01	0.83 ± 0.04	2.3 ± 0.12	0.15 ± 0.01	0.64 ± 0.07	33.4 ± 3.34	17 (26)	53.3	52.3 ± 6.3	MIS 3	Base transgression

^aIn situ moisture content, with figures in parentheses indicating saturation values (in weight %). Ages calculated using approximately 70% of saturation values.

^bAnalyses obtained using inductively coupled plasma mass spectrometry (ICP-MS). All errors were obtained with calibration standards (i.e. K% error = 3%, U and Th ppm error = 5%).

^cCosmic doses and attenuation with depth were calculated using the methods of Prescott and Hutton (1994). See text for details.

^dNumber of replicated equivalent dose (De) estimates used to calculate the equivalent dose. Figures in parentheses indicate total number of measurements included in calculating the equivalent dose and age using the central age model (CAM), while the * represents the minimum age model (MAM).

^eDefined as "over-dispersion" of the De values. Obtained by taking the average over the standard deviation. Values >20% are considered to be poorly bleached, mixed, or bioturbated sediments.

^fDose rate and age for fine-grained 250-180 micron sized quartz. Exponential + linear fit used on equivalent doses; errors to two sigma; ages and errors rounded.

^g70% of average field capacity moisture content from other samples used for dose-rate calculation

^hInterpreted MIS correlations based on highest sea level within 2-sigma sample error range based on proxies indicated in Figure 3 of manuscript

ⁱFurther work is in progress on this sample to identify stratigraphic reversal between this sample and the sample above

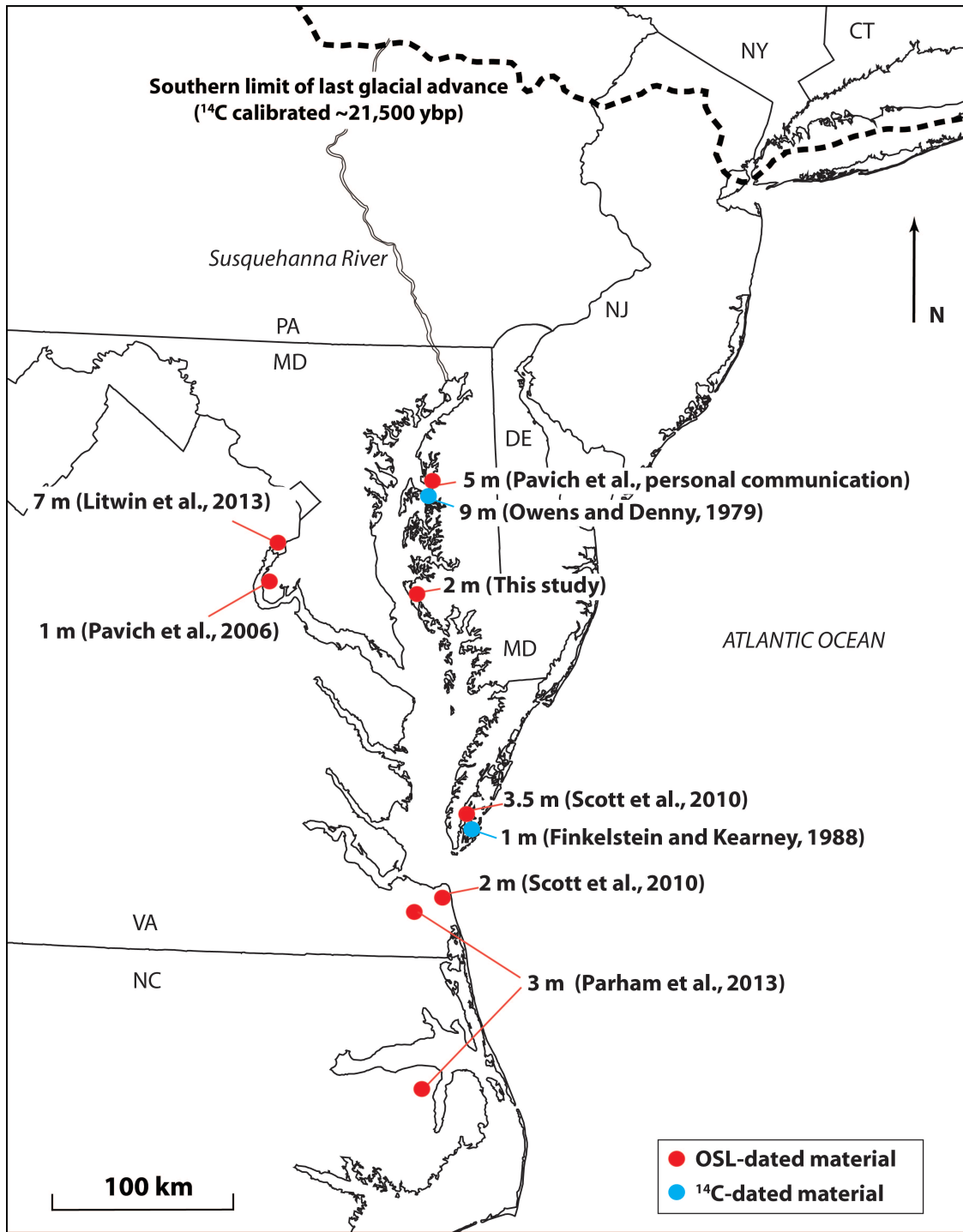


Figure 2-13 (SD8) Variability in surface elevations of MIS 3 deposits dated using both OSL and ¹⁴C dating. To the knowledge of the authors, no emerged MIS 3 units have been dated and reported in the literature north or south of this region.

Table 2-3 (SD3) Radiocarbon ages produced for the Holocene stratigraphy of the BNWR

TABLE SD3. Radiocarbon ages produced for the Holocene stratigraphy of the BNWR

USGS ID	Core	Location	Elevation (m)	¹⁴ C AGE ^a	Calibrated age (yBP) ^b	Description
WW6532			-3.7	--	Modern	Plant material; base of peat
WW6533	Barbadoes		-3.8	863 ± 43	691-907	Plant material; top of silt below peat
WW6535	Island (BI)	38°24'45.98"N 76° 5'16.85"W	-7.8	1584 ± 35	1400-1550	Plant material in silt
WW6536			-8.0	2087 ± 37	1950-2149	Plant material in silt
WW6537			-8.3	1921 ± 36	1740-1949	Plant material in silt
WW6539	BW Transect 5		-3.9	--	Modern	Plant material; base of peat
WW6540 ^c	(BWT5)	38°25'12.60"N 76° 5'49.78"W	-8.4	129 ± 34	8-277	Plant material in silt
WW6541			-8.6	4660 ± 40	5310-5572	Plant material in silt

^aStandard ¹⁴C age (yr) using the Libby half life of 5568 years

^bCalibrated to calendar years before present (1950) using the INTCAL 13 curve (Reimer et al., 2013) in CALIB 7.0 (Stuiver and Reimer, 1993), full 2-sigma range.

Ages were rounded to 102 years and expressed as "ka" for consistency in Figure 5.

^cSample assumed to be out of place and drug in during drilling

References cited (Supplementary Data)

- Aitken, M.J. 1998: An Introduction to Optical Dating: The dating of Quaternary sediments by the use of photon-stimulated luminescence. New York, Oxford University Press, 267 pp.
- Balco, G., and Rovey, C. W., 2008, An isochron method for cosmogenic-nuclide dating of buried soils and sediments: *American Journal of Science*, v. 308, no. 10, p. 1083-1114.
- Finkelstein, K. F., and Kearney, M. S., 1988, Late Pleistocene barrier-island sequence along the southern Delmarva Peninsula: Implications for middle Wisconsin sea levels: *Geology*, v. 16, p. 41-45.
- Galbraith, R.F., Roberts, R.G., Laslett, G.M., Yoshida, H., Olee, J.M., 1999. Optical dating of single and multiple grains of quartz from Jinmium Rock Shelter, northern Australia: Part I, experimental design and statistical models: *Archaeometry*, v. 41, p. 339-364.
- Genau, R. B., Madsen, J. A., McGeary, S., and Wehmiller, J. F., 1994, Seismic-Reflection Identification of Susquehanna River Paleochannels on the Mid-Atlantic Coastal Plain: *Quaternary Research*, v. 42, p. 166-174.
- Granger, D. E., 2014, Cosmogenic Nuclide Burial Dating in Archaeology and Paleoanthropology: *Treatise on Geochemistry*, v. 14, p. 81-97.
- Guerin, G., Mercier, N., Adamiec, G., 2011. Dose-rate conversion factors: update: *Ancient TL*, v. 29, p. 5-8.

- Jull, A. J. T., Scott, E. M., and Bierman, P., in press, The CRONUS-Earth inter-comparison for cosmogenic isotope analysis: *Quaternary Geochronology*.
- Kohl, C. P., and Nishiizumi, K., 1992, Chemical isolation of quartz for measurement of in-situ-produced cosmogenic nuclides: *Geochimica et Cosmochimica Acta*, v. 56, p. 3583-3587.
- Litwin, R. J., Smoot, J. P., Pavich, M. J., Markewich, H. W., Brook, G., and Durika, N. J., 2013, 100,000-year-long terrestrial record of millennial-scale linkage between eastern North American mid-latitude paleovegetation shifts and Greenland ice-core oxygen isotope trends: *Quaternary Research*, v. 80, no. 2, p. 291-315.
- Mallinson, D., Burdette, K., Mahan, S., and Brook, G., 2008, Optically stimulated luminescence age controls on late Pleistocene and Holocene coastal lithosomes, North Carolina, USA: *Quaternary Research*, v. 69, no. 1, p. 97-109.
- Murray, A.S., Wintle, A.G., 2000. Luminescence dating of quartz using an improved single aliquot regenerative-dose protocol: *Radiation Measurements* v. 32, p. 57-73.
- Murray, A.S., Wintle, A.G., 2003. The single aliquot regenerative dose protocol: potential for improvements in reliability: *Radiation Measurements* v. 37, p. 377-381.
- Nishiizumi, K., Imamura, M., Caffee, M. W., Southon, J. R., Finkel, R. C., and McAninch, J., 2007, Absolute calibration of ^{10}Be AMS standards: *Nuclear*

Instruments and Methods in Physics Research Section B: Beam Interactions with Materials and Atoms, v. 258, no. 2, p. 403-413.

Olley, J. M., Caitcheon, G. G., and Murray, A. S., 1998, The distribution of apparent dose as determined by optically stimulated luminescence in small aliquots of fluvial quartz: implications for dating young sediments: *Quaternary Science Reviews*, v. 17, p. 1033-1040.

Owens, J. P., and Denny, C. S., 1979, Upper Cenozoic deposits of the Central Delmarva Peninsula, Maryland and Delaware, USGS Professional Paper 1067-A: Washington, DC, 27 pp.

Parham, P. R., Riggs, S. R., Culver, S. J., Mallinson, D. J., Jack Rink, W., and Burdette, K., 2013, Quaternary coastal lithofacies, sequence development and stratigraphy in a passive margin setting, North Carolina and Virginia, USA: *Sedimentology*, v. 60, no. 2, p. 503-547.

Pavich, M. J., and Markewich, H. W., 2006, Significance of Kent Island Formation to geomorphic history of the Mid-Atlantic region: *Geological Society of America, Abstracts with programs* 38, p. 226.

Prescott, J. R., Hutton, J.T., 1994. Cosmic ray contributions to dose rates for luminescence and ESR dating: *Radiation Measurements* 23, 497-500.

Reimer, P. J., Bard, E., Bayliss, A., Beck, J. W., Blackwell, P. G., Bronk Ramsey, C., Buck, C. E., Cheng, H., Edwards, R. L., Friedrich, M., Grootes, P. M., Guilderson, T. P., Haflidason, H., Hajdas, I., Hatté, C., Heaton, T. J., Hoffmann,

- D. L., Hogg, A. G., Hughen, K. A., Kaiser, K. F., Kromer, B., Manning, S. W., Niu, M., Reimer, R. W., Richards, D. A., Scott, E. M., Southon, J. R., Staff, R. A., Turney, C. S. M., and van der Plicht, J., 2013, INTCAL13 and marine13 radiocarbon age calibration curves 0–50,000 years CAL BP: *Radiocarbon*, v. 55, no. 4, p. 1869-1887.
- Reuter, J., 2005, Erosion rates and pattern inferred from cosmogenic ^{10}Be in the Susquehanna River Basin. Unpublished Masters thesis, University of Vermont, 160 p.
- Rittenour, T.M., Goble, R.J., Blum, M.D., 2003, An Optical Age Chronology of Fluvial Deposits in the Northern Lower Mississippi Valley: *Quaternary Science Reviews*, v. 22, p. 1105-1110.
- Rittenour, T.M., Goble, R.J., Blum, M.D., 2005, Development of an OSL chronology for late Pleistocene channel belts in the lower Mississippi valley: *Quaternary Science Reviews*, v.24, p.2539-2554.
- Rood, D.H., Hall, S., Guilderson, T.P., Finkel, R.C., Brown, T.A., 2010, Challenges and opportunities in high-precision Be-10 measurements at CAMS, *Nuclear Instruments and Methods B: Beam Interactions with Materials and Atoms*, v. 268, no. 7-8, p. 730-732.
- Rood, D.H., Brown, T.A., Finkel, R.C., Guilderson, T.P., 2013, Poisson and non-Poisson uncertainty estimations of $^{10}\text{Be}/^9\text{Be}$ measurements at LLNL–CAMS, *Nuclear Instruments and Methods B: Beam Interactions with Materials and Atoms*, v.

294, p. 426-429.

- Scott, T. W., Swift, D. J. P., Whittecar, G. R., and Brook, G. A., 2010, Glacioisostatic influences on Virginia's late Pleistocene coastal plain deposits: *Geomorphology*, v. 116, no. 1-2, p. 175-188.
- Stauch, G., Ijmker, J., Pötsch, S., Zhao, H., Hilgers, A., Diekmann, B., Dietze, E., Hartmann, K., Opitz, S., Wünnemann, B., and Lehmkuhl, F., 2012, Aeolian sediments on the north-eastern Tibetan Plateau: *Quaternary Science Reviews*, v. 57, p. 71-84.
- Stuiver, M., and Reimer, P. J., 1993, Extended ^{14}C database and revised CALIB radiocarbon calibration program: *Radiocarbon* v. 35, p. 215-230.
- Wintle, A.G. Murray, A.S., 2006, A review of quartz optically stimulated luminescence characteristics and their relevance in single-aliquot regenerative protocols: *Radiation Measurements*, v. 41, p. 369-391.
- Xu, S., Dougans, A.B., Freeman, S.P.H.T., Schnabel, C., Wilcken, K.M, 2010, Improved ^{10}Be and ^{26}Al -AMS with a 5 MV spectrometer: *Nuclear Instruments and Methods in Physics Research B*, v. 268, p. 736–738.
- Xu, S., Freeman, S.P.H.T., Rood, D.H., Shanks, R.P., 2014, ^{26}Al interferences in accelerator mass spectrometry measurements, *Nuclear Instruments and Methods in Physics Research B*, v. 333, p. 42-45.

**CHAPTER 3: OPTIMIZING COSMOGENIC BURIAL ISOCHRONS USING
MUON-INCLUSIVE SIMPLE BURIAL DATING**

*Submitted for publication in Nuclear Instruments and Methods in Physics Research
Section B: Beam Interactions with Materials and Atoms*

Benjamin D. DeJong, U.S. Geological Survey, Reston, VA, 20192, and
Rubenstein School of the Environment and Natural Resources, University of Vermont,
Burlington, VT 05405, bdejong@usgs.gov, 435-760-5440

Alan J. Hidy, Center for Accelerator Mass Spectrometry, Lawrence Livermore National
Laboratory, Livermore, CA 94550, hidy3@llnl.gov, 925-423-8877

Paul R. Bierman, Geology Department and Rubenstein School of the Environment and
Natural Resources, University of Vermont, Burlington, VT, 05405, pbierman@uvm.edu,
802-238-6826

3.1. Abstract

Isochron burial dating with cosmogenic nuclides presents new opportunities for determining the deposition age of Plio-Pleistocene gravels. The method uses paired measurements of ^{26}Al and ^{10}Be from individual clasts and is able to generate ages even if burial histories are complex and poorly constrained. Critical to the isochron method is the assumption that gravel is deposited with a predictable $^{26}\text{Al}/^{10}\text{Be}$ ratio, based on near-surface production rates, that then decreases due to radioactive decay after burial. If all clasts are collected from the same depth in a deposit, they share the same history of post-burial production and decay. Because decay constants are known, a line regressed through a bivariate plot of ^{26}Al and ^{10}Be concentrations represents an isochron, the slope of which is related to burial duration. The method is ideal when samples are numerous (≥ 5 data points) and yield a spread of concentrations such that linear regression can resolve a meaningful slope, but logistics, costs, and site geology can preclude such ideal datasets. Additionally, it can be difficult to identify and reject samples that may have been deposited with nuclide ratios resulting from prior burial that have the potential to contaminate isochron age estimates. Here we present a methodology for checking the integrity of small isochron datasets (≤ 4 samples) by co-applying a muon-inclusive simple burial dating algorithm that scales muogenic production with shielding mass (cover density * depth). This analysis uses the same ^{26}Al and ^{10}Be concentrations as the isochron method, but incorporates assumptions based on site geology to independently validate and inform isochron results. We use two examples to demonstrate how these

burial calculations can increase confidence in isochron results, show when the isochron method is inappropriately applied, and provide criteria for rejection of data points in isochrons.

3.2. Introduction

Paired cosmogenic nuclides are used in different geologic settings to help constrain the burial age of deposits (Granger and Muzikar, 2001). The most common nuclides used in burial dating are ^{26}Al and ^{10}Be , which are produced with a predictable ratio at Earth's surface (nominally 6.75:1 for spallogenic production at sea level [Nishiizumi et al., 1986, 2007], but note recent suggestions that the ratio may be 5% higher and altitude-dependent [Argento et al., 2013; Lifton et al., 2014]). Once sediment is buried, production greatly diminishes; ^{26}Al and ^{10}Be decay with different half-lives so that the measured ratio of the two isotopes can be used as a burial clock (Klein et al., 1986).

The classic, or “simple” cosmogenic nuclide ^{26}Al - ^{10}Be burial dating method assumes a two-stage transport-burial history of material that 1) is exposed in one event during which ^{26}Al and ^{10}Be accumulate at the surface production ratio of these isotopes, and 2) is then buried deeply enough to shield it from further cosmic ray flux (Granger et al., 2001). This method works best when applied to sediments deposited in caves (Granger et al., 1997; Granger, 2006) or in deep lakes (Balco et al., 2013) where overburden is sufficient such that the cosmic flux at depth is negligible and post-

depositional production can be ignored. But many samples do not conform to this relatively simple, two-stage history, because they are incompletely buried such that post-depositional (dominantly muogenic) production must be modeled (Hidy et al., 2013).

The isochron burial dating method deals with more complex burial histories by explicitly separating postburial production from isotope concentrations inherited at the time of burial for an assemblage of samples buried together (Balco and Rovey, 2008; Granger, 2014). Clasts and sand fractions are likely sourced from different locations in the catchment landscape, and thus were subject to different pre-burial exposure histories. However, all clasts and sand share a similar post-burial nuclide production history and burial age because they were deposited simultaneously at the same depth. If all clasts and sand fractions are derived from sites with a wide range of erosion rates that are high enough (greater than a few meters per million years) such that radioactive decay during exposure and transport can be disregarded, so that they are deposited with an $^{26}\text{Al}/^{10}\text{Be}$ ratio similar to the spallogenic production ratio, then they will form a linear relationship, or an isochron, in a bivariate plot of ^{26}Al and ^{10}Be concentrations. The isochron age is indicated by the slope, which depends only on the $^{26}\text{Al}/^{10}\text{Be}$ ratio at deposition, the ^{26}Al and ^{10}Be decay constants, and the burial time, but it is independent of the postburial component, which is indicated by the intercept of the isochron.

Isochron burial dating is becoming an important tool in solving a variety of previously intractable Earth surface processes questions (e.g. Balco and Rovey, 2010; Erlanger et al., 2012; Balco et al., 2013; Granger, 2014), but the reliability of the method

when applied to small datasets, such as those produced from mass-limited sediment cores, is uncertain. In instances where just 3-4 clasts are available for sampling, age regression may be complicated by a minimal spread in nuclide concentrations, or by line-fitting that introduces uncertainties greater than that of individual measurements. Additionally, clasts that were recycled from older deposits into sampled gravels may contain “inherited” ^{26}Al and ^{10}Be concentrations from an unknown and potentially complex prior history of exposure and burial. These clasts commonly have relatively low $^{26}\text{Al}/^{10}\text{Be}$ ratios, which are easily identified in larger datasets and rejected as outliers (e.g. Erlanger et al., 2012), but may be difficult to identify in smaller datasets.

These challenges suggest the importance of additional information when evaluating isochron ages regressed from few (≤ 4) data points. Simple burial analysis that explicitly considers post-burial muogenic production, a parameter on which the isochron age regression does not depend, can provide an additional estimate for burial age, help identify outlying data, and increase confidence in isochrons with few data points. Here, we present a simple method of checking the integrity of isochrons by simultaneously calculating muon-inclusive simple burial ages for individual clasts included in isochrons. Because this method incorporates estimates for post-burial production, it provides age estimates that rely on different assumptions and are thus in part independent from those determined using the isochron method.

3.3. Methods

To prove the concept of joint isochron-simple burial analysis, we apply both methods to gravels sampled from 2 deposits on the eastern shore of Chesapeake Bay on the mid-Atlantic coast of the United States (figure 3-1). The Pleistocene stratigraphy in the region is defined by deep (~20-60 m) paleochannels that incised and back-filled repeatedly from major sea-level fluctuations (Colman et al., 1990). Samples were collected from ~11 cm diameter boreholes, with limited clasts available at each horizon. We first analyze cosmogenic data for suites of clasts and grain-size separates from the same depth using the isochron method of Granger (2014), which uses a linearization factor to improve regression of clasts derived from sources with low erosion rates where $^{26}\text{Al}/^{10}\text{Be}$ ratios at deposition are lower than 6.75 (samples that plot far to the right of the “erosion banana” in figure 3-2).

We then analyze each clast individually using a muon-inclusive simple burial approach (sensu Hidy, 2013), which estimates the muogenic component from the burial mass depth (depth times shielding material density) based on bulk density estimates from the lithology of overburden. The stacked nature of cut-fill deposits in the field area (figure 3-1) suggests a complex history of cutting and filling, meaning effective burial depths likely changed over time, which is why the isochron method is preferred. However, we assume that each subsequent incised valley was back-filled with similar estuarine sediments, so that the overburden today is representative of the long-term average. And since all samples share a similar burial history, inaccuracy of the chosen

integrated mass-depth estimate is systematically shared by all clasts and grain size separates. In general, the simpler the overlying stratigraphy, the simpler the history of burial, and thus the more accurate the estimate of muogenic production.

If the assumptions regarding the pre-burial surface source and mass depth since burial are correct, then all samples must plot within the contoured region of the burial plot (figure 3-2). Otherwise, they are in a “forbidden zone” (gray area of figure 3-2), and either one or both of these assumptions have been violated, or there is a problem with the measurement itself. The most likely explanation for samples plotting in the forbidden zone is a poor estimate of the time-averaged post-depositional production rate; however, in some cases a clast that plots well within the forbidden zone may be explained by isotope concentrations in part inherited from a previous burial event. Because all samples share any inaccuracy in the initial estimate for muon production, in some instances the location of one sample in relation to the muogenic production line can help constrain the degree to which one can modify the initial muogenic production rate estimate. For example, if a sample plots near this line in the contoured burial region, the estimate for muogenic production can be increased, thus shifting the burial contours right, only until that sample intersects the production curve, but not beyond this limit so as to prevent forcing that sample into the forbidden zone.

Since this muon-inclusive approach yields maximum apparent burial ages, it follows that the sample with the lowest inherited burial signal will indicate the youngest and most accurate individual burial age. However, because the calculated post-

depositional muon production may be incorrect, which will change apparent burial ages more significantly for lower concentration samples (note larger vertical spacing between age contours for a sample that experienced 0.1 Ma of surface exposure versus one that experienced 0.01 Ma of exposure), we first consider the sample with the highest ^{10}Be concentration. If this sample yields the youngest apparent burial age, then this age is the best estimate from the simple burial method. If there are samples with younger apparent ages, then we attempt to perturb the assumed post-depositional muon production rate to align these samples to the burial contour that runs through the highest concentration sample ellipse. If this cannot be done, then we assume that the highest concentration sample has experienced a prior episode of burial, and we analyze the sample with the next-highest concentration, and so forth, until the sample with the youngest maximum apparent burial age is found that can be imposed on all other samples by perturbing the assumed post-depositional production rate. This youngest maximum apparent burial age is considered the “best” estimate from simple burial and is then compared with the isochron age.

3.4. Results

Two isochrons clearly illustrate the utility of our method as shown in figure 3-3 with relevant data presented in Table 3-1. For sample set KENW53.5, four clasts appear to lie on an isochron, while one clast is significantly below the line (figure 3-3a). The isochron age from a 4-clast regression that excludes the low-ratio point is 2.06 ± 0.07 Ma

(all errors presented as 1σ). Following the methodology indicated above, we use the highest concentration clast for simple burial to calculate an age of $2.22^{+0.17}_{-0.15}$ Ma (figure 3-3b; probability distribution function inset). This youngest maximum apparent burial age can be imposed upon the lower concentration samples if we slightly increase our initial estimate for the muogenic production rate (which would shift burial contours to the right in figure 3-3b). Thus, isochron and simple burial ages agree within 1σ error for this deposit. Additionally, the outlier sample in the isochron of KENW53.5 falls well within the forbidden zone, which suggests it was deposited with a $^{26}\text{Al}/^{10}\text{Be}$ ratio lower than the others because it had a complex burial and exposure history prior to deposition. Post-burial nuclide production analysis thus independently supports our rejection of this data point from the isochron age regression.

For sample site MT39.5, four clasts were available for measurement, all of which appear to lie near an isochron (gray line, figure 3-3c). The age calculated from regression of these 4 points is 0.58 ± 0.08 Ma. Checking this age using simple burial, however, we find that one sample lies outside the contoured region and in the “forbidden zone” (figure 3d; note this sample plots far to the right in the inset probability distribution plots). Again, the low $^{26}\text{Al}/^{10}\text{Be}$ ratio suggests that this clast had a complex exposure history prior to deposition. The clast with the highest nuclide concentration indicates an apparent burial age of $0.94^{+0.19}_{-0.12}$ Ma. This age could be imposed upon samples with lower concentrations if the initial estimate for the muogenic production was slightly increased. However, the proximity of the clast in the forbidden zone to the muogenic exposure

curve suggests that we slightly overestimated the muogenic production, and so the initial estimate for muogenic production cannot be increased. Thus, the best apparent single-clast age is $0.94^{+0.19}_{-0.12}$ Ma. Having rejected one clast as an outlier based on results of muon-inclusive burial dating, we re-calculated the isochron age based on the remaining three data points (black line, figure 3-3c). The revised isochron has an age of 0.91 ± 0.09 Ma.

3.5. Discussion

Co-application of muon-inclusive simple burial dating and isochron burial dating significantly improved the interpretation of isotope data presented here. With limited data, the use of these methods in tandem reveals important details about the burial history of the two deposits. In the case of KENW53.5, both methods, which compute ages based on different sets of assumptions, indicate a long burial time and similar age. We may have underestimated muogenic production for this sample set, as the blue burial contours can be shifted to the right in figure 3-3b so that all 1-sigma sample ellipses fit well with one age contour. Because we slightly underestimated the muogenic component, the clast with the best apparent simple burial age estimate ($2.22^{+0.17}_{-0.15}$ Ma) may actually be too young. Conversely, we must also consider that this clast may have experienced a prior episode of burial, making its apparent age a maximum. However, since any prior burial history would have had to be the same for all three clasts based on simple burial results, we deem such burial, highly unlikely. Because the apparent simple burial age is statistically inseparable from the isochron age (2.06 ± 0.07 Ma), we interpret the isochron

age as representative. Additionally, the outlier sample with an anomalously low $^{26}\text{Al}:$ ^{10}Be ratio in the isochron also plots outside the contoured region in the simple burial plot, well within the muogenic “forbidden zone”. This indicates either an extended prior period of burial, or problems with the chemistry or AMS measurement, and supports removal of this sample from isochron age regression.

For MT 39.5, simple burial dating on single clasts significantly helped refine isochron age estimates by identifying outlier data. The isochron age regression based on all 4 points appears to be reliable (gray line, figure 3-3c). But by plotting the data on the simple burial diagram (figure 3-3d), and identifying one clast that experienced significant prior burial, we were able to refine isochron results. This reduced the isochron to just 3 points, two of which are statistically overlapping; isochron age regression is effectively based on two points. However, because we have evidence from simple burial that we slightly overestimated the muogenic component, so that a burial contour could easily be regressed through all 3 data points by slightly reducing post-burial production, we interpret the isochron result as a reliable age constraint.

These examples demonstrate that by co-applying both isochron and muon-inclusive simple burial dating, one can provide complementary age constraints on the burial history of gravel deposits, even with relatively few data points. Sample set KENW53.5 shows how simple burial can provide fully complimentary age analysis and provide a process argument for rejecting outlier data that are easily identified in both methods. Sample set MT39.5 presents the risk of including a sample in isochron age

regression that has experienced a prior episode of burial that is not obvious from isochron plots. This sample is readily identified and rejected using the simple burial method. While co-application of simple burial and isochron dating methods is necessary for increasing confidence in isochrons regressed from few data points, and particularly for identifying clasts that experienced prior burial and rejecting them as outlier data, this method could also be utilized as a powerful quality control measure for larger datasets as well. This simple procedural check improves interpretation of cosmogenic nuclide isochron data and prevents presentation of misleading age estimates.

3.6. Acknowledgements

We would like to thank the Eastern Geology and Paleoclimate Science Center of the U.S.G.S. for financially supporting this research, E. Cobbs III and J. Grey for drilling, G. Balco and D. Granger for providing Matlab scripts for isochron methods, and D. Rood and S. Zimmerman for ^{26}Al and ^{10}Be AMS measurements, respectively.

3.7. References

- Argento, D. C., Reedy, R. C., and Stone, J. O., 2013, Modeling the earth's cosmic radiation Nuclear Instruments and Methods in Physics Research, Section B, Beam Interactions with Materials and Atoms, v. 294, p. 464–469.
- Balco, G., and Rovey, C. W., 2008, An isochron method for cosmogenic-nuclide dating of buried soils and sediments: American Journal of Science, v. 308, no. 10, p.

1083-1114.

- Balco, G., and Rovey, C.W., 2010, Absolute chronology for major Pleistocene advances of the Laurentide Ice Sheet: *Geology*, v. 38, no. 9, p. 795-798.
- Balco, G., Soreghan, G. S., Sweet, D. E., Marra, K. R., and Bierman, P. R., 2013, Cosmogenic-nuclide burial ages for Pleistocene sedimentary fill in Unaweep Canyon, Colorado, USA: *Quaternary Geochronology*, v. 18, p. 149-157.
- Colman, S. M., Halka, J. P., Hobbs III, C. H., Mixon, R. B., and Foster, D. S., 1990, Ancient channels of the Susquehanna River beneath Chesapeake Bay and the Delmarva Peninsula: *Geological Society of America Bulletin*, v. 102, p. 1268-1279.
- Erlanger, E. D., Granger, D. E., and Gibbon, R. J., 2012, Rock uplift rates in South Africa from isochron burial dating of fluvial and marine terraces: *Geology*, v. 40, no. 11, p. 1019-1022.
- Granger, D. E., 2006, A review of burial dating methods using ^{26}Al and ^{10}Be , *in* Siame, I. L., Bourlies, D. L., and Brown, E. T., eds., *In Situ-Produced Cosmogenic Nuclides and Quantification of Geological Processes: Geological Society of America Special Paper 415, Volume 415*, p. 1-16.
- Granger, D. E., 2014, *Cosmogenic Nuclide Burial Dating in Archaeology and Paleoanthropology: Treatise on Geochemistry*, v. 14, p. 81-97.
- Granger, D. E., Kirchner, J. W., and Finkel, R. C., 1997, Quaternary downcutting rate of the New River, Virginia, measured from differential decay of cosmogenic ^{26}Al

- and ^{10}Be in cave-deposited alluvium: *Geology*, v. 25, no. 2, p. 107-110.
- Granger, D. E., and Muzikar, P. F., 2001, Dating sediment burial with in situ-produced cosmogenic nuclides: theory, techniques, and limitations: *Earth and Planetary Science Letters*, v. 188, p. 269-281.
- Hidy, A. J., Gosse, J. C., Froese, D. G., Bond, J. D., and Rood, D. H., 2013, A latest Pliocene age for the earliest and most extensive Cordilleran Ice Sheet in northwestern Canada: *Quaternary Science Reviews*, v. 61, p. 77-84.
- Jacobs, J. M., 1980, Stratigraphy and lithology of Quaternary landforms on the eastern coast of the Chesapeake Bay [MS: University of Delaware, 81 p.
- Klein, J., Giegengack, R., Middleton, R., Sharma, P., Underwood, J. R., and Weeks, R. A., 1986, Revealing histories of exposure using *in situ* produced ^{26}Al and ^{10}Be in Libyan desert glass.
- Lifton, N., Sato, T., and Dunai, T. J., 2014, Scaling in situ cosmogenic nuclide production rates using analytical approximations to atmospheric cosmic-ray fluxes: *Earth and Planetary Science Letters*, v. 386, p. 149-160.
- Nishiizumi, K., Imamura, M., Caffee, M. W., Southon, J. R., Finkel, R. C., and McAninch, J., 2007, Absolute calibration of ^{10}Be AMS standards: *Nuclear Instruments and Methods in Physics Research B*, v. 258, no. 2, p. 403-413.
- Nishiizumi, K., Lal, D., Klein, J., Middleton, R., and Arnold, J. R., 1986, Production of ^{10}Be and ^{26}Al by cosmic rays in terrestrial quartz in situ and implications for erosion rates: *Nature*, v. 319, p. 134-136

Xu, S., Dougans, A. B., Freeman, S. P. H. T., Schnabel, C., and Wilcken, K. M., 2010, Improved ^{10}Be and ^{26}Al -AMS with a 5 MV spectrometer: Nuclear Instruments and Methods in Physics Research B, v. 268, p. 736–738.

Xu, S., Freeman, S. P. H. T., Rood, D. H., and Shanks, R. P., 2014, ^{26}Al interferences in accelerator mass spectrometry measurements: Nuclear Instruments and Methods in Physics Research B, v. 333, no. 42-45.

3.8. Figure captions

Figure 3-1. Map showing location of study area. Inset map on upper right corner shows location of Chesapeake Bay (C.B.), with the rectangle indicating the location of the Light Detection and Ranging (LiDAR) imagery. Line A-A' shows the location of the borehole cross-section below, which demonstrates the stacked nature of deposits from which KENW53.5 and MT39.5 were sampled.

Figure 3-2. The simple burial plot explained. Solid red lines represent continuous surface and burial (muogenic) exposure curves, solid green lines represent continuous exposure with successively increasing surface erosion rates; together, these comprise the “erosion banana” where samples are presumed to plot prior to burial. Red and blue numbers have units of Ma. If the assumptions regarding the pre-burial surface source and mass depth since burial are correct, then all samples must plot within the contoured region. Upon burial, samples follow a path parallel to the dashed black lines, such as that

indicated by black arrows, with the burial duration indicated by dotted blue lines. The gray “forbidden zone” indicates problems with assumptions or with measurement, as described in the text. The example ellipse shows a sample that experienced 0.1 Ma of exposure and 1.0 Ma of burial.

Figure 3-3. Isochron and simple burial plots for samples analyzed in this study. Ellipses indicate 68% confidence regions (1σ) and include errors related to decay constant uncertainties. A. Isochron burial dating results for KENW53.5. Raw data are shown as light blue ellipses, refined (linearized) data are shown in dark blue. Open ellipse indicates a clast with significantly lower $^{26}\text{Al} : ^{10}\text{Be}$ ratios compared with other clasts in each deposit. B. Simple burial dating results for KENW53.5, as explained in figure 2. Inset probability distribution functions (pdfs) for individual clasts indicate relative probability on the y-axis and burial age (Ma) on the x-axis. C. Isochron burial dating results for MT39.5 with (gray line) and without (black line) including outlier data point identified by the open ellipse. D. Simple burial dating results for MT 39.5 with inset pdfs. The clast with the highest concentration and best apparent age for both KENW53.5 and MT39.5 are colored magenta on both the burial plots and the pdfs in B. and D., respectively.

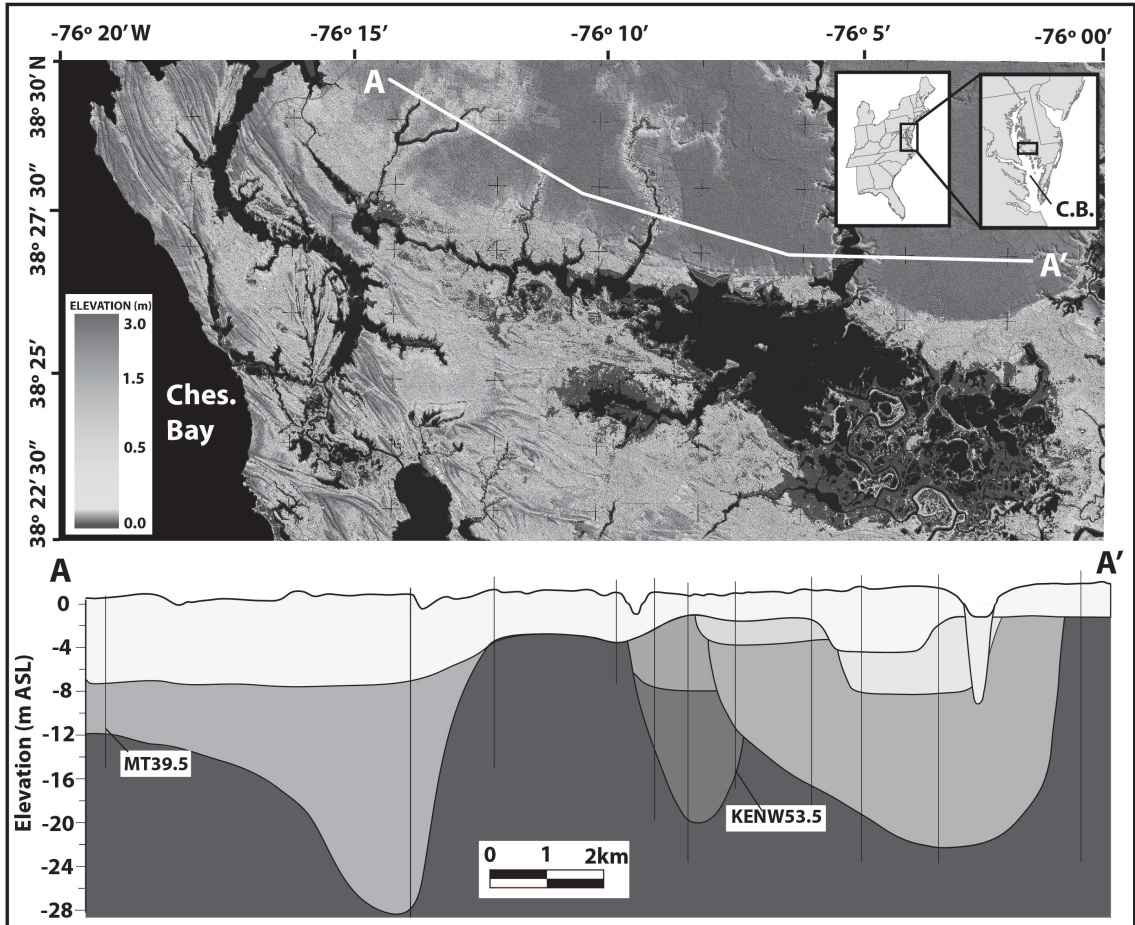


Figure 3-1 Map showing location of study area

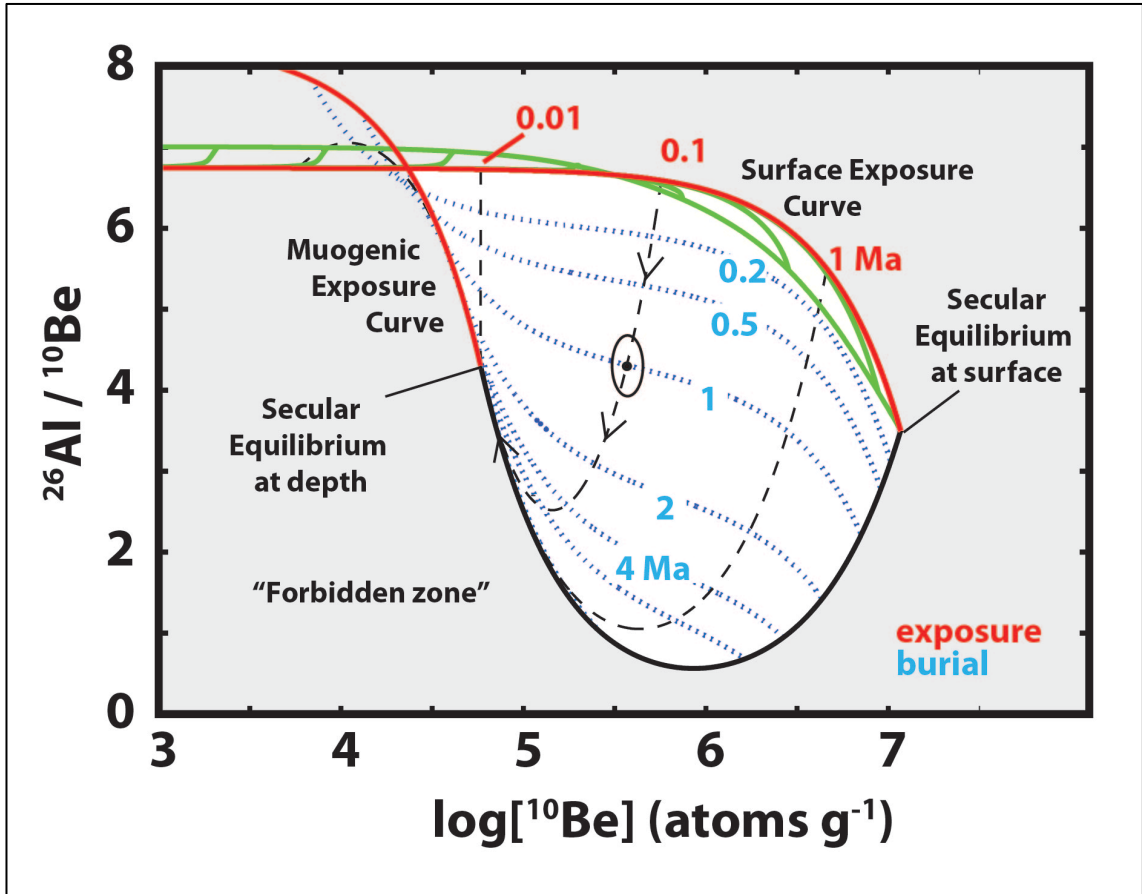


Figure 3-2 The simple burial plot explained

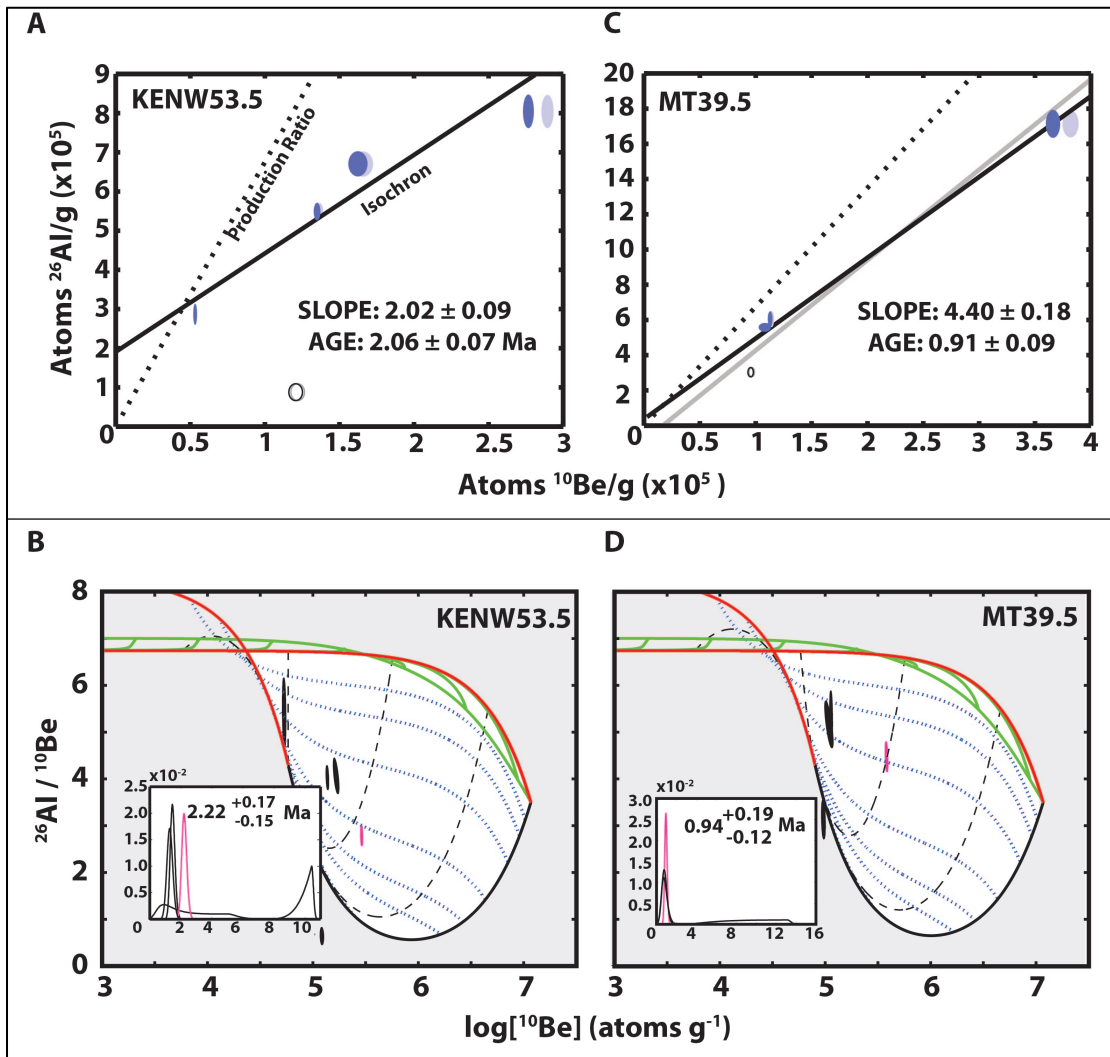


Figure 3-3 Isochron and simple burial plots for samples analyzed in this study

TABLE 1 Cosmogenic radionuclide data and burial age estimates

Isochron	Sample ID (UVM ID)	Location	Depth in core (m)	¹⁰ Be Concentration* (Measured; atoms/g)	²⁶ Al Concentration* (Measured; atoms/g)	²⁶ Al/ ¹⁰ Be	Isochron Age ^f (Ma)	Cumulative Bulk Density (g/cm ³)	Simple burial age ^g (Ma)	1σ (+)	1σ (-)
KENW53.5	513BL18	38.448047°N, 76.124019°W	16.3	5.34E+04 ± 1.24E+03	2.88E+05 ± 2.77E+04	5.39 ± 0.53	2.06 ± 0.07	1.77	0.94	3.65	0.10
	513BL19			1.37E+05 ± 2.30E+03	5.52E+05 ± 2.19E+04	4.03 ± 0.17			1.46	0.16	0.14
	513BL20			2.90E+05 ± 4.08E+03	8.09E+05 ± 4.31E+04	2.79 ± 0.15			2.22	0.17	0.15
	B517BL21	76.124019°W		1.22E+05 ± 3.28E+03	7.80E+04 ± 1.58E+04	0.64 ± 0.13			FZ ^h	--	--
	556BL41			1.66E+05 ± 6.82E+03	6.74E+05 ± 3.22E+04	4.05 ± 0.25			1.34	.19	.18
MT39.5	B517BL28	38.495698°N, 76.237045°W	12.0	3.82E+05 ± 7.20E+03	1.71E+06 ± 7.70E+04	4.47 ± 0.22	0.91 ± 0.09	1.73	0.94	0.19	0.12
	B517BL29			9.61E+04 ± 2.50E+03	3.01E+05 ± 2.64E+04	3.13 ± 0.29			FZ	--	--
	513BL27			1.14E+05 ± 2.15E+03	6.02E+05 ± 4.52E+04	5.29 ± 0.41			0.71	0.40	0.20
	556BL30B			1.09E+05 ± 5.65E+03	5.56E+05 ± 2.40E+04	5.10 ± 0.34			0.88	0.28	0.23

^aMeasured at the Lawrence Livermore National Laboratory and normalized to the 'D7KNSTD' standard with an assumed ratio of 2.85 x 10⁻¹². See [3]

^bMeasured at the Scottish Universities Environmental Research Centre and normalized to the Z92-0222 standard with defined ratio of 4.11 x 10⁻¹¹. See [16, 17]

^cAll ages reported to 1 sigma uncertainty

^dBest apparent age indicated in bold

^eSamples labeled FZ fall into the muogenic "forbidden zone" (see figure 2)

Table 3-1 Cosmogenic radionuclide data and burial age estimates

**CHAPTER 4: ESTUARIES PRESERVE LONG RECORD OF PLEISTOCENE
GLACIAL-INTERGLACIAL LANDSCAPE CHANGE**

For submission to Nature Geoscience

Benjamin D. DeJong, U.S. Geological Survey, Reston, VA, 20192, and
Rubenstein School of the Environment and Natural Resources, University of Vermont,
Burlington, VT 05405, bdejong@usgs.gov, 435-760-5440

Paul R. Bierman, Geology Department and Rubenstein School of the Environment and
Natural Resources, University of Vermont, Burlington, VT, 05405, pbierman@uvm.edu,
802-238-6826

Darryl Granger, Department of Earth, Atmospheric, and Planetary Sciences, Purdue
University, 550 Stadium Mall Drive Purdue University, West Lafayette, IN 47907, 765-
494-0043

Alan J. Hidy, Center for Accelerator Mass Spectrometry, Lawrence Livermore National
Laboratory, Livermore, CA 94550, hidy3@llnl.gov, 925-423-8877

Dylan H. Rood, Scottish Universities Environmental Research Centre (SUERC),
University of Glasgow, East Kilbride G750QF, Scotland, UK; now at Department of
Earth Science and Engineering, Imperial College London, South Kensington Campus,
London SW7 2AZ, UK, d.rood@imperial.ac.uk, +44 (0)20 7594 7333

Eric W. Portenga, School of Geographical and Earth Sciences, University of Glasgow,
East Kilbride G750QF, Scotland, UK

4.1. Introductory paragraph

The world's major coastal plain estuaries preserve, in their sediments, a record of both terrestrial and marine responses to climate change (Dalrymple et al., 1992). Situated at the interface between terrestrial sediment sources and marine sediment sinks, estuaries repeatedly alternated between fluvial and near-shore subaqueous environments as sea level, driven by the coming and going of ice sheets, fluctuated during the Pleistocene. However, difficulty in dating old estuarine sediment has stymied the interpretation of estuarine sedimentary records. Here, we use cosmogenic radionuclide burial dating to date sediment underlying Chesapeake Bay, the largest estuary in North America. Age data indicate that sediments underlying the Bay preserve a record of glacial-interglacial, cut-fill processes stretching back nearly to the onset of the Pleistocene, many times the previously assumed age of paleochannels associated with Chesapeake Bay (Colman et al., 1990). Comparing decay-corrected ^{10}Be concentrations in the oldest sampled gravels with contemporary river sand samples from never-glaciated areas of the Susquehanna River Basin indicates that erosion rates are at least 50% higher in late Pleistocene than they were at the start of the Pleistocene – presumably a response to changing climate and base level.

4.2. Article text

Major coastal plain estuaries, which are drowned, distal river valleys, repeatedly alternated between fluvial and estuarine regimes as climate and thus sea level fluctuated

over the Pleistocene (Perillo, 1991). During sea-level high stands, estuaries were sediment sinks, preserving records of both terrestrial and marine processes. During low stands, channels incised deep valleys that provided accommodation space for deposition during the subsequent high stand. As a result, estuaries preserve a large range of deposits from lowstand, glacio-fluvial channel sand and gravels, which are commonly used to interpret local-to-regional impacts of climate cycling in up-catchment settings (Hidy et al., 2014), to highstand estuarine and marine muds. Provided an adequately large channel basin where river meets sea, and a shifting channel through time, coastal plain estuaries thus present unique opportunities to preserve in their sedimentary record a long and detailed history of upland landscape evolution.

The Chesapeake Bay (Figure 4-1) is one of the largest and most thoroughly studied coastal plain estuaries in the world (Perillo, 1995). Chesapeake Bay occupies the drowned, distal valley of the Susquehanna River (Figure 4-1), which acted as a significant conduit for sand and gravel during glacial periods (e.g. Pazzaglia and Gardner, 1993), when sea levels were up to ~140 m below present (Miller et al., 2005), and as a major sediment sink during sea-level high-stands both for terrestrial material eroded from the Susquehanna River watershed (71,225 km²) and marine material transported from the shelf (Owens and Denny, 1979). The alternating erosional and depositional regimes of the distal Susquehanna River resulted in a stratigraphy of deeply incised channels back-filled by interglacial sediments that have been identified in boreholes (Mixon, 1985) and in seismic profiling of the Chesapeake region (Colman et al., 1990; Genau, 1994; Oertel

and Foyle, 1995).

The combined lateral migration of the Susquehanna River through time (Colman et al., 1990) and the vertical stacking of progressively younger fill units within individual paleovalley locations (Genau, 1994; Oertel and Foyle, 1995; DeJong et al., in press) preserves a sedimentary record of major sea-level fluctuations. This record has long been used to discern the Late Pleistocene history of the Chesapeake Bay and the greater mid-Atlantic region of the United States (Cronin, 1981; Colman et al., 1990; Wehmiller et al., 2004). Other local paleochannels provide additional constraints on the evolution of the Delmarva Peninsula, which separates the Chesapeake Bay from the Atlantic Ocean (Figure 4-1).

Exploiting the long stratigraphic record under Chesapeake Bay to constrain the history of incision and aggradation and to understand the response of upstream landscapes to the initiation of Pleistocene glaciation requires age control. Previous attempts at constraining ages of paleochannels in Chesapeake Bay focused on dating shells (amino acid racemization; AAR) and encrusting corals on shells (Uranium series dating; U-series) within emerged interglacial deposits interpreted as highstand counterparts from the same sea level cycle during which channels were incised (Cronin et al., 1984; Szabo, 1985; Colman et al., 1990). However, these chronologies have been the source of considerable debate and confusion; results from various dating methods conflict (e.g. Colman and Mixon, 1990), and ages disagree with global sea-level records accepted for given time periods (Cronin, 1981; Wehmiller et al., 2004). Additionally, seismic

evidence suggests channels were active during multiple glacial cycles, so that ages of bounding highstand deposits do not necessarily constrain initial cutting of channels (Oertel and Foyle, 1995). As a result, the ages of Chesapeake Bay paleochannels remain poorly known. Presumed ages (<0.5 Ma) imply a large (10^5 - 10^6 year) time gap between Plio-Pleistocene development of the Delmarva Peninsula as a barrier spit (Mixon, 1985) and the age of the Susquehanna River paleochannel estimated from AAR results on bounding sediments (Colman et al., 1990).

In this paper, we use cosmogenic radionuclides to directly determine the range of time represented by the Susquehanna River paleochannel stratigraphy. Burial dating uses the measurement of the rare isotopes ^{26}Al and ^{10}Be that are produced on Earth's surface by nuclear reactions with cosmic rays. Simple burial dating assumes a two-stage exposure-burial history, with initial exposure followed by deep burial (Granger and Muzikar, 2001). While some gravel deposits in the Chesapeake Bay stratigraphy may conform to this simple, two-stage history, many likely do not, and geologic evidence alone cannot confirm exposure and burial history *a priori*. An alternative burial dating method deals better with more complex histories (Balco and Rovey, 2008; Granger, 2014). The cosmogenic nuclide burial isochron method involves sampling several (≥ 3) clasts and/or grain size separates from the same horizon that presumably begin burial with different ^{26}Al and ^{10}Be concentrations, but share post-burial nuclide production and decay history. If these criteria are satisfied, the ^{26}Al and ^{10}Be concentrations from all clasts and grain size separates form a linear relationship, or an isochron, in a bivariate

plot of ^{26}Al and ^{10}Be concentrations. The slope of this isochron depends on the $^{26}\text{Al}/^{10}\text{Be}$ production ratio, the ^{26}Al and ^{10}Be decay constants, and on the burial time, but it is independent of the production of nuclides during burial. So if clasts are derived from sites with a range of erosion rates, and erosion rates in the watershed are high enough (greater than a few meters per million years) that radioactive decay can be disregarded, the slope of the isochron drawn through ^{26}Al and ^{10}Be concentrations can indicate a burial age for the deposit even when inherited ^{26}Al and ^{10}Be concentrations and burial histories are unknown. We apply isochron burial dating to 9 major channel sequences underlying Chesapeake Bay allowing direct dating of units over 10^5 - 10^6 year timescales.

4.3. Results

Cosmogenic ^{26}Al - ^{10}Be isochron data provide the first numerical ages for stacked paleochannel gravel deposits on the eastern shore of Chesapeake Bay (Table SI1). Ages range from 2.06 ± 0.07 to 0.28 ± 0.05 Ma, spanning the Early-Middle Pleistocene time range (Figure 4-2). Each age includes an isochron age regressed from at least three ^{26}Al - ^{10}Be measurements; all samples were also analyzed using a muon-inclusive simple burial method, which relies on assumptions about on post-burial production (see methods and supplementary information). Because isochrons are insensitive to post-burial production, simple burial provides an independent age estimate (*sensu* DeJong et al., in review).

We also analyzed shells for AAR that were collected from fill units superimposed over deposits with dated gravels. Values are reported as the ratio of the dextro (D) form

of an amino acid to its levo (L) counterpart, or D/L value, which is assigned to well-established “aminozones” of the East Coast (e.g. Wehmiller et al., 2013). Results indicate the presence of shells from aminozones IIc, and II d’, a range that spans the Early to Middle Pleistocene (Figure 4-3, Table SI2). While the analyses were completed on friable specimens of oysters (*Crassostrea*) and clams (*Mulinia*), and thus are non-ideal, the aminozones are generally consistent with the regional aminostratigraphy, and they support the burial isochron ages.

Isochron burial ages are consistent with muon-inclusive simple burial dating and AAR results and indicate that cut-fill processes of the paleo-Susquehanna River have shaped the Chesapeake Bay estuary over multi-million year timescales (Figure 4-3). Isochron ages unambiguously show that Susquehanna River paleochannels and their tributaries have been active for more than 2 My, many times longer than previously assumed (Figure 4-3). The new ages support the interpretation that paleochannels were incised early in the Pleistocene and then re-occupied repeatedly (Oertel and Foyle, 1995) and are consistent with field evidence upstream in the Susquehanna basin that suggests multiple periods of fluvial reactivation during early Pleistocene glaciations (Pazzaglia and Gardner, 1993). That fill ages span nearly the entire Pleistocene is important, because it means that sediments within the estuary contain a several-million year archive of landscape and marine history.

For example, we use our oldest isochron ages to calculate the concentration of ^{10}Be in sediment when it was deposited in paleo Chesapeake Bay. This allows us to

calculate paleo-erosion rates. Susquehanna gravels, tributary gravels, and local gravel lag deposits in the early record (>1.6 Ma) all have median decay-corrected concentrations that are $>4.0 \times 10^5$ atoms/g; after that time, median concentrations are similar to or less than ^{10}Be concentrations measured in contemporary Susquehanna mainstem channel sands from parts of the basin that were never glaciated ($\sim 2.5 \times 10^5$ atoms/g; Figure 3B, Table SI3). We interpret the high ^{10}Be concentrations in the older sediments as reflecting initial glacial stripping of Tertiary regolith, which accumulated ^{10}Be prior to the first glacial advance around 2.4 Ma (Balco and Rovey, 2010). The similarity of decay-corrected ^{10}Be concentrations in sediment deposited after 1.6 Ma reflects relative consistency in landscape processes over the glacial-interglacial climate fluctuations of the Pleistocene.

For unglaciated drainage basins, ^{10}Be concentrations in river sand can be used to calculate long-term, basin-average erosion rates (integrated over 10^3 to 10^4 yr timescales; Brown et al., 1995; Bierman and Steig, 1996; Granger et al., 1996). Assuming that high ^{10}Be concentrations in the early record indicate pre-glacial regolith, we can infer paleo-erosion rates from decay-corrected ^{10}Be concentrations in the oldest gravels and compare them with erosion rates calculated for present-day Susquehanna sub-basins that were never glaciated. The oldest paleo-channel sample (2.06 Ma) indicates an apparent erosion rate of 12.4 ± 1.1 m/Ma, within uncertainty of the average rate (11.6 ± 1.7 m/Ma) calculated from all sand and clasts associated with gravel deposits >1.7 Ma ($n=9$). The average erosion rate from modern sand in non-glaciated basins ($n=18$) is 19.0 ± 1.2

m/Ma. We interpret the 50% increase in apparent erosion rates from pre-glacial regolith to Late Pleistocene sediments as evidence of accelerated erosion due to glacial-interglacial climate cycling of the Late Pleistocene. These results support the idea that erosion rates increased in mountainous regions during the Pleistocene (Herman et al., 2013), even in the absence of active tectonics. If global weathering fluxes indeed remained constant over the Plio-Pliocene boundary (Willenbring and von Blackenburg, 2010), our data support a requisite, opposing reduction of erosion rates in what must be increasingly stable, low-relief regions (Hidy et al., 2014).

Our isochron burial ages show that major estuaries can provide multi-million year records of landscape response to climate change. For Chesapeake Bay, our ages suggest that major cutting and filling from glacial-interglacial climate fluctuations commenced at the onset of the Pleistocene. The consistency in decay-corrected ^{10}Be concentrations, following the initial high values in the early Pleistocene, reflects consistency of landscape processes despite climate fluctuations of the last ~ 1.6 My. Our cosmogenic nuclide ages show promise for improving correlation of buried paleochannel deposits with onshore records and for establishing paleoclimate records over 10^6 year timescales for a more complete understanding of landscape evolution during major Pleistocene climate perturbations.

4.4. Methods

Gravel and sand fractions collected from sediment cores were processed at the University of Vermont. Sand fractions were sieved and gravel clasts were crushed and ground to 125-250 μm and 250-500 μm fractions. Quartz was purified using selective acid etching (Kohl and Nishiizumi, 1992) and Be and Al were isolated using HF dissolution and ion exchange chromatography (Corbett et al., 2011). Using accelerator mass spectrometry, ^{10}Be was measured at the Lawrence Livermore National Laboratory, and ^{26}Al was measured at the Scottish Universities Environmental Research Centre; reported values include 1σ measurement uncertainties. Measured ratios of $^{10}\text{Be}/^9\text{Be}$ were normalized to the 07KNSTD standard with an assumed ratio of 2.85×10^{-12} (Nishiizumi et al., 2007), and $^{26}\text{Al}/^{27}\text{Al}$ to Z92-0222 standard with an assumed ratio of 4.11×10^{-11} (Xu et al., 2010, 2014); all samples were corrected using process blanks run with each batch of samples. Erosion rate values were calculated from ^{10}Be and ^{26}Al measurements corrected for decay and for post-burial production for individual clasts and sand fractions using the CRONUS online calculator (<http://hess.ess.washington.edu/>); average catchment geometry for the Susquehanna watershed and for the Delmarva Peninsula were used to estimate production rates of isotopes for mainstem and tributary streams, respectively.

Two separate methodologies were used to calculate burial ages, after DeJong and others (in review). The CRN isochron burial ages were calculated using a methodology from Granger (2014) that depends on the $^{26}\text{Al} / ^{10}\text{Be}$ production ratio, the

^{26}Al and ^{10}Be decay constants, and on the burial time, but it is independent of the production of nuclides during burial. Samples derived from source areas with low erosion rates may be deposited with ratios lower than the production ratio, and this method uses iteration to "linearize" the data. Simple burial ages were calculated using a methodology that relies heavily on estimates for post-burial (muogenic) production (sensu Hidy, 2013); we use time-averaged bulk density measurements to quantify muogenic contribution.

We calculate depositional ^{10}Be concentrations using the ^{10}Be decay constant ($4.99 \times 10^{-7} \text{ atoms} \cdot \text{yr}^{-1}$) (Balco et al., 2008) and the post-burial component indicated by the intercept of the isochron (Granger, 2014).

4.5. Acknowledgements

We thank E. Cobbs and J. Grey of the US Geological Survey for drilling and J. Wehmiller for AAR analyses. M. Whitbeck provided access at the Blackwater NWR. Research funded by USGS and NSF EAR-0034447 and EAR-0310208. ^{10}Be measurements performed under the auspices of the U. S. Department of Energy by the University of California, Lawrence Livermore National Laboratory under Contract No. W-7405-Eng-48.

4.6. Author contributions

B.D.D. and P.R.B. instigated this work and carried out sample collection and processing. G.B/ D.G., and A.H. provided isochron and burial dating Matlab scripts and analyses, respectively. D.H.R. made AMS measurements. E.P. helped analyze cosmogenic data. All authors contributed to manuscript preparation

4.7. References

- Perillo, G.M.E., ed., 1995, *Geomorphology and Sedimentology of Estuaries*, Amsterdam, Elsevier.
- Balco, G., and Rovey, C. W., 2008, An isochron method for cosmogenic-nuclide dating of buried soils and sediments: *American Journal of Science*, v. 308, no. 10, p. 1083-1114.
- Balco, G., and Rovey, C.W., 2010, Absolute chronology for major Pleistocene advances of the Laurentide Ice Sheet: *Geology*, v. 38, no. 9, p. 795-798.
- Bierman, P. R., and Steig, E. J., 1996, Estimating rates of denudation using cosmogenic isotope abundances in sediment: *Earth Surface Processes and Landforms*, v. 21, p. 125-139.
- Brown, E., Stallard, R. F., Larsen, M. C., Raisbeck, G. M., and Yiou, F., 1995, Denudation rates determined from the accumulation of in situ-produced ^{10}Be in the Luquillo Experimental Forest, Puerto Rico: *Earth and Planetary Science Letters*, v. 129, p. 193–202.

- Colman, S. M., Halka, J. P., Hobbs III, C. H., Mixon, R. B., and Foster, D. S., 1990, Ancient channels of the Susquehanna River beneath Chesapeake Bay and the Delmarva Peninsula: Geological Society of America Bulletin, v. 102, p. 1268-1279.
- Corbett, L. B., Young, N. E., Bierman, P. R., Briner, J. P., Neumann, T. A., Rood, D. H., and Graly, J. A., 2011, Paired bedrock and boulder ^{10}Be concentrations resulting from early Holocene ice retreat near Jakobshavn Isfjord, western Greenland: Quaternary Science Reviews, v. 30, no. 13-14, p. 1739-1749.
- Cronin, T. M., 1981, Rates and possible causes of neotectonic vertical crustal movements of the emerged southeastern United States Atlantic Coastal Plain: Geological Society of America Bulletin, v. 92, no. 11, p. 812-833.
- Cronin, T. M., Bybell, L. M., Poor, R. Z., Blackwelder, B. W., Liddicoat, J. C., and Hazel, J. E., 1984, Age and correlation of emerged Pliocene and Pleistocene deposits, U.S. Atlantic coastal plain: Pelogeography, Palaeoclimatology, Palaeoecology, v. 47, p. 21-51.
- Dalrymple, R. W., Zaitlin, B. A., and Boyd, R., 1992, Estuarine facies models: conceptual basis and stratigraphic implications: Journal of sedimentary petrology, v. 62, p. 1130-1146.
- DeJong, B. D., Bierman, P. R., Newell, W. L., Rittenour, T. M., Mahan, S. A., Balco, G., and Rood, D. H., In press, Pleistocene relative sea levels in the Chesapeake Bay region and their implications for the next century: GSA Today.

- Genau, R. B., Madsen, J. A., McGeary, S., and Wehmiller, J. F., 1994, Seismic-Reflection Identification of Susquehanna River Paleochannels on the Mid-Atlantic Coastal Plain: *Quaternary Research*, v. 42, p. 166-174.
- Granger, D. E., 2014, Cosmogenic Nuclide Burial Dating in Archaeology and Paleoanthropology: *Treatise on Geochemistry*, v. 14, p. 81-97.
- Granger, D. E., Kirchner, J. W., and Finkel, R., 1996, Spatially averaged long-term erosion rates measured from in-situ produced cosmogenic nuclides in alluvial sediment: *Journal of Geology*, v. 104, p. 249-257.
- Granger, D. E., and Muzikar, P. F., 2001, Dating sediment burial with in situ-produced cosmogenic nuclides: theory, techniques, and limitations: *Earth and Planetary Science Letters*, v. 188, p. 269-281.
- Herman, F., Seward, D., Valla, P. G., Carter, A., Kohn, B., Willett, S. D., and Ehlers, T. A., 2013, Worldwide acceleration of mountain erosion under a cooling climate: *Nature*, v. 504, no. 423-426.
- Hidy, A. J., Gosse, J. C., Blum, M. D., and Gibling, M. R., 2014, Glacial–interglacial variation in denudation rates from interior Texas, USA, established with cosmogenic nuclides: *Earth and Planetary Science Letters*, v. 390, p. 209-221.
- Hidy, A. J., Gosse, J. C., Froese, D. G., Bond, J. D., and Rood, D. H., 2013, A latest Pliocene age for the earliest and most extensive Cordilleran Ice Sheet in northwestern Canada: *Quaternary Science Reviews*, v. 61, p. 77-84.
- Kohl, C. P., and Nishiizumi, K., 1992, Chemical isolation of quartz for measurement of

- in-situ-produced cosmogenic nuclides: *Geochimica et Cosmochimica Acta*, v. 56, p. 3583-3587.
- Korschinek, G., Bergmaier, A., Faestermann, T., Gerstmann, U. C., Knie, K., Rugel, G., Wallner, A., Dillmann, I., Dollinger, G., von Gostomski, C. L., Kossert, K., Maiti, M., Poutivtsev, M., and Remmert, A., 2010, A new value for the half-life of ^{10}Be by heavy-ion elastic recoil detection and liquid scintillation counting: *Nuclear Instruments and Methods in Physics Research B*, v. 268, p. 187-191.
- Miller, K. G., and al., e., 2005, The Phanerozoic record of global sea-level change: *Science*, v. 310, p. 1293-1298.
- Mixon, R. B., 1985, Stratigraphic and Geomorphic Framework of Uppermost Cenozoic Deposits in the Southern Delmarva Peninsula, Virginia and Maryland, USGS Professional Paper 1067-G: Reston, VA, 53 pp.
- Nishiizumi, K., Imamura, M., Caffee, M. W., Southon, J. R., Finkel, R. C., and McAninch, J., 2007, Absolute calibration of ^{10}Be AMS standards: *Nuclear Instruments and Methods in Physics Research B*, v. 258, no. 2, p. 403-413.
- Oertel, G. F., and Foyle, A. M., 1995, Drainage Displacement by Sea-Level Fluctuation at the Outer Margin of the Chesapeake Seaway: *Journal of Coastal Research*, v. 11, no. 3, p. 583-604.
- Owens, J. P., and Denny, C. S., 1979, Upper Cenozoic deposits of the Central Delmarva Peninsula, Maryland and Delaware, USGS Professional Paper 1067-A: Washington, DC, 27 pp.

- Pazzaglia, F. J., 1993, Stratigraphy, petrography, and correlation of late Cenozoic middle Atlantic Coastal Plain deposits: Implications for late-stage passive-margin geologic evolution: *GSA Bulletin*, v. 105, p. 1617-1634.
- Szabo, B. J., 1985, Uranium-series dating of fossil corals from marine sediments of southeastern United States Atlantic coastal plain: *Geological Society of America Bulletin*, v. 96, p. 398–406.
- Wehmiller, J. F., 2013, United States Quaternary coastal sequences and molluscan racemization geochronology – What have they meant for each other over the past 45 years? *Quaternary Geochronology*, v. 16, p. 3-20.
- Wehmiller, J. F., Simmons, K. R., Cheng, H., Edwards, L. R., Martin-McNaughton, J., York, L. L., Krantz, D. E., and Shen, C.-C., 2004, Uranium-series coral ages from the US Atlantic Coastal Plain—the “80ka problem” revisited: *Quaternary International*, v. 120, no. 1, p. 3-14.
- Willenbring, J. K., and von Blanckenburg, F., 2010, Long-term stability of global erosion rates and weathering during late-Cenozoic cooling: *Nature*, v. 465, p. 211-214.
- Xu, S., Dougans, A. B., Freeman, S. P. H. T., Schnabel, C., and Wilcken, K. M., 2010, Improved ^{10}Be and ^{26}Al -AMS with a 5 MV spectrometer: *Nuclear Instruments and Methods in Physics Research B*, v. 268, p. 736–738.
- Xu, S., Freeman, S. P. H. T., Rood, D. H., and Shanks, R. P., 2014, ^{26}Al interferences in accelerator mass spectrometry measurements: *Nuclear Instruments and Methods in Physics Research B*, v. 333, no. 42-45.

4.8. Figure captions

Figure 4-1. Study area showing Chesapeake Bay and the contributing area of the Susquehanna River watershed. Up to 40% of the basin was intermittently glaciated during the Pleistocene.

Figure 4-2. Isochron ages shown in cross-section. See supplemental Figure 2-8 for A-A' location. X-axes indicate atoms $^{10}\text{Be}/\text{g}$ ($\times 10^5$), Y-axes indicate atoms $^{26}\text{Al}/\text{g}$ ($\times 10^5$). Ellipses indicate 68% confidence regions (1σ) and include errors related to decay constant uncertainties; raw data are shown as light gray ellipses, refined (linearized) data are shown in dark gray. Open ellipses indicate clasts with significantly lower $^{26}\text{Al} : ^{10}\text{Be}$ ratios compared with other clasts in each deposit. Dark gray substrate represents the Miocene substrate; progressively lighter shades represent younger cut-fill paleochannels. MD33 and KENS are AAR samples indicating deposition during MIS 17-21 (~ 0.87 - 0.68 Ma) and MIS 7 (~ 0.24 - 0.20 Ma), respectively.

Figure 4-3. Cosmogenic ages and concentrations through time. A. Age-elevation relationships of isochrons plotted alongside a eustatic sea-level curve for the Pleistocene (Miller et al., 2005). Gray shaded region indicates the presumed age range of Susquehanna River paleochannels prior to this study (Colman et al., 1990). B. Box and whisker plots showing the maximum, third quartile, median, first quartile, and minimum values of decay-corrected ^{10}Be from clasts and sand fractions from each gravel unit

plotted against time.

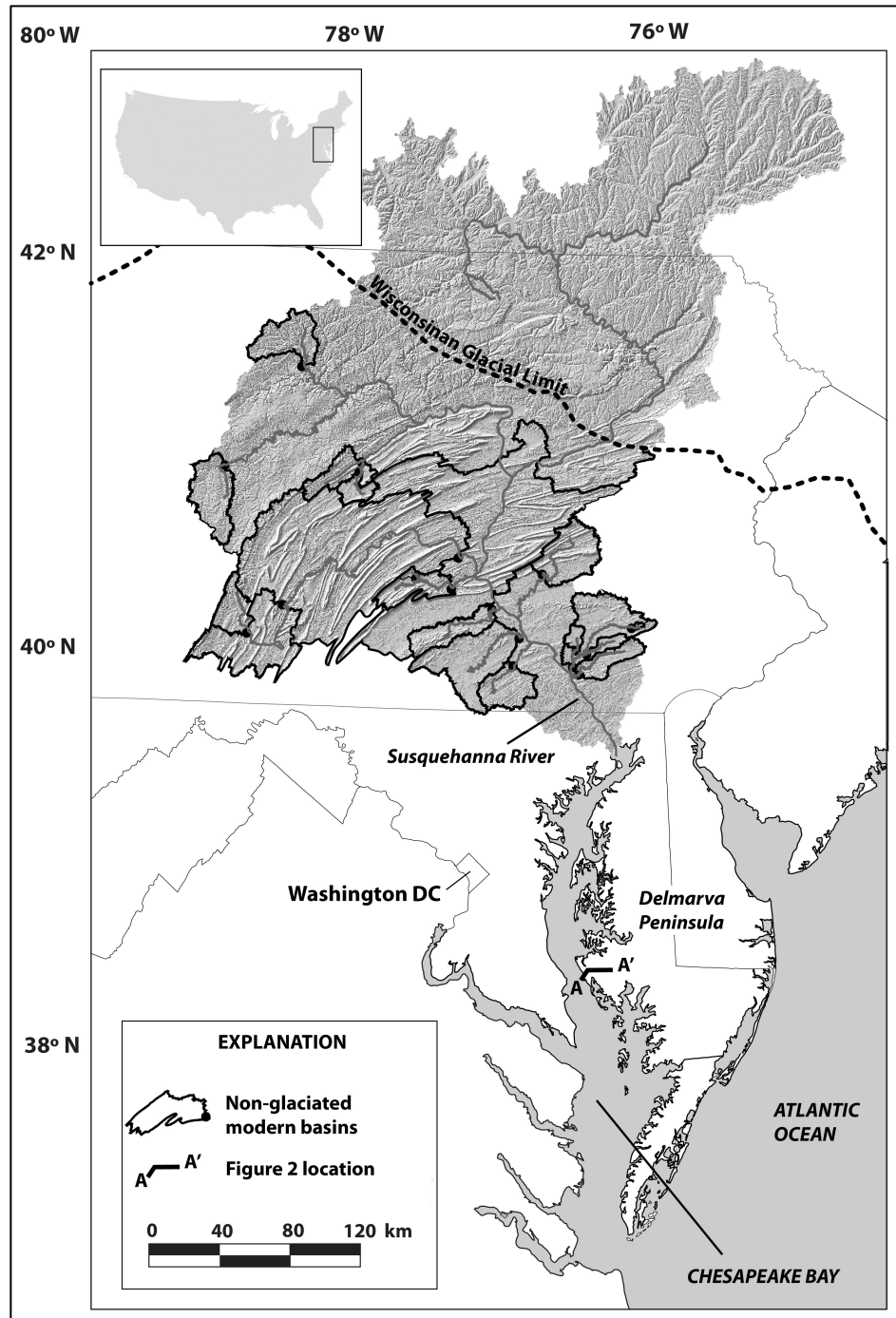


Figure 4-1 Study area showing Chesapeake Bay and the contributing area of the Susquehanna River watershed

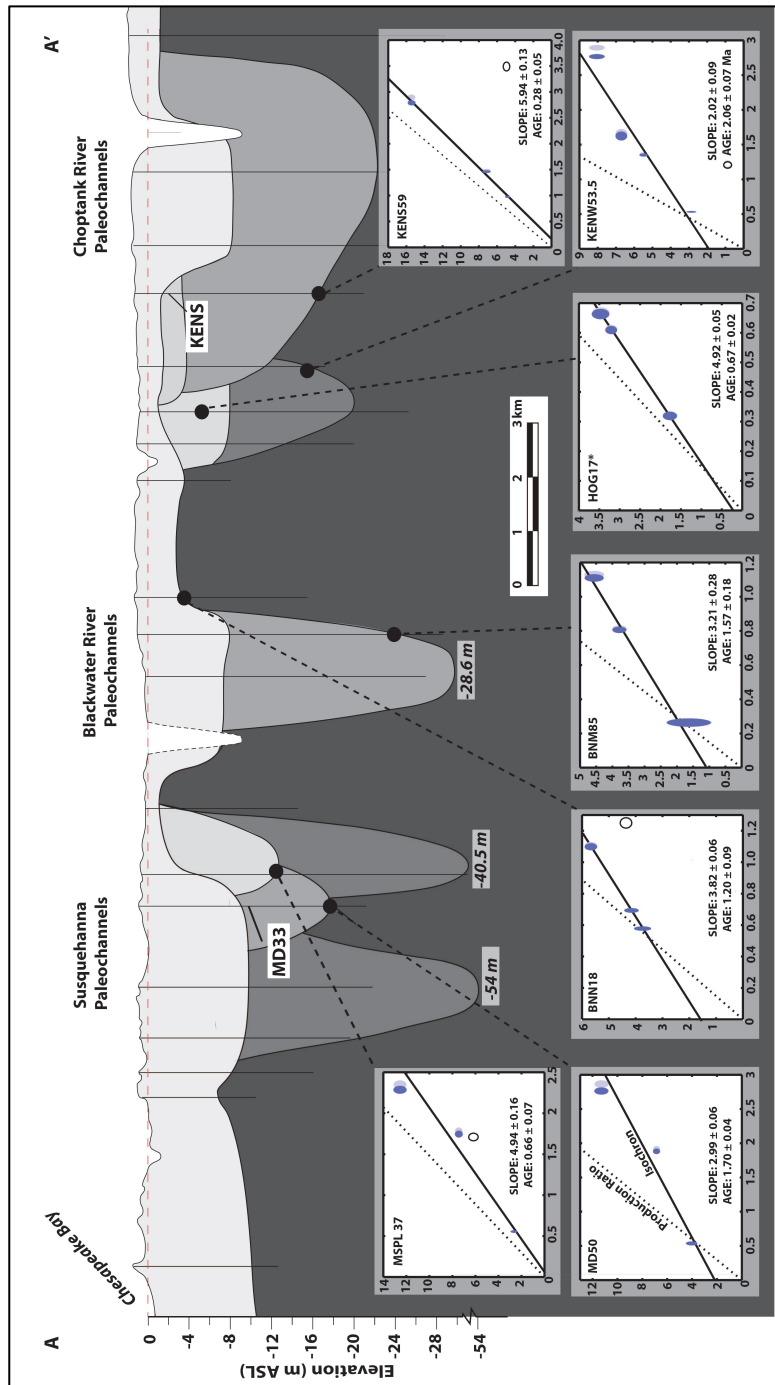


Figure 1-2 Isochron ages shown in cross-section

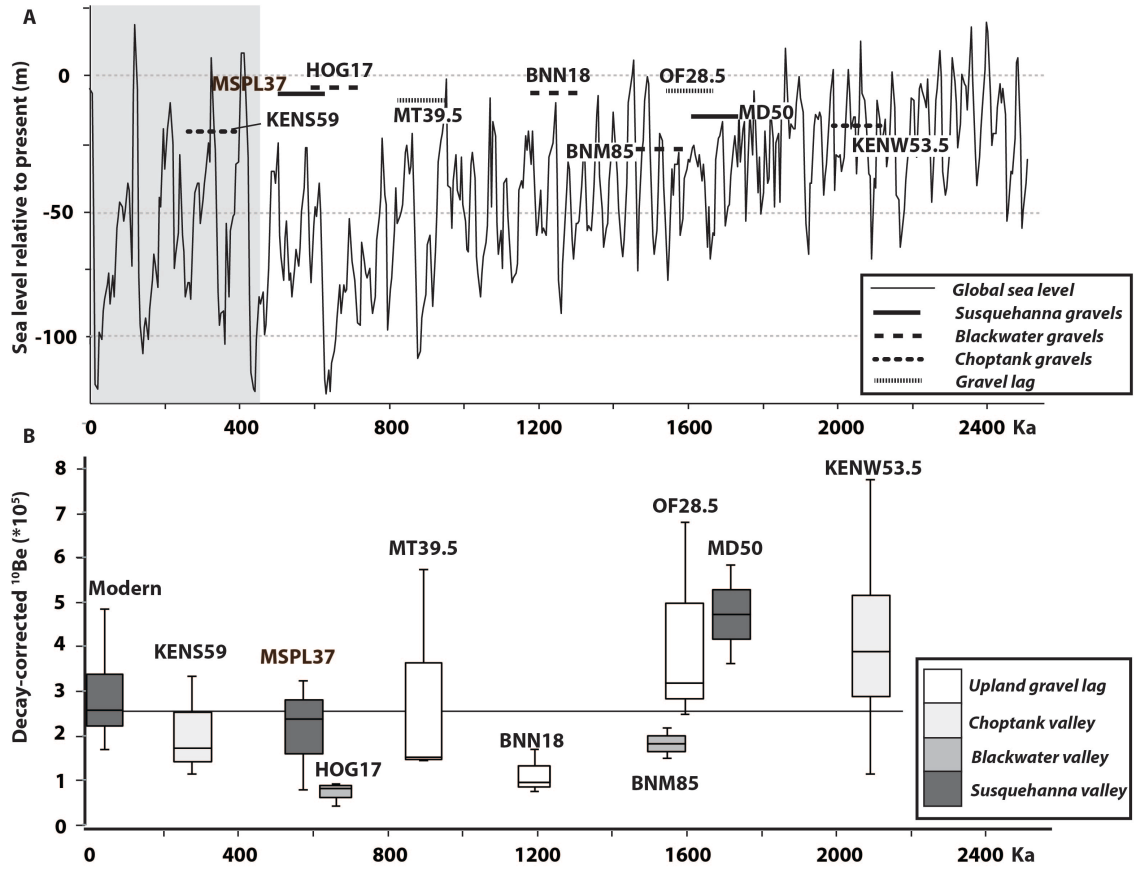


Figure 4-3 Cosmogenic ages and concentrations through time

4.9. Supplemental information

Table 4-1 (S11) Cosmogenic nuclide data table associated with isochron and simple burial ages

TABLE S11 Cosmogenic radionuclide data and burial age estimates

Isochron	Sample ID (UVM ID)	Location	Depth in core (m)	Type	¹⁰ Be Concentration ^g (Measured, atoms/g)	²⁶ Al Concentration ^h (Measured, atoms/g)	²⁶ Al/ ¹⁰ Be	Isochron Age ^f (Ma)	Cumulative Bulk Density (g/cm ³)	Simple burial age ^d (Ma)	1σ (+)	1σ (-)
BNM85	B525BL2	38.46009°N, -76.179611°W	25.9	clast	1.13E+05 ± 2.28E+03	4.54E+05 ± 3.03E+04	4.02 ± 0.28		1.83	1.33	0.23	0.18
	B525BL3			clast	2.59E+04 ± 2.50E+03	1.61E+05 ± 6.97E+04	6.23 ± 2.76	1.57 ± 0.18		1.02	3.05	-0.29
	B518BL4B			250-500 ^f	8.13E+04 ± 1.89E+03	3.76E+05 ± 2.21E+04	4.63 ± 0.29			1.02	0.21	0.18
HOG17	513BL10			clast	6.46E+05 ± 9.59E+03	1.18E+06 ± 3.33E+04	1.82 ± 0.06	0.67 ± 0.02	1.89	3.71	0.13	0.11
	B518BL11	38.448609°N, -76.143293°W	5.2	clast	3.18E+04 ± 1.46E+03	1.77E+05 ± 1.72E+04	5.58 ± 0.60			FZ	--	--
	B518BL12			clast	6.14E+04 ± 1.40E+03	3.22E+05 ± 1.42E+04	5.25 ± 0.26			FZ	--	--
KENV53	B518BL13			clast	6.70E+04 ± 1.77E+03	3.48E+05 ± 2.11E+04	5.20 ± 0.34			FZ	--	--
	513BL18			clast	5.34E+04 ± 1.24E+03	2.88E+05 ± 2.77E+04	5.39 ± 0.53			0.94	3.65	0.10
	513BL19	38.448047°N, -76.124019°W	16.3	clast	1.37E+05 ± 2.30E+03	5.52E+05 ± 2.19E+04	4.03 ± 0.17	2.06 ± 0.07	1.77	1.46	0.16	0.14
MSP137	513BL20			clast	2.90E+05 ± 4.08E+03	8.09E+05 ± 4.31E+04	2.79 ± 0.15			2.22	0.17	0.15
	B517BL21			clast	1.22E+05 ± 3.28E+03	7.80E+04 ± 1.38E+04	0.64 ± 0.13			FZ	--	--
	B556BL41			clast	1.66E+05 ± 6.82E+03	6.74E+05 ± 3.22E+04	4.05 ± 0.25			1.34	0.19	0.18
MD50	513B23			clast	5.61E+04 ± 1.58E+03	2.61E+05 ± 2.83E+04	4.65 ± 0.52			FZ	--	--
	B517BL24	38.434958°N, -76.225146°W	11.3	clast	1.71E+05 ± 3.30E+03	6.17E+05 ± 2.94E+04	3.60 ± 0.19	0.66 ± 0.07	1.89	1.95	0.24	0.19
	B517BL26			clast	2.33E+05 ± 5.24E+03	1.23E+06 ± 5.51E+04	5.28 ± 0.26			0.58	0.14	0.12
BNN18	B556BL47			clast	1.77E+05 ± 4.47E+03	7.30E+05 ± 3.22E+04	4.12 ± 0.209			1.4	0.18	0.17
	513BL35	38.433425°N, -76.229417°W	15.2	clast	5.47E+04 ± 2.82E+03	4.03E+05 ± 4.60E+04	7.36 ± 0.92			FZ	--	--
	B517BL36			clast	2.86E+05 ± 5.44E+03	1.13E+06 ± 5.54E+04	3.95 ± 0.21	1.70 ± 0.04	1.84	1.27	0.14	0.14
KENS59	B525BL37A			500-850	1.92E+05 ± 4.14E+03	6.86E+05 ± 2.72E+04	3.57 ± 0.16			1.69	0.15	0.13
	513BL6			clast	1.09E+05 ± 2.07E+03	5.67E+05 ± 2.25E+04	5.18 ± 0.23			FZ	--	--
	B518BL7	38.464564°N, -76.172321°W	5.5	clast	1.25E+05 ± 2.36E+03	4.36E+05 ± 1.54E+04	3.49 ± 0.14	1.20 ± 0.09	1.69	FZ	--	--
MT39.5	B518BL8			clast	5.72E+04 ± 1.19E+03	3.72E+05 ± 3.10E+04	6.51 ± 0.56			FZ	--	--
	B518BL14B			clast	6.87E+04 ± 1.29E+03	4.14E+05 ± 2.60E+04	6.03 ± 0.39			FZ	--	--
	513BL15	38.45228°N, -76.11493°W	18.0	250-500	2.89E+05 ± 5.37E+03	1.55E+06 ± 4.37E+04	5.36 ± 0.18	0.28 ± 0.05	1.71	0.50	0.08	0.08
OF28.5	B517BL16			clast	3.49E+05 ± 6.07E+03	4.96E+05 ± 2.56E+04	1.42 ± 0.08			4.18	0.21	0.17
	B517BL17			clast	9.88E+04 ± 2.06E+03	4.74E+05 ± 2.82E+04	4.80 ± 0.30			0.97	0.27	0.17
	B517BL28			clast	1.49E+05 ± 2.70E+03	7.10E+05 ± 4.68E+04	4.76 ± 0.33			0.89	0.22	0.17
BS56BL30B	B517BL29	38.495698°N, -76.237045°W	12.0	clast	3.82E+05 ± 7.20E+03	1.71E+06 ± 7.70E+04	4.47 ± 0.22	0.91 ± 0.09	1.73	0.94	0.19	0.12
	513BL27			clast	9.61E+04 ± 2.50E+03	3.01E+05 ± 2.64E+04	3.13 ± 0.29			FZ	--	--
	B556BL30B			250-500	1.14E+05 ± 2.15E+03	6.02E+05 ± 4.52E+04	5.29 ± 0.41			0.71	0.40	0.20
BS17BL32	513BL31			clast	1.09E+05 ± 5.65E+03	5.56E+05 ± 2.40E+04	5.10 ± 0.344			0.88	0.28	0.23
	B517BL32	38.483996°N, -76.130518°W	8.7	clast	3.15E+05 ± 4.63E+03	1.21E+06 ± 4.28E+04	3.83 ± 0.15	1.65 ± 0.07	1.69	1.50	0.12	0.12
	B518BL33			clast	5.36E+05 ± 1.00E+04	1.33E+06 ± 4.39E+04	2.48 ± 0.09			2.51	0.11	0.11
BS18BL34	B518BL33			clast	1.26E+05 ± 2.47E+03	6.47E+05 ± 2.67E+04	5.12 ± 0.23			0.94	0.28	0.16
	B518BL34			clast	1.57E+05 ± 3.51E+03	8.07E+05 ± 3.07E+04	5.15 ± 0.23			0.80	0.19	0.13

^aMeasured at the Lawrence Livermore National Laboratory and normalized to the ¹⁰Be standard with an assumed ratio of 2.85 x 10⁻¹². See [3].
^bMeasured at the Scottish Universities Environmental Research Centre and normalized to the Z92-0222 standard with defined ratio of 4.11 x 10⁻¹¹. See [16, 17].
^cAll ages reported to 1 sigma uncertainty
^dBest apparent age indicated in bold
^eSamples labeled FZ fall into the muogenic "forbidden zone" (DeLong et al., submitted)
^fGrain size of sand (µm)

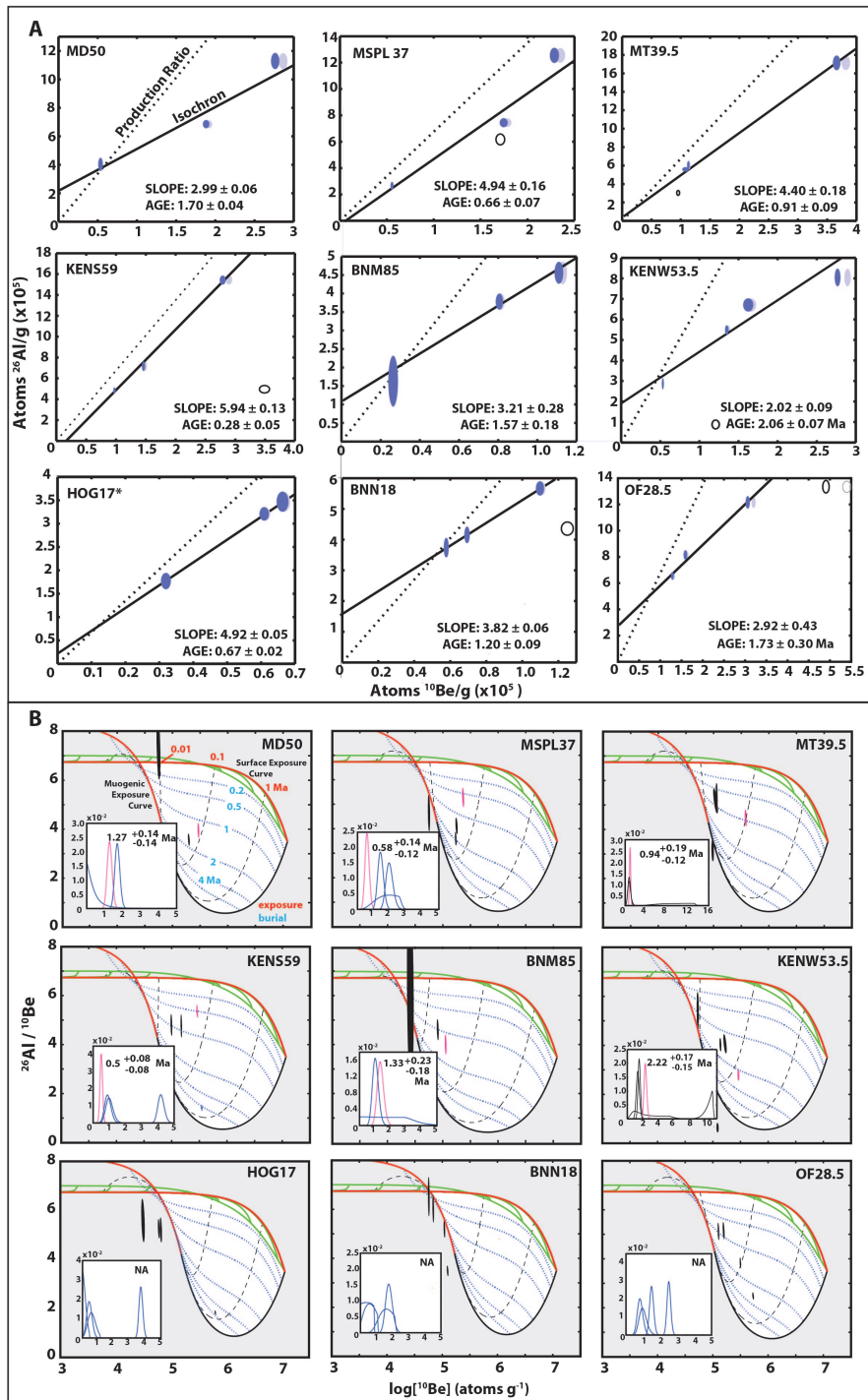


Figure 4-4 (SI1) Isochron and simple burial plots. A. Isochron plots, B. Simple burial plots.

Table 4-2 (SI2) Amino acid racemization sample details

Table SI2 Amino acid racemization data					
Sample	Locality	Elevation (m)	Aminozone	MIS Correlation ^b	Notes
BNM	38.46009°N, -76.179611°W	-3.4 to -7.8	IIa/IIb	MIS 5 (?)	<i>Crassostrea</i> ; soft but very clean
MY	38.448984°N, -76.091742°W	-6.3	IIa/IIb	MIS 5 (?)	<i>Crassostrea</i> ; visible layers but robust
KENS	38.45228°N, -76.11493°W	-2.4	IIc	MIS 7-9	<i>Mulinia</i> (?); probable, robust
MD33 ^c	38.433425°N, -76.229417°W	-9.5	II d'	MIS 17-21 (?)	<i>Mercenaria</i> (?); chalky but robust
DCMD ^d	38.4775°N, -76.2779°W	-9.1	II d'	MIS 17-21	<i>Rangia</i>
BNN	38.464564°N, -76.172321°W	-15.3	IIe	Pre-Pleistocene	<i>Mercenaria</i> ; Miocene Choptank Fm.
Golden Hill/MSS	38.424934°N, -76.206338°W	-6.9	IIe	Pre-Pleistocene	<i>Mulinia</i> (?); Miocene Choptank Fm.

^aSee Figure SI2 for detailed AAR results
^bMIS correlations from Groot and others (1990)
^cCollected from the same channel fill as isochron MD50 and AAR sample DCMD
^dFrom Jacobs (1980); reported in Genau et al., (1994)

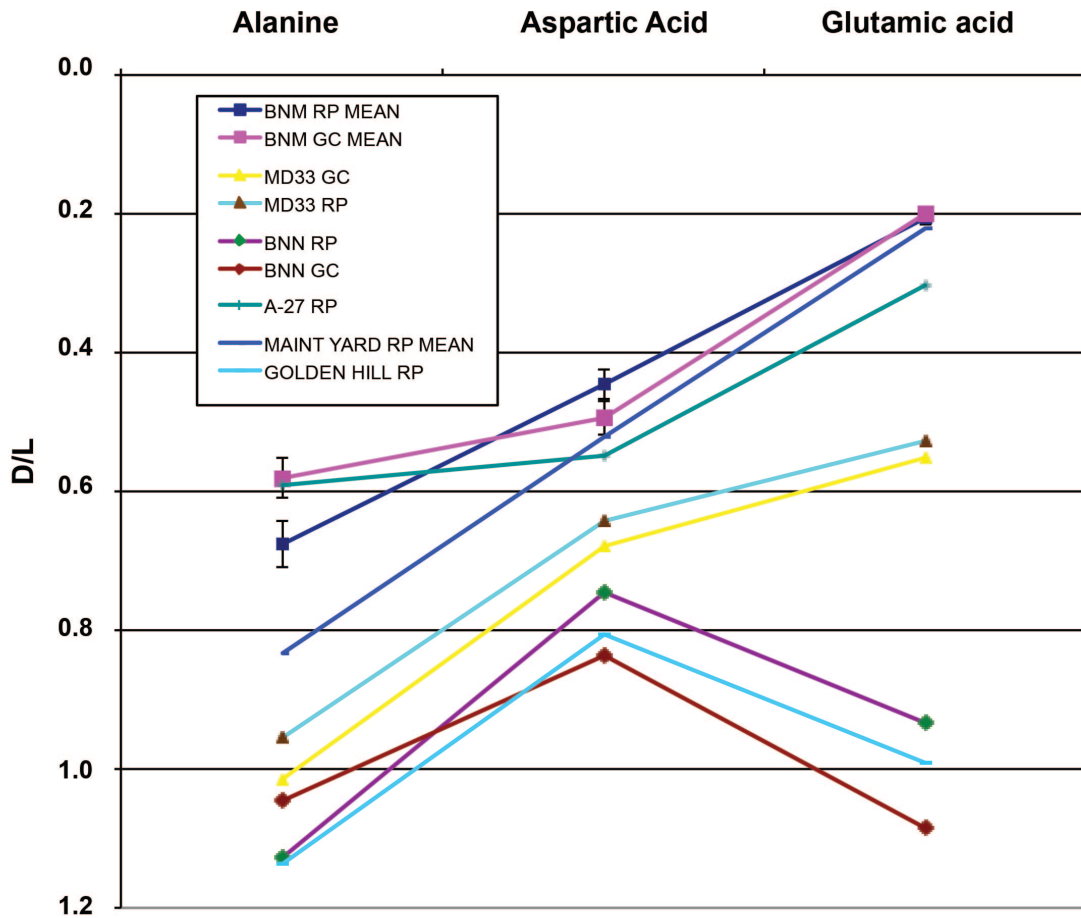


Figure 4-5 (SI2) Amino acid D-L values associated with amino acid racemization samples. Samples labeled with “RP” were processed using reverse phase liquid chromatography (Kaufman and Manley, 1998) at Northern Arizona University. Samples labeled “GC” were processed using amino acid racemization gas chromatography (Wehmiller and Miller, 2000) at the University of Delaware.

Table 4-3 (SI3) ^{10}Be data and erosion rate estimates associated with non-glaciated Susquehanna basins

TABLE SI3 ^{10}Be data and erosion rate estimates associated with non-glaciated Susquehanna basins

Sample	LLNL ID	Location (Dec. degrees lat, long)	Basin Elevation (m)	^{10}Be Concentration ^a (Atoms/g \pm 1 sigma)	Erosion Rate ^b (m/Ma \pm 1 sigma)
JSQ_039	BE18404	40.043, -76.578	239	2.60E+05 \pm 7.17E+03	18.61 \pm 1.40
JSQ_042	BE18405	39.946, -76.368	149	1.82E+05 \pm 5.03E+03	25.75 \pm 1.87
JSQ_043	BE18406	40.010, -76.278	134	2.95E+05 \pm 7.44E+03	14.86 \pm 1.11
JSQ_044	BE18409	40.145, -75.989	195	3.53E+05 \pm 9.55E+03	12.76 \pm 0.99
JSQ_045	BE18653	39.906, -76.329	157	1.71E+05 \pm 5.28E+03	27.53 \pm 2.03
JSQ_001	BE18022	39.946, -76.756	216	2.57E+05 \pm 6.60E+03	18.41 \pm 1.37
JSQ_002	BE18576	40.082, -76.720	194	2.47E+05 \pm 6.55E+03	18.96 \pm 1.41
JSQ_003	BE18023	40.225, -76.898	252	1.89E+05 \pm 5.38E+03	26.6 \pm 1.96
JSQ_005	BE18025	40.323, -77.169	318	3.43E+05 \pm 8.44E+03	14.54 \pm 1.10
JSQ_006	BE18026	40.371, -77.043	287	4.76E+05 \pm 2.46E+04	9.83 \pm 0.92
JSQ_007	BE18528	40.478, -77.129	393	2.18E+05 \pm 5.85E+03	25.18 \pm 1.86
JSQ_009	BE18654	40.890, -77.794	394	3.12E+05 \pm 7.60E+03	17.17 \pm 1.29
JSQ_010	BE18028	40.943, -77.787	412	2.55E+05 \pm 6.73E+03	21.72 \pm 1.62
JSQ_011	BE18027	40.897, -78.677	529	2.39E+05 \pm 6.98E+03	25.24 \pm 1.91
JSQ_012	BE18400	40.216, -78.266	468	4.64E+05 \pm 1.12E+04	11.61 \pm 0.91
JSQ_013	BE18401	40.072, -78.493	496	4.86E+05 \pm 1.19E+04	11.27 \pm 0.89
JSQ_101	BE18533	41.413, -78.197	548	2.20E+05 \pm 6.41E+03	28.25 \pm 2.13
JSQ_165	BE18606	40.021, -76.359	118	3.31E+05 \pm 7.93E+03	12.91 \pm 0.97

^aMeasured at the Lawrence Livermore National Laboratory and normalized to the "07KNSTD" standard with an assumed ratio of 2.85×10^{12} .

^bCalculated using the CRONUS online calculator (Balco et al., 2008)

References Cited (Supplemental Information)

- Genau, R. B., Madsen, J. A., McGeary, S., and Wehmiller, J. F., 1994, Seismic-Reflection Identification of Susquehanna River Paleochannels on the Mid-Atlantic Coastal Plain: *Quaternary Research*, v. 42, p. 166-174.
- Groot, J. J., Ramsey, K. W., and Wehmiller, J. F., 1990, Ages of the Bethany, Beaverdam, and Omar Formations of southern Delaware: Delaware Geological Survey.
- Jacobs, J. M., 1980, Stratigraphy and lithology of Quaternary landforms on the eastern coast of the Chesapeake Bay [MS: University of Delaware, 81 p.]
- Kaufman, D. S., and Manley, W. F., 1998, A new procedure for determining DL amino acid ratios in fossils using reverse phase liquid chromatography: *Quaternary Science Reviews (Quaternary Geochronology)*, v. 17, p. 987–1000.
- Nishiizumi, K., Imamura, M., Caffee, M. W., Southon, J. R., Finkel, R. C., and McAninch, J., 2007, Absolute calibration of ^{10}Be AMS standards: *Nuclear Instruments and Methods in Physics Research B*, v. 258, no. 2, p. 403-413.
- Wehmiller, J. F., and Miller, G. H., 2000, Aminostratigraphic dating methods in Quaternary geology, *in* Noller, J. S., Sowers, J.M., Lettis, W.R., ed., *Quaternary Geochronology, Methods and Applications, Volume 4*, American Geophysical Union Reference Shelf, p. 187–222.
- Xu, S., Dougans, A. B., Freeman, S. P. H. T., Schnabel, C., and Wilcken, K. M., 2010, Improved ^{10}Be and ^{26}Al -AMS with a 5 MV spectrometer: *Nuclear Instruments*

and Methods in Physics Research B, v. 268, p. 736–738.

Xu, S., Freeman, S. P. H. T., Rood, D. H., and Shanks, R. P., 2014, ^{26}Al interferences in accelerator mass spectrometry measurements: Nuclear Instruments and Methods in Physics Research B, v. 333, no. 42-45.

**CHAPTER 5: QUATERNARY GEOLOGIC EVOLUTION OF EAST-
CENTRAL CHESAPEAKE BAY**

For submission to Geosphere

Benjamin D. DeJong, U.S. Geological Survey, Reston, VA, 20192, and
Rubenstein School of the Environment and Natural Resources, University of Vermont,
Burlington, VT 05405, bdejong@usgs.gov, 435-760-5440

Paul R. Bierman, Geology Department and Rubenstein School of the Environment and
Natural Resources, University of Vermont, Burlington, VT, 05405, pbierman@uvm.edu,
802-238-6826

Wayne L. Newell, U.S. Geological Survey, Reston, VA, 20192, wnewell@usgs.gov, 703-
648-6991

Bryan Landacre, U.S. Geological Survey, Reston, VA, 20192, blandacre@usgs.gov, 703-
648-6085

Lucy Edwards, U.S. Geological Survey, Reston, VA, 20192, leedwards@usgs.gov, 703-
648-5272

5.1. Abstract

The Chesapeake Bay, one of the most recognizable and most thoroughly studied coastal features on the East Coast of the United States, took shape over numerous major fluctuations of sea level during the Pleistocene. Ideally, reconstructing this history would include constraining the longest possible section of stratigraphic units both in space and time, but until recently no dating techniques were available for dating large portions of the stratigraphy either due to the paucity of fossil material or because deposits are older than the limit of dating methods. Optically stimulated luminescence and cosmogenic nuclides enable dating of quartz-bearing materials spanning the full Pleistocene. We apply these methods to a high-resolution framework of cut-fill deposits in east-central Chesapeake Bay that include both the oldest recognized Susquehanna paleochannels and the youngest, Late Pleistocene estuarine fill deposit. Limited amino acid racemization ages support cosmogenic nuclide ages, and radiocarbon dating of Holocene sediments reconstructed in three dimensions help understand the Holocene inundation and sediment accumulation. Higher resolution sedimentology, age control and palynology provide paleoenvironmental paleoclimatic proxies for Late Pleistocene deposits. Results indicate that major fluvial cut-fill processes were initiated by at least ~2 Ma, shortly after the onset of North American continental glaciation, and dominated landscape evolution through the Pleistocene. Optically stimulated luminescence ages indicate departures in relative sea level in Chesapeake Bay from eustatic sea-level curves during at least marine isotope stages 5 and 3, and ages are supported by paleoclimate proxies. Holocene

sediments, which form a continuum with marsh habitat threatened by sea-level rise, fills an antecedent topography that was formed during MIS 2; ongoing conversion of salt marsh to open water does not appear to correlate with compressibility of shallow substrate but rather with glaciostatic lowering of the land surface. By establishing age control for a well-defined framework of cut-fill deposits, we show that the Chesapeake Bay subsurface architecture preserves a long and relatively complete record of localized processes, making for a highly complex Pleistocene stratigraphic record.

5.2. Introduction

Despite being the focus of study for over a century, our understanding of Chesapeake Bay's geologic history continues to evolve with more sophisticated and detailed methods of inquiry. Early studies consisted almost exclusively of geomorphic observation (Shattuck, 1901, 1902, 1906). Geologists used the low-relief surfaces separated by scarps that dominate the landscape to form the "marine terrace concept" in which terraces up to ~80 m asl were interpreted as interstadial marine benches and correlated hundreds of kilometers based on surface elevation (Cooke, 1930, 1958). However, local observations indicated problems with this model (Flint, 1940, Hack, 1957), and it was largely abandoned with the first detailed stratigraphic study of units below terrace surfaces, which indicated far greater complexity than could be explained by single transgressive events (Oaks and Coch 1963).

Following the pioneering work of Oaks and Coch (1963), multiple, isolated

observations of paleochannel segments were reported east of Chesapeake Bay (Hansen, 1966; Weigle, 1972; Schubel and Zabawa, 1973; Kehrin et al., 1980; Mixon, 1985) that identified a need to correlate these features regionally. Colman and Mixon (1988) responded with extensive seismic reflection profiles in Chesapeake Bay, which identified a network of three major Susquehanna River paleochannels that crossed under the southern Delmarva Peninsula (Figure 5-1; Colman and Mixon, 1988). A new model of Chesapeake Bay evolution resulted from this work whereby the Delmarva Peninsula progressively grew southward as a barrier system during interglacial highstands that were punctuated by periods of paleochannel incision during glacial periods when sea level fell (Figure 5-1; Colman et al., 1990). Each channel was interpreted as unique to one sea-level cycle, and because the channels cross the southern Delmarva Peninsula under prevalent Late Pleistocene shoreline units (gray shading, Figure 5-1) that were dated by uranium-series (U-series) and amino acid racemization (AAR) methods (Oaks et al., 1974; Cronin, 1981; Mixon, 1985; Szabo, 1985; Wehmiller et al., 1988), the ages produced for emerged shorelines were used to constrain the cutting of channels (Colman et al., 1988). This provided the first-ever model of Chesapeake Bay evolution constrained in space and time.

But more recent seismic work on the Atlantic side of southern Delmarva Peninsula further refined this model by showing that Susquehanna River paleochannels include multiple, stacked cut-fill deposits (Oertel and Foyle, 1995). Albeit this study was not substantiated by sediment coring or age control, seismic facies successions suggest

that paleochannels were reoccupied during multiple sea-level low stands, so each channel does not represent one unique incision event in Chesapeake Bay history as previously assumed (Colman et al., 1990) but rather a long and complex history of cutting and filling. And while further seismic work (Genau et al., 1994) and detailed subsurface studies (Flemming et al., 2011) have validated multiple, stacked fill deposits in paleochannels, the paucity of fossils and uniformity of stacked units limit differentiation into multiple strata (Owens and Denny, 1986).

Additionally, advancements in dating techniques continue to improve our understanding of the Pleistocene geologic history of the mid-Atlantic region. For example, the vast majority of u-series ages produced for emerged units both on southern Delmarva Peninsula and in southwest Virginia, in part used to constrain channel ages by Colman and others (1990), correlates with marine isotope stage (MIS) 5a (review in Wehmiller et al., 2004), when proxies for eustatic sea level indicate seas were >20 m lower than present (Lambeck et al., 2002). First considered controversial, these ages have now become widely recognized as evidence for glacioisostatic adjustment (GIA) of the land surface following the MIS 6 glaciation (Potter and Lambeck, 2003). More recently, optically stimulated luminescence (OSL) dating of fluvio-estuarine deposits from central Chesapeake Bay (DeJong et al., in press) to the southern tip of Delmarva and the Virginia-North Carolina coastal boundary (Mallinson et al., 2008; Scott et al., 2010; Parham et al., 2013) verify the MIS 5a U-series ages and indicate MIS 3 ages for subtle, lower-elevation estuarine surfaces in these locations. Prior to OSL methods,

regional correlation of these surfaces remained difficult because units either lack fossil material or are too old for traditional dating methods such as radiocarbon or u-series. OSL chronologies suggest that GIA-driven subsidence proceeded for many tens of millennia following retreat of MIS 6 ice (Scott et al., 2010) and will maintain high rates of relative sea-level rise in the Chesapeake Bay for the foreseeable future, partially driving conversion of salt marsh to open water along Chesapeake Bay coastlines (DeJong et al., in press).

In this paper we reconstruct the longest Pleistocene stratigraphic record possible for Chesapeake Bay to better understand its early evolution, relative sea-level history, and ongoing sea-level threats. We focus on a region that includes the oldest recognized Susquehanna River paleochannels, the geomorphic surface correlative with MIS 3 deposits, and extensive Holocene accretionary deposits. We work from boreholes to place lithostratigraphic details into a well-defined geologic framework. Multiple dating techniques provide ages from the early Pleistocene to the Holocene; higher-resolution dating and palynology help determine the age and conditions during deposition of Late Pleistocene to Holocene units to reconstruct the Late Pleistocene relative sea-level history. Results indicate a high degree of lithologic variability and stratigraphic complexity that primarily result from sea-level fluctuations dating back to the beginning of the Pleistocene. Two preserved estuarine units date to the cool-temperate MIS 3, which truncate less extensive, erosional remnants of warm-temperate MIS 5a and MIS 5e deposits. The Holocene transgressive deposits, including sediments that form a

continuum with threatened marsh habitat, suggest the Blackwater River channel levees and adjacent marsh kept pace with relative sea level rise over millennial timescales until a threshold was crossed during the 20th century. By placing paleoenvironmental, age, and climate proxies together into a framework, we present a multi-million year, Pleistocene geologic history of complex valley cutting and filling.

5.3. Setting

To reconstruct the geologic history of Chesapeake Bay, we focus on the stratigraphy below the Blackwater National Wildlife Refuge (BNWR), which includes the earliest known paleochannels of the Susquehanna River and the latest highstand deposits of the Pleistocene (DeJong et al., in press). The BNWR is a ~110 km² preserve of tidal lowlands on the western margin of the Delmarva Peninsula below the prominent ~6-7 m Princess Anne-Oak Hall Scarp (Figure 5-1). The surficial unit in the majority of these lowlands has previously been mapped as the Kent Island Formation (Owens and Denny, 1986; Mixon et al., 1989), a lithologically variable map unit in Maryland that is correlative with other shoreline deposits near sea-level with MIS 3 ages (Figure SD1; references therein). Previous investigation of the Kent Island Formation near the field area included extremely limited lithologic, palynologic, and age data, and the topographic maps available at the time were too coarse to identify many of the geomorphic features (Owens and Denny, 1986). So the BNWR surface was interpreted as a featureless, estuarine landscape possibly deposited in a barrier-back-barrier system during either the

Mid-Wisconsinan or the Sangamon (Owens and Denny, 1979; Owens and Denny, 1986). The Kent Island Formation reportedly overlies a clay unit with Pleistocene-aged shells and pollen indicating warm climate and presumed to be equivalent with the Omar Formation of eastern and southern Delmarva Peninsula (see Figure SD1 for regional correlation chart), but its similarity to the Kent Island Formation precluded differentiation of the two units in the field area (Owens and Denny, 1986). Here, we differentiate the Kent Island Formation from the presumed Omar Formation and older units below based on lithology, age, and pollen data.

5.4. Methods

To define the Pleistocene geologic framework of the BNWR we use a dense network of boreholes (n=70) drilled through prominent geomorphic landforms identified in the LiDAR (Light Detection And Radar) DEM (digital elevation model; Figure 5-2). We define the Miocene basement using biostratigraphy (dinoflagellates). The Pleistocene deposits were characterized based on grain size, mineralogy, color, and sedimentary structures (where preserved in cores) to define lithofacies and place them into depositional sequences. Units are placed into a chronostratigraphic framework using cosmogenic nuclide, AAR, and OSL ages. Additionally, we cored 2 parallel transects normal to the Blackwater River valley where ponding has degraded marshes to define the antecedent topography of marsh and see if significant marsh degradation is related to the framework of underlying sediments. We use pollen assemblages as a proxy for climate

at the time of deposition for Late Pleistocene to Holocene deposits. Analyses include moderate-resolution records for two cores that we compare against a high-resolution, ~100 ka pollen record produced in Hybla Valley (Figure 5-1; Litwin et al., 2013), a location that provided continuous accommodation for Pleistocene sediments possibly due to its proximity to a normal fault (Mixon and Newell, 1977). Because oak and pine span a broad range of climatic tolerance but show high frequency change in response to shifting climate in the Hybla record, we use pine-oak proportions as well as presence of cold-tolerant spruce and fir to delineate major climate shifts in the BNWR record. Our moderate-resolution pollen analyses help guide interpretation of pollen data produced from major lithologic units within cores that have age constraints.

5.6. Results

5.6.1. Geomorphology

The LiDAR elevation data (Figure 5-2a) reveal a suite of landforms derived from the most recent processes active on the west-central Delmarva landscape. The geomorphology of the field area can be separated into two prominent zones that are separated by a ~1.2 m, ESE- WNW wave-cut scarp (DeJong et al., in press) with associated beach ridges (orange lines, Figure 5-2b). North of the scarp, the geomorphology is subtle, with a surface that gently rises in elevation from ~1.0 to 3.0 meters and hosts expansive freshwater swamps. South of the scarp, a broad region of ~1-3 km long, curvilinear features interpreted as very large, wave-built sand bars deposited

in long-shore fashion (blue lines, Figure 5-2b) parallel the scarp and overprint a flat, low-elevation (~0.25-0.5 m) surface on which the BNWR marsh is accreting. These long, coast-parallel landforms helped previous workers recognize the landscape as part of back-barrier, estuarine system (Jacobs, 1980; Owens and Denny, 1986), but their full distribution and relationship to previously unrecognized coastal features seen in LiDAR elevation data help to better contextualize these features and confirm the origin of these features in an estuarine setting. In the western portion of the field area, the bars are truncated by a north-south trending meander channel with associated scroll bars (red lines; Figure 5-2b) and by oval depressions (purple lines; Figure 5-2b) interpreted in nearby areas on Delmarva as “Maryland Bays”, ephemeral active basins formed by niveo-eolian processes (Newell and Clark, 2008).

5.6.2. Stratigraphy, lithology, and age

The Quaternary stratigraphy in the field area is largely defined by deeply incised (up to 60 m) paleovalleys cut into the underlying Miocene Chesapeake Group and filled with multiple, vertically stacked transgressive deposits clearly indicating valley reoccupation (Figure 5-3). The “Exmore” and “Eastville” channels of Colman and others (1988), major paleochannels of the Susquehanna River, are oriented north to south on the western end of the field area. Two other local paleochannel systems are also present, one in association with the paleo-Choptank River (Flemming et al., 2011), and one that is geographically located between the two (Figure 5-3). East of the Choptank River

paleochannel, the Quaternary stratigraphy is much thinner and the Tertiary stratigraphy more complete. The valley fill generally consists of transgressive facies successions including basal, sandy gravel grading upward to silty sand and clayey silt with variable shell, sand, and gravel abundances.

The oldest Pleistocene units in the field area include full or nearly full transgressive sequences and were observed in the deepest and most extensive paleovalley fills. Long (>27 m) sequences of massive silt indicate deep valley incision during sea-level lowstands followed by back filling with bay mud during the subsequent rise in sea level (Figure 5-3). Several major gravel units have been dated via cosmogenic radionuclide and amino acid racemization methods in the field area (Table 5-1). These ages indicate channel cutting and filling going back to just after presumed onset of Pleistocene glaciation at ~2 Ma and continuing through the rest of the Pleistocene.

Stratigraphically above the older paleochannel fills, we locally encountered beds that have been previously correlated with the Omar Formation (Figures 5-3, 5-4) of eastern and southern portions of the Delmarva Peninsula (Owens and Denny, 1986). Remnants of this unit consist primarily of dark gray silty clay with locally abundant oyster (*Crassostrea virginica*) shells, though coarsening-upward sequences of peaty silt to silty sand with shell fragments also occur. All sampled units in this age range are truncated to an unknown extent by younger cut-fill deposits, so their pre-erosional elevation range remains unknown. OSL ages from these units range 92.5 ± 14.2 to 68.7 ± 15.2 ka (n=4; all ages reported with 2σ error). We tentatively correlate all units with MIS

5a, recognizing that one sample (USU-1203) statistically could correlate with MIS 5c. On the eastern end of the field area, away from major paleochannels, we also penetrated a dark gray, silty, medium sand below the Kent Island Formation that was not observed elsewhere. One OSL age on these sands indicates 125.0 ± 16.0 ka. We tentatively interpret this deposit as fluvio-estuarine sands deposited during MIS 5e.

The Kent Island Formation directly overlies units of different age, from the Miocene to MIS 5a beds (Figure 5-3). The Kent Island Formation ranges from ~2-9 m in thickness and includes at least two distinct depositional units in the field area separated by unconformities. The lower unit consists of dark greenish gray sandy silt with locally abundant burrows, shells and pebbles. OSL ages from this unit range 54.9 ± 9.2 to 44.8 ± 10.9 ka (n=3). This is interpreted as a paleovalley fill deposited in a low-energy, outer estuarine environment during early MIS 3. The upper unit represents the most laterally extensive unit in the field area and has variable lithofacies. Above the scarp, the upper unit consists of dark gray silty, pebbly sand grading up to a grayish brown, heavily burrowed silt. Below the scarp, in the vicinity of the large sand bars, the Kent Island Formation consists of laminated sand with mud drapes and heavy mineral laminae. Material in the upper unit ranges in age from 62.0 ± 10.8 to 34.9 ± 7.5 ka (n=15). Based on the lithology, geomorphic features, and age, this unit represents a continuum of features characteristic of a shallow-water, estuarine environment during a MIS 3 high stand.

The surface of the Kent Island Formation is unconformably capped by up to 3.0 m

(but typically less than 2.0 m) of mottled, massive silt with variable amounts of very fine sand and clay. This silt package subdues the geomorphology of the area, thinly mantling ridges and filling swales, as observed in a focused study by Jacobs (1980); soils in the BNWR formed predominantly in this parent material.

Holocene deposits accumulated on top of MIS 3-aged sediments of the Kent Island Formation in a valley cut up to -9 m asl during MIS 2 (Figure 5-3). The Holocene stratigraphy includes two primary units in the center of the Blackwater River valley (Figure 5-4). The lower unit ~1.0-6.0 m thick in the middle of the Blackwater River valley, where it consists of massive silt on levees of the present channel, and of alternating laminae of sand, silt, and peat outside of levees (e.g. BARB). The iron phosphate mineral vivianite precipitates locally from finely laminated clay, silt, and sand from this lower unit, which has been identified as an indicator of anoxic, freshwater environments in deposits of the Chesapeake region (Bricker et al., 2003). The lower unit is progressively thinner toward the northern end of the flooded Blackwater River valley. Radiocarbon ages from the lower deposit range ~5500-700 cal ybp. Superimposed on the lower unit is a well-developed grassy peat deposit ranging from ~2.0-4.0 m thick in the Blackwater River valley. Radiocarbon data from the peat indicate modern ages. Based on the 3-dimensional reconstruction of Holocene deposits near the confluence of the Blackwater and Little Blackwater Rivers, antecedent topography formed during low sea levels of MIS 2 primarily controls the thickness and distribution of Holocene sediments, and marsh inundation is not correlated with the thickness of underlying, compressible

Holocene sediments.

5.5.3. Paleoclimate

Pollen analyses provide proxies for climate during deposition of the Late Pleistocene and Holocene sedimentary units of the BNWR stratigraphy (Figures 5-4, 5-5). Results show that the MIS 5a unit includes a *Quercus* (oak)-*Pinus* (pine)-*Carya* (hickory)-*Fagus* (beech) assemblage with lesser amounts of *Liquidambar* (sweet gum), *Tsuga* (hickory) and *Osmunda* (ferns). This assemblage and the relative proportions of fauna are in general agreement with the MIS 5a pollen abundances in the Hybla record, where it was interpreted as humid-subtropical (Litwin et al., 2013). One pollen sample was also collected from the MIS 5e sediments (KD, Figure 5-6), and results indicate a relatively lower pine:oak ratio and a spike in sweet gum, supporting the MIS 5e age of those sediments indicated by OSL.

The Kent Island Formation indicates a significant decrease in the arboreal component with a pine-oak-hickory (lowlands) and pine-oak-spruce (uplands) assemblage with presence of *Abies* (fir); open vegetation plants such as *Poaceae* (grasses), *Asteraceae* (asters), and ferns dominate. Litwin and others (2013) show the largest and most frequently alternating pollen assemblages during MIS 3, and it is likely that our low-moderate resolution records are not capable of recording such changes. We interpret the overall decrease in the arboreal component, increase in pine-oak ratio, increase in open vegetation flora, with the presence of cold-tolerant taxa such as spruce

and fir to indicate a transition to cooler, wetter conditions.

We use these higher resolution records to contextualize and interpret lower resolution pollen records from multiple cores (Figure 5-5). Results show that general patterns are traceable in the subsurface, and that pine-oak ratios mimic those observed in other MIS 3 deposits on Delmarva (e.g. Owens and Denny, 1979; Finkelstein and Kearney, 1988). These climate proxies provide additional confidence in OSL ages by providing relative climate changes between MIS 5e, MIS 5a, and MIS 3.

5.6. Discussion

The Pleistocene stratigraphy underlying the BNWR indicates a higher density of paleochannels and greater complexity than expected based on previous work (Owens and Denny, 1986) and suggests that the region experienced a long history of sea-level fluctuation. By establishing age control for a well-defined framework of paleochannel systems, we show that the Chesapeake Bay subsurface architecture preserves a long and relatively complete record of landscape evolution during the Pleistocene.

5.6.1. Early-Mid Pleistocene paleovalley cutting and filling

Ages produced from gravels collected from paleochannel systems show that major cut-fill processes have been active in the field area for nearly the entire Pleistocene. Cosmogenic nuclide ages ranging from 2.06 ± 0.12 Ma to 0.28 ± 0.10 Ma suggest far longer timescales of fluvial action than previously estimated (Colman et al.,

1990) and indicate active cut-fill processes between deposition of Miocene and Pliocene gravel sheets that form the spine of Delmarva (see textures in Figure 5-1) and the most recent cut-fill units commonly observed on Chesapeake coastlines today. Sample MD50 (1.70 ± 0.08 Ma) appears to be associated with earliest cutting of the Eastville Paleochannel of Colman and others (1990). This age is consistent with the AAR sample MD33, collected from overlying sediments in the same core, and sample DCMD, collected from the same paleochannel to the north (Jacobs, 1980) indicating cut-fill deposits prior to the Exmore paleochannel as suggested by Genau and others (1994). Based on the complexity of channel fills, and the large range in cosmogenic burial and AAR ages produced from stacked deposits, the BNWR stratigraphy supports seismic evidence that paleovalleys were re-occupied multiple times (Oertel and Foyle, 1995) and do not represent singular sea-level cycles (e.g. Colman et al., 1990).

5.6.2. MIS 5: Recognition of mid-Atlantic sea-level anomalies

Based on OSL ages produced on estuarine units at depth in the BNWR stratigraphy, there were two high stands of sea level during MIS 5. The older unit, which produced an age of 125 ± 16 ka ($n=1$) from the uppermost preserved sediments, is from a deposit on the far eastern end of the field area, just outside of the heavily channelized zone. While this is the only preserved erosional remnant dating to MIS 5e age, and we only have one OSL age for this unit, the pollen data as well as amino acid racemization age estimates for *Mercenaria* shells ranging from 130 to 120 ka in several subsurface

units of North Carolina support this interpretation (Wehmiller et al., 2010). Directly dated MIS 5e deposits near present sea level are generally lacking in the mid-Atlantic region (Wehmiller et al., 2004), perhaps due in part to the paucity of datable fossil material, and, to our knowledge, this is the first quantified MIS 5e age on Delmarva. Our data show that OSL can provide a means to identify the extent of MIS 5e material in the region.

We encountered remnants of MIS 5a deposits in several locations under BNWR. OSL ages from these deposits are consistent with chronologies from similar units near present sea level in Virginia and North Carolina (Mallinson et al., 2008; Scott et al., 2010; Parham et al., 2013) that have been the focus of chronostratigraphic studies spanning several decades (the “80 ka problem”; Wehmiller et al., 2004). Long considered spurious, the greater distribution of MIS 5a ages produced for emerged deposits relative to MIS 5e ages has been attributed to intermediate-field effects of GIA from the Laurentide Ice Sheet. The age-elevation relationships of these deposits, and specifically latitudinal trends in these relationships have been used to constrain GIA following deglaciation of the MIS 6 termination (Potter and Lambeck, 2003). The presence of MIS 5a deposits at or near sea level suggests that today’s landscape remains uplifted ~23-29 m above equilibrium (Potter and Lambeck, 2003; Mallinson et al., 2008). The lithology, elevation, and age control of MIS 5a highstand deposits under the BNWR further support the notion that the mid-Atlantic region remains isostatically uplifted (Wehmiller et al., 2004; Mallinson et al., 2008; Scott et al., 2010; Parham et al., 2013).

5.6.3. MIS 3: Expansion of the “80 ka problem”

Similar to MIS 5a deposits, we interpret the geomorphology, lithology, and OSL ages associated with the Kent Island Formation in the BNWR as indicative of shallow-water, estuarine deposition during MIS 3. This interpretation echoes several recent studies from Virginia (Pavich et al., 2006; Scott et al., 2010) to North Carolina (Mallinson et al., 2008; Litwin et al., 2013; Parham et al., 2013) that also employ OSL dating techniques to constrain ages of Late Pleistocene estuarine-marine units. These observations continue to build upon decades of observations suggesting MIS 3 highstand deposition in the mid-Atlantic region (Susman and Heron, 1978; Owens and Denny, 1979; Finkelstein and Kearney, 1988) that have been controversial (Colman et al., 1989; Wellner et al., 1993).

A MIS 3 highstand implies further deviation in mid-Atlantic relative sea levels from eustatic sea level curves, likely due to GIA. Multiple sea-level proxies, including oxygen isotope records from benthic and planktonic foraminifera and ice cores, sedimentary sequences, and dated coral reef terrace records indicate eustatic sea levels ~40 to 80 m below present during MIS 3, with at least four large magnitude (10-20 m) fluctuations between these levels during this time (review and references in Siddall et al., 2008). But corals in Vanuatu (Cabioch and Ayliffe, 2001) and offshore sequences in passive margins with minimal influence of GIA (Rodriguez et al., 2000; Murray-Wallace et al., 1993) suggest sea levels rose as high as 15-22 m below present during this time. Provided the mid-Atlantic region was glacioisostatically lowered by as much as 26 m

relative to present by MIS 5a (Potter and Lambeck, 2003; Mallinson et al., 2008), and continued to subside between MIS 5a and MIS 3, low-elevation mid-Atlantic surfaces could easily have been submerged, if for only short time periods. The relative paucity of emergent MIS 3 shorelines reported in the literature globally, except in areas with rapidly uplifting coastlines (review in Pedoja et al., 2014), and the results of several glacio-isostatic models identifying the mid-Atlantic region as the apex of a glacial forebulge (Peltier, 1986; Davis and Mitrovica, 1986; Potter and Lambeck, 2003; Peltier, 2009) suggests the MIS 3 shoreline features near present sea level in the mid-Atlantic region are unique, and likely related to the continued effects of GIA.

At least two MIS 3 units with statistically overlapping 2-sigma OSL ages and separated by an unconformity are observed under the BNWR. This observation is consistent with short-lived periods of submersion in which relatively low-elevation portions of mid-Atlantic coastlines, which were isostatically lowered during that time (Potter and Lambeck, 2003), were locally impacted by high-frequency and high magnitude sea-level fluctuations (Siddall et al., 2008). The two MIS 3 units are not preserved over the entire field area, but based on the localized nature of cut-fill processes in this landscape based on the full distribution of Pleistocene deposits in the BNWR stratigraphy, we would not anticipate laterally extensive units preserved from previous high stands. The localized, short-lived nature of MIS 3 deposition that we observed based on firm, numerical dating may help reconcile seemingly contrasting observations in the mid-Atlantic during this time. For example, it is possible that loess deposition

(Lowery et al., 2011) or upland bog sedimentation (Ramsey, 2010) proceeded in slightly higher elevation areas while the lowest-elevation coastlines were submerged.

5.6.4. MIS 2: Low sea levels and a frozen landscape

The youngest age recorded for Kent Island estuarine deposits at the BNWR is 34.9 ± 7.5 ka. This age marks the onset of major ice-sheet growth in the Northern Hemisphere (Winograd, 2001), a significant drop in eustatic sea level (Lisiecki and Raymo, 2005), and a pulse of rapid incision on upstream reaches of the Susquehanna and Potomac Rivers (Reusser et al., 2004). The paleoclimate record from Hybla Valley indicates a regional transition from cold-temperate conditions at terminal MIS 3 to high boreal conditions during MIS 2 (Litwin et al., 2013). OSL ages from elliptical basins formed in bar sands of the Kent Island Formation range from 30.4 ± 3.4 to 25.8 ± 4.7 ka, (n=3), indicating cryoburbation processes became active shortly after the land surface became emerged. These ages are consistent with the onset of major periglacial dune activity by at least ~ 33 ka west of Chesapeake Bay (Markewich et al., 2009) and by ~ 30 ka on the uplands of Delmarva (Denny and Owens, 1979; Denny et al., 1979). Based on the distribution of thermal contraction crack polygons observed in the mid-Atlantic coastal plain, the BNWR sits right at the southern boundary of continuous permafrost during the Last Glacial Maximum (Gao, 2014).

The sandy silt unit that variably caps the BNWR surface has been a focus of previous investigation (Jacobs, 1980; Wah, 2003). Previous interpretations suggest this

unit is a terminal-Pleistocene loess package that draped large portions of the Delmarva landscape (Foss et al., 1979). The loess at the BNWR has previously been correlated to a well-preserved exposure on Tilghman's Island, ~35 km north of the BNWR, where archeological evidence suggests that loess deposition ceased by ~11,500 years ago (Lowery et al., 2010).

5.6.5. MIS 1: Marsh establishment, growth, and submergence

Holocene sediments within the Blackwater River valley rest unconformably over the Kent Island Formation. The BNWR became inundated by at least 5310-5572 cal ybp, the oldest age we produced for the basal silt package. Near Blackwater River levees, rapidly alternating facies at the base of Holocene sediments (BARB and HARPB locations; Figure 4), and precipitation of vivianite, an indicator of fresh-water river inputs, suggest that the Blackwater River has been active in these locations since ~2000 cal ybp. This implies that Blackwater River levee accretion has kept pace with sea-level rise over millennial timescales with minimal lateral migration. This stability was disturbed during the 20th century, based on major conversion of salt marsh to open water in this locality between 1938 and the present (Figure 4). This may be the result of a 20th century acceleration in relative sea-level rise (Engelhart et al., 2009), leading to suboptimum elevations of adjacent marsh. This results in reduced root growth and a reduced rate of marsh accretion for BNWR marshes (Kirwan and Guntenspergen, 2012). Importantly, these processes will likely continue for the foreseeable future as relative sea-

level rise accelerates (Engelhart et al., 2009) and the land surface continues to subside from GIA (DeJong et al., in press), irrespective of management practices such as the frequency and intensity of prescribed burns of salt marsh (Cahoon et al., 2010).

5.7. Conclusions

Recognition of the detailed geologic evolution of the Chesapeake Bay continues to improve with advancements in methods available to interrogate the stratigraphy. Our development of multi-proxy chronostratigraphic and paleoenvironmental datasets within the complete Pleistocene framework under the BNWR offers important details regarding the Pleistocene evolution of Chesapeake Bay, the largest estuary in North America. Using cosmogenic nuclides we show that Chesapeake Bay evolution spans far greater timescales than previously understood, $> 2\text{My}$. Processes related to major cutting and filling of paleochannels dominate the Pleistocene geologic history. During the Late Pleistocene, there is clear evidence, from the stratigraphy and OSL chronology of the BNWR, indicating departures in relative sea levels of the mid-Atlantic from global trends. The building consensus that the landscape was submerged during MIS 3 implies long timescales of GIA in the intermediate field of Laurentide ice, and that high rates of sea-level rise in the region are rooted in geologic processes that will continue for the foreseeable future (DeJong et al., in press). Subsurface details of the Holocene stratigraphy at the BNWR, part of the most expansive and threatened expanse of tidal marsh in the Chesapeake Bay, suggest that marsh accretion is relatively young ($<1,000$

yr), and that 21st century inundation and conversion of marsh to open water reflects disequilibrium in the Blackwater River and marsh accretionary processes that were metastable over millennial timescales.

5.8. Acknowledgements

This research was supported by the USGS. M. Whitbeck (USFWS) and colleagues granted access to the BNWR, and many residents provided access to their private property. USGS drillers E. Cobbs, J. Grey make this work possible. We thank many who assisted in data collection, analysis, and interpretation including M. Nelson, A. Benthem, J. Wehmiller, I. Clark, H. Pierce, D. Powars, M. Pavich, J. McGeehin, and J. Smoot.

5.9. References

- Bricker, O. P., Newell, W. L., and Simon, N. S., 2003, Bog Iron Formation in the Nassawango Watershed, Maryland: USGS Open File Report 2003-346.
- Cabioch, G., and Ayliffe, L. K., 2001, Raised Coral Terraces at Malakula, Vanuatu, Southwest Pacific, Indicate High Sea Level During Marine Isotope Stage 3: *Quaternary Research*, v. 56, no. 3, p. 357-365.
- Cahoon, D. R., G. Guntnerspergen, S. Baird, J. Nagel, P. Hensel, J. Lynch, D. Bishara, P. Brennand, J. Jones, and C. Otto. 2010. Do annual prescribed fires enhance or slow the loss of coastal marsh habitat at Blackwater National Wildlife Refuge? Final

Project Report (JFSP Number: 06-2-1-35) March 31, 2010. Beltsville, MD.

- Colman, S. M., Halka, J. P., Hobbs III, C. H., Mixon, R. B., and Foster, D. S., 1990, Ancient channels of the Susquehanna River beneath Chesapeake Bay and the Delmarva Peninsula: *Geological Society of America Bulletin*, v. 102, p. 1268-1279.
- Colman, S. M., and Mixon, R. B., 1988, The record of major Quaternary sea-level changes in a large coastal plain estuary, Chesapeake Bay, Eastern United States: *Palaeogeography, Palaeoclimatology, Palaeoecology*, v. 68, p. 99-116.
- Colman, S. M., Mixon, R. B., Rubin, M., Bloom, A. L., and Johnson, G. H., 1989, Comments and Reply on "Late Pleistocene barrier-island sequence along the southern Delmarva Peninsula: Implications for middle Wisconsin sea levels": *Geology*, v. 17, no. 1, p. 84.
- Cooke, C. W., 1930, Correlation of Coastal Terraces: *The Journal of Geology*, v. 38, p. 577-589.
- Cooke, C. W., 1958, Pleistocene shorelines in Maryland: *Geological Society of America Bulletin*, v. 69, no. 9, p. 1187-1190.
- Cronin, T. M., Szabo, B. J., Ager, T. A., Hazel, J. E., and Owens, J. P., 1981, Quaternary Climates and Sea Levels of the U.S. Atlantic Coastal Plain: *Science*, v. 211, no. 4479, p. 233-240.
- Davis, J. L., and Mitrovica, J. X., 1996, Glacial isostatic adjustment and the anomalous tide gauge record of eastern North America: *Nature*, v. 379, p. 331-333.

- DeJong, B. D., Bierman, P. R., Newell, W. L., Rittenour, T. M., Mahan, S. A., Balco, G., and Rood, D. H., In press, Pleistocene relative sea levels in the Chesapeake Bay region and their implications for the next century: *GSA Today*.
- Denny, C. S., and Owens, J. P., 1979, Sand Dunes on the Central Delmarva Peninsula, Maryland and Delaware, US Geological Survey Professional Paper 1067-C, p. 1-15.
- Denny, C. S., Owens, J. P., Sirkin, L. A., and Rubin, M., 1979, The Parsonsburg Sand in the Central Delmarva Peninsula, Maryland and Delaware, US Geological Survey Professional Paper 1067-B, p. 1-16.
- Engelhart, S. E., Horton, B. P., Douglas, B. C., Peltier, W. R., and Tornqvist, T. E., 2009, Spatial variability of late Holocene and 20th century sea-level rise along the Atlantic coast of the United States: *Geology*, v. 37, no. 12, p. 1115-1118.
- Finkelstein, K. F., and Kearney, M. S., 1988, Late Pleistocene barrier-island sequence along the southern Delmarva Peninsula: Implications for middle Wisconsin sea levels: *Geology*, v. 16, p. 41-45.
- Fleming, B. J., DeJong, Benjamin D., Phelan, Daniel J., 2011, *Geology, Hydrology, and Water Quality of the Little Blackwater River Watershed, Dorchester County, Maryland, 2006-2009*. US Geological Survey Special Investigations Report 2011-5054 p. 1-27.
- Flint, R. F., 1940, Pleistocene features of the Atlantic Coastal Plain, *Am. Jour. Sci.*, v. 238, no. 11, p. 757-787.

- Foss, J. E., Fanning, D. S., Miller, F. P., and Wagner, D. P., 1978, Loess deposits of the Eastern Shore of Maryland: *Soil Science Society of America Journal*, v. 42, no. 2, p. 329-334.
- Gao, C., 2014, Relict Thermal-contraction-crack Polygons and Past Permafrost South of the Late Wisconsinan Glacial Limit in the Mid-Atlantic Coastal Plain, USA: *Permafrost and Periglacial Processes*, p. 144-149.
- Genau, R. B., Madsen, J. A., McGeary, S., and Wehmiller, J. F., 1994, Seismic-Reflection Identification of Susquehanna River Paleochannels on the Mid-Atlantic Coastal Plain: *Quaternary Research*, v. 42, p. 166-174.
- Hack, J. T., 1957, Submerged river system of Chesapeake Bay: *Geological Society of America Bulletin*, v. 68, no. 7, p. 817-830.
- Hansen, H. J., 3rd, 1966, Pleistocene stratigraphy of the Salisbury area, Maryland, and its relationship to the lower Eastern Shore—A subsurface approach, Maryland Geological Survey Report of Investigations 2, p. 56.
- Jacobs, J. M., 1980, Stratigraphy and lithology of Quaternary landforms on the eastern coast of the Chesapeake Bay [unpublished MS thesis: University of Delaware], 81 p.
- Kerhin, 1974, Recognition of beach and nearshore depositional features of Chesapeake Bay: *MD Geol. Surv. Paper M2*, p. 1269-1274.
- Kirwan, M. L., and Guntenspergen, G. R., 2012, Feedbacks between inundation, root production, and shoot growth in a rapidly submerging brackish marsh: *Journal of*

- Ecology, v. 100, no. 3, p. 764-770.
- Lambeck, K., Yokoyama, Y., and Purcell, A., 2002, Into and out of the Last Glacial Maximum: sea-level change during Oxygen Isotope Stages 3 and 2: Quaternary Science Reviews, v. 21, p. 343-360.
- Lisiecki, L. E., and Raymo, M. E., 2005, A Pliocene-Pleistocene stack of 57 globally distributed benthic $\delta^{18}\text{O}$ records: Paleoceanography, v. 20, no. 1, p. 1-17.
- Litwin, R. J., Smoot, J. P., Pavich, M. J., Markewich, H. W., Brook, G., and Durika, N. J., 2013, 100,000-year-long terrestrial record of millennial-scale linkage between eastern North American mid-latitude paleovegetation shifts and Greenland ice-core oxygen isotope trends: Quaternary Research, v. 80, no. 2, p. 291-315.
- Lowery, D. L., O'Neal, M. A., Wah, J. S., Wagner, D. P., and Stanford, D. J., 2010, Late Pleistocene upland stratigraphy of the western Delmarva Peninsula, USA: Quaternary Science Reviews, v. 29, no. 11–12, p. 1472-1480.
- Mallinson, D., Burdette, K., Mahan, S., and Brook, G., 2008, Optically stimulated luminescence age controls on late Pleistocene and Holocene coastal lithosomes, North Carolina, USA: Quaternary Research, v. 69, no. 1, p. 97-109.
- Markewich, H. W., Litwin, R. J., Pavich, M. J., and Brook, G. A., 2009, Late Pleistocene eolian features in southeastern Maryland and Chesapeake Bay region indicate strong WNW–NW winds accompanied growth of the Laurentide Ice Sheet: Quaternary Research, v. 71, no. 3, p. 409-425.
- Mixon, R. B., 1985, Stratigraphic and Geomorphic Framework of Uppermost Cenozoic

- Deposits in the Southern Delmarva Peninsula, Virginia and Maryland, US Geological Survey Professional Paper 1067-G, 53 pp.
- Mixon, R. B., Berquist, C. R., Newell, W. L., and Johnson, G. H., 1989, Geologic map and generalized cross sections of the coastal plain and adjacent parts of the piedmont, Virginia, Reston, Virginia.
- Murray-Wallace, C. V., Belperio, A. P., Gostin, V. A., and Cann, J. H., 1993, Amino acid racemization and radiocarbon dating of interstadial marine strata (oxygen isotope stage 3), Gulf St. Vincent, South Australia: *Marine Geology*, v. 110, p. 83–92.
- Newell, W. L., and Clark, I., 2008, Geomorphic map of Worcester County, Maryland, interpreted from a LiDAR-based digital elevation model, US Geological Survey Open File Report 2008-1005, p. 34.
- Newell, W. L., and DeJong, B. D., 2011, Cold-climate slope deposits and landscape modifications of the Mid-Atlantic Coastal Plain, Eastern USA: *Geological Society, London, Special Publications*, v. 354, no. 1, p. 259-276.
- Oaks, R. A., Coch, N. K., Sanders, J. E., and Flint, R. F., 1974, Post-Miocene shorelines and sea levels, Southeastern Virginia, *in* Oaks, R. A., and DuBar, J. R., eds., *Post-Miocene Stratigraphy Central and Southern Atlantic Coastal Plain*: Logan, UT, Utah State University Press, p. 53-87.
- Oaks, R. Q., Jr., and Coch, N. K., 1963, Pleistocene Sea Levels, Southeastern Virginia: *Science*, v. 140, no. 3570, p. 979-983.
- Oertel, G. F., and Foyle, A. M., 1995, Drainage Displacement by Sea-Level Fluctuation

- at the Outer Margin of the Chesapeake Seaway: *Journal of Coastal Research*, v. 11, no. 3, p. 583-604.
- Owens, J. P., and Denny, C. S., 1979, Upper Cenozoic deposits of the Central Delmarva Peninsula, Maryland and Delaware, US Geological Survey Professional Paper 1067-A, p. 1-28.
- Owens, J. P., and Denny, C. S., 1986, Geologic Map of Dorchester County: US Geological Survey Printing, Reston, VA.
- Parham, P. R., Riggs, S. R., Culver, S. J., Mallinson, D. J., Jack Rink, W., and Burdette, K., 2013, Quaternary coastal lithofacies, sequence development and stratigraphy in a passive margin setting, North Carolina and Virginia, USA: *Sedimentology*, v. 60, no. 2, p. 503-547.
- Pavich, M. J., Markewich, H. W., and Brook, G. A., 2006, Significance of Kent Island Formation to geomorphic history of the Mid-Atlantic region, Geological Society of America, Volume Abstracts with programs 38, p. 226.
- Pedoja, K., Husson, L., Johnson, M. E., Melnick, D., Witt, C., Pochat, S., Nexer, M., Delcaillau, B., Pinegina, T., Poprawski, Y., Authemayou, C., Elliot, M., Regard, V., and Garestier, F., 2014, Coastal staircase sequences reflecting sea-level oscillations and tectonic uplift during the Quaternary and Neogene: *Earth-Science Reviews*, v. 132, p. 13-38.
- Peltier, W. R., 1986, Deglaciation induced vertical motion of the North American continent and transient lower mantle rheology: *Journal of Geophysical Research*,

v. 91, no. B8, p. 9099-9123.

Peltier, W.R., 2009, Closure of the budget of global sea level rise over the GRACE era: the importance of magnitudes of the required corrections for global glacial isostatic adjustment: *Quaternary Science Reviews*, v. 28, p. 1658-1674.

Potter, E.-K., and Lambeck, K., 2003, Reconciliation of sea-level observations in the Western North Atlantic during the last glacial cycle: *Earth and Planetary Science Letters*, v. 217, no. 1-2, p. 171-181.

Ramsey, K. W., 2010, Stratigraphy, correlation, and depositional environments of the middle to late Pleistocene interglacial deposits of southern Delaware, Delaware Geological Survey Report of Investigations 76, Newark, Delaware, p. 43.

Reusser, L. J., Bierman, P. R., Pavich, M. J., Zen, E.-a., Larsen, J., and Finkel, R. C., 2004, Rapid Late Pleistocene Incision of Atlantic Passive-Margin River Gorges: *Science*, v. 305, p. 499-502.

Rodriguez, A. B., Anderson, J. B., Banfield, L. A., Taviani, M., Abdulah, K., and Snow, J. N., 2000, Identification of a -15 m middle Wisconsin shoreline on the Texas inner continental shelf: *Palaeogeography, Palaeoclimatology, Palaeoecology*, v. 158, p. 25-43.

Schubel, J. R., and Zabawa, C. F., 1972, A Pleistocene Susquehanna River Channel Connects the Lower Reaches of the Chester, Miles, and Choptank Estuaries: *Chesapeake Biological Laboratory Special Report*, v. 24.

Scott, T. W., Swift, D. J. P., Whittecar, G. R., and Brook, G. A., 2010, Glacioisostatic

- influences on Virginia's late Pleistocene coastal plain deposits: *Geomorphology*, v. 116, no. 1-2, p. 175-188.
- Siddall, M., Rohling, E. J., Thompson, W. G., and Waelbroeck, C., 2008, Marine isotope stage 3 sea level fluctuations: Data synthesis and new outlook: *Reviews of Geophysics*, v. 46, no. 4, p. 29 p.
- Shattuck, G. B., 1901, The Pleistocene problem of the North Atlantic Coastal Plain, *American Geologist*, v. 28, p. 87-107.
- Shattuck, G. B., 1902, The geology of the Coastal Plain formations, *in* The physical features of Cecil County, Maryland Geol. Survey, Cecil County [Volume], p. 149-194.
- Shattuck, G.B., 1906, The Pliocene and Pleistocene deposits of Maryland: Maryland Geol. Survey, Pliocene and Pleistocene [Volume], p. 21-137.
- Susman, K. R., and Heron, S. D., 1979, Evolution of a barrier island—Shackleford Banks, Carteret County, North Carolina: *Geological Society of America Bulletin*, v. 90, p. 205-215.
- Szabo, B. J., 1985, Uranium-series dating of fossil corals from marine sediments of southeastern United States Atlantic coastal plain: *Geological Society of America Bulletin*, v. 96, p. 398–406.
- Wah, J. S., 2003, The origin and pedogenic history of quaternary silts on the Delmarva Peninsula in Maryland [unpublished PhD]: University of Maryland, College Park.
- Wehmiller, J. F., Belknap, D. F., Boutin, B. S., Mirecki, J. E., Rahaim, S. D., and York,

- L. L., 1988, A review of the aminostratigraphy of Quaternary mollusks from United States Atlantic Coastal Plain sites: GSA Special Paper, v. 227, p. 69-110.
- Wehmiller, J. F., Simmons, K. R., Cheng, H., Edwards, L. R., Martin-McNaughton, J., York, L. L., Krantz, D. E., and Shen, C.-C., 2004, Uranium-series coral ages from the US Atlantic Coastal Plain—the “80ka problem” revisited: Quaternary International, v. 120, no. 1, p. 3-14.
- Wehmiller, J. F., Thieler, E. R., Miller, D., Pellerito, V., Bakeman Keeney, V., Riggs, S. R., Culver, S., Mallinson, D., Farrell, K. M., and York, L. L., 2010, Aminostratigraphy of surface and subsurface Quaternary sediments, North Carolina coastal plain, USA: Quaternary Geochronology, v. 5, no. 4, p. 459-492.
- Weigle, J. M., 1972, Exploration and mapping of Salisbury paleochannel, Wicomico County, Maryland: Maryland Geological Survey Bulletin, v. 31, no. 2, p. 61-123.
- Wellner, R. W., Ashley, G. M., and Sheridan, R. E., 1993, Seismic stratigraphic evidence for a submerged middle Wisconsin barrier: Implications for sea-level history: Geology, v. 21, no. 2, p. 109-112.
- Winograd, I. J., 2001, The magnitude and proximate cause of ice-Sheet growth since 35,000 yr B.P.: Quaternary Research, v. 56, p. 299-307.

5.10. Figure captions

Figure 5-1. Map of the mid-Atlantic region. Pleistocene marine highstand coastal and estuarine terrace deposits (gray shading) are superimposed upon deeply weathered,

Miocene–Pliocene upland gravel (circle-and-dot hatching) with oldest Miocene deltaic deposits (dot pattern) shown. White areas within coastlines indicate flowing or standing water and fringing Holocene sediments; arrows indicate paleoflow directions of Pliocene gravels; star indicates location of the Hybla Valley. Paleochannel locations from Colman et al., 1990 (see Figure SD2 for higher resolution); modified from Newell and DeJong (2011).

Figure 5-2. LIDAR imagery, geology, and geomorphology of the BNWR. A. LiDAR-derived DEM of the BNWR. Cell size is 2.5 by 2.5 m; graduated elevation scale indicated to the left of the image exaggerates subtle features in the lowest elevation ranges. White outline indicates location of the BNWR. B. Geology and geomorphology as referenced in the text draped over LiDAR imagery as in A.

Figure 5-3. Cross-section with age proxies. This line shows the full distribution of the Pleistocene stratigraphy under the BNWR with OSL (*italic*), isochron (underlined), and AAR (**bold**) ages as well as dinoflagellate zones (DN#) established for the Miocene stratigraphy (see Figure SD3 for dinoflagellate zonation and correlation chart). A-A' location shown in Figure 2.

Figure 5-4. Transect across the Blackwater River valley showing the Holocene stratigraphy overlapping sediments of MIS3-2 age. Ages are in calibrated radiocarbon

ybp. A moderate-resolution pollen assemblage is provided for the far northeastern core showing paleoenvironmental change. Location is indicated in Figure 2.

Figure 5-5. Cross-sectional diagram of pollen data indicating paleo-environmental change. Note the MY core is of highest resolution; others were sampled primarily at major changes in lithology. Texture key as in Figure 3.

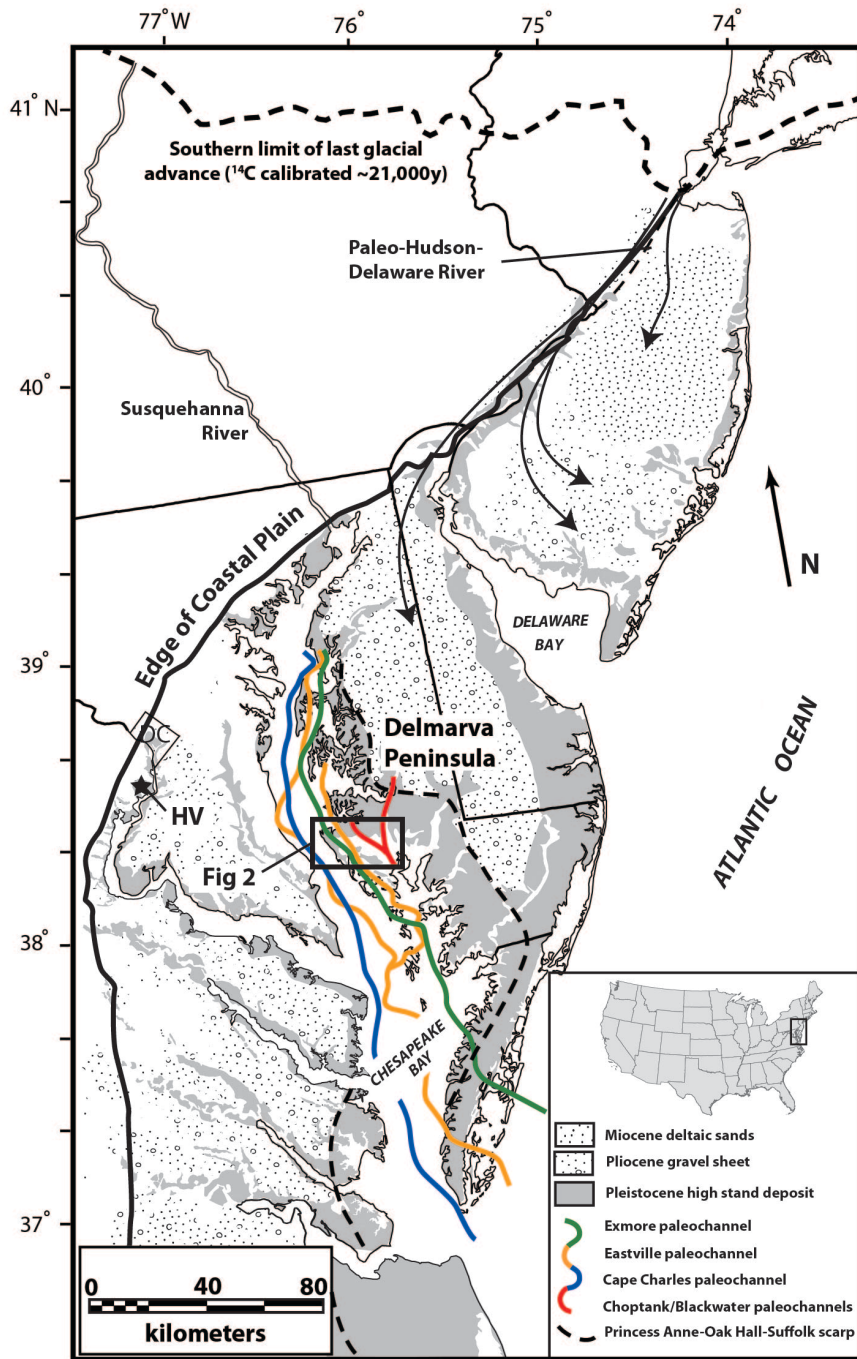


Figure 5-1 Map of the mid-Atlantic region

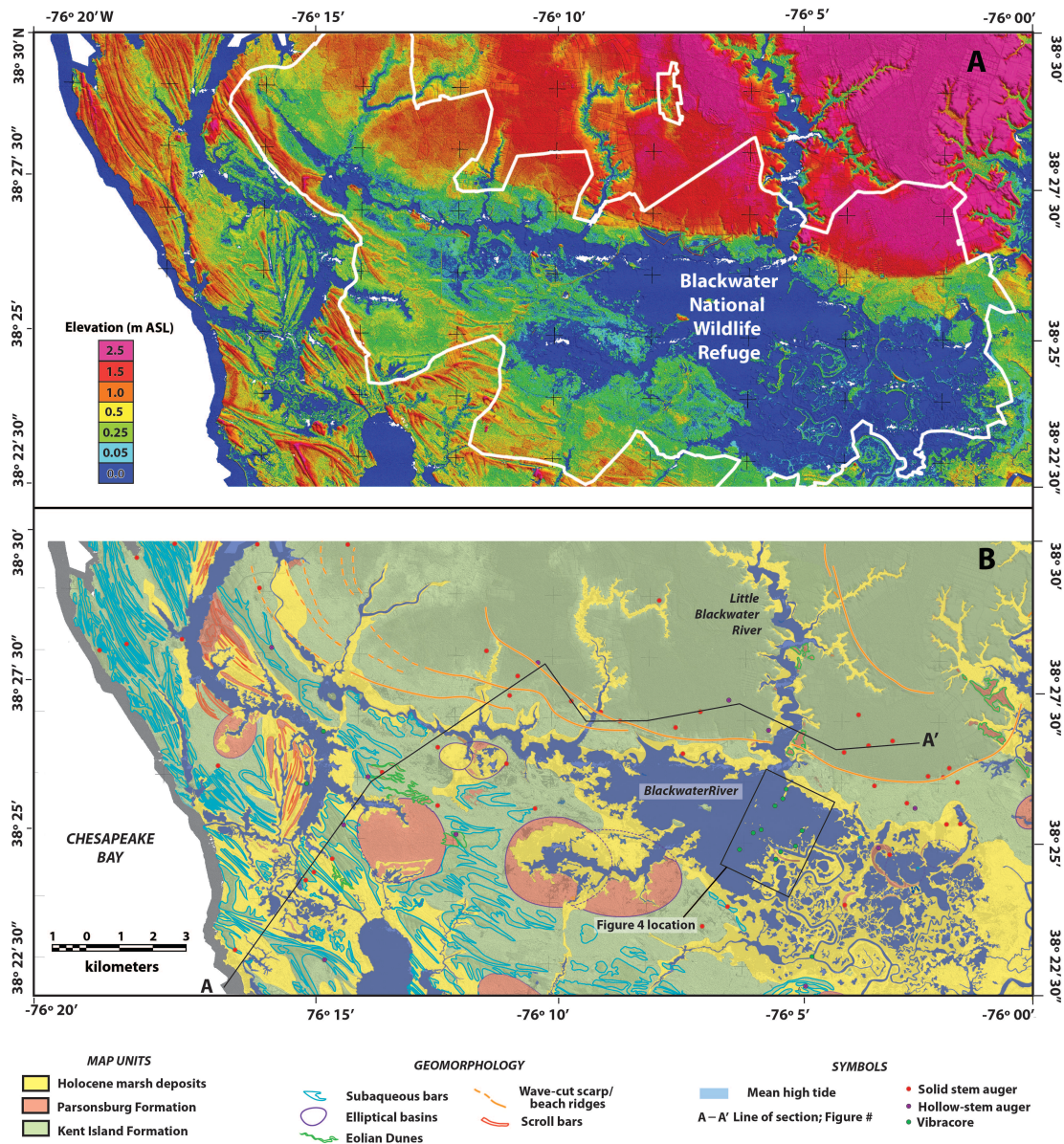


Figure 5-2 LIDAR imagery, geology, and geomorphology of the BNWR

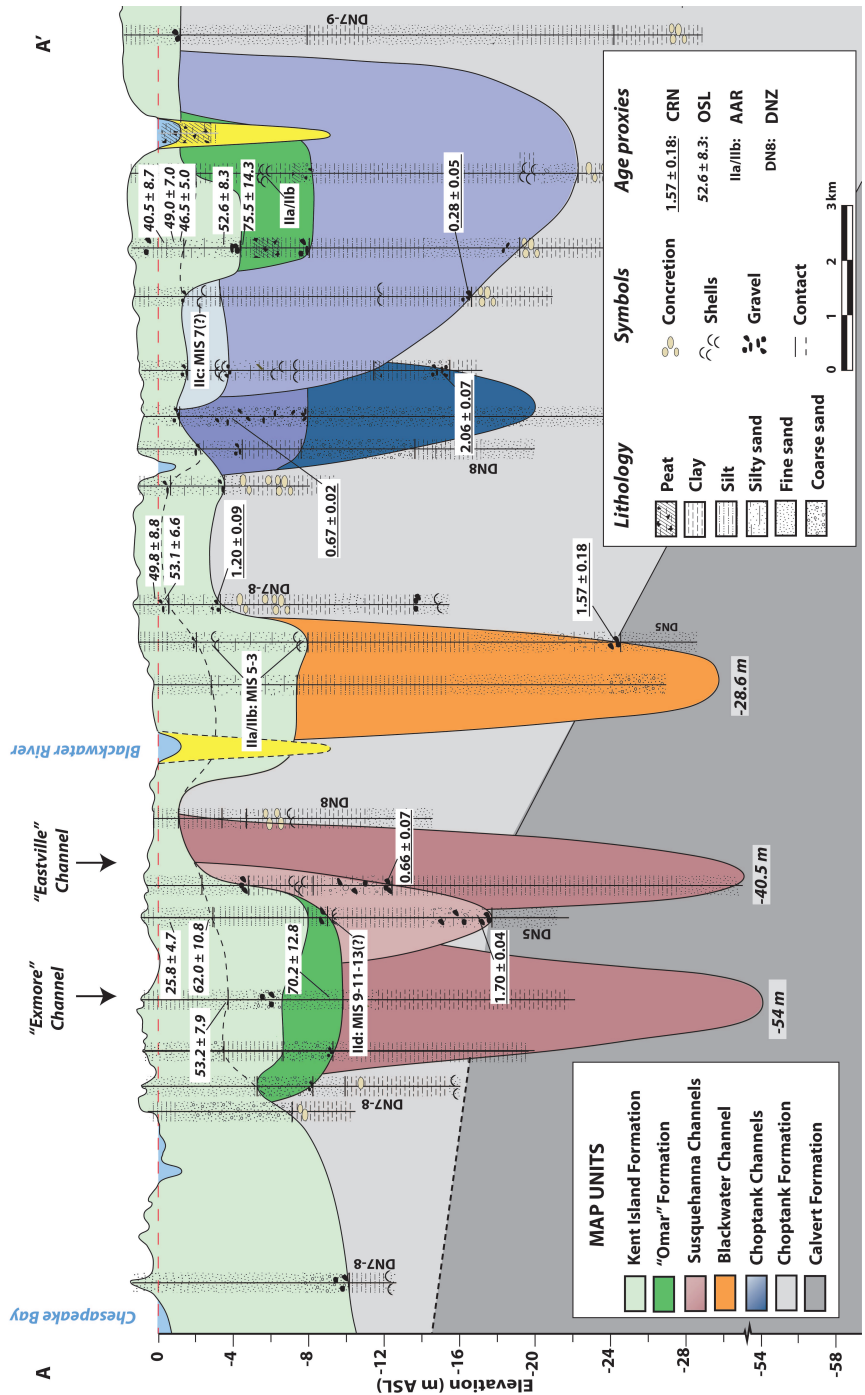


Figure 5-3 Cross-section with age proxies

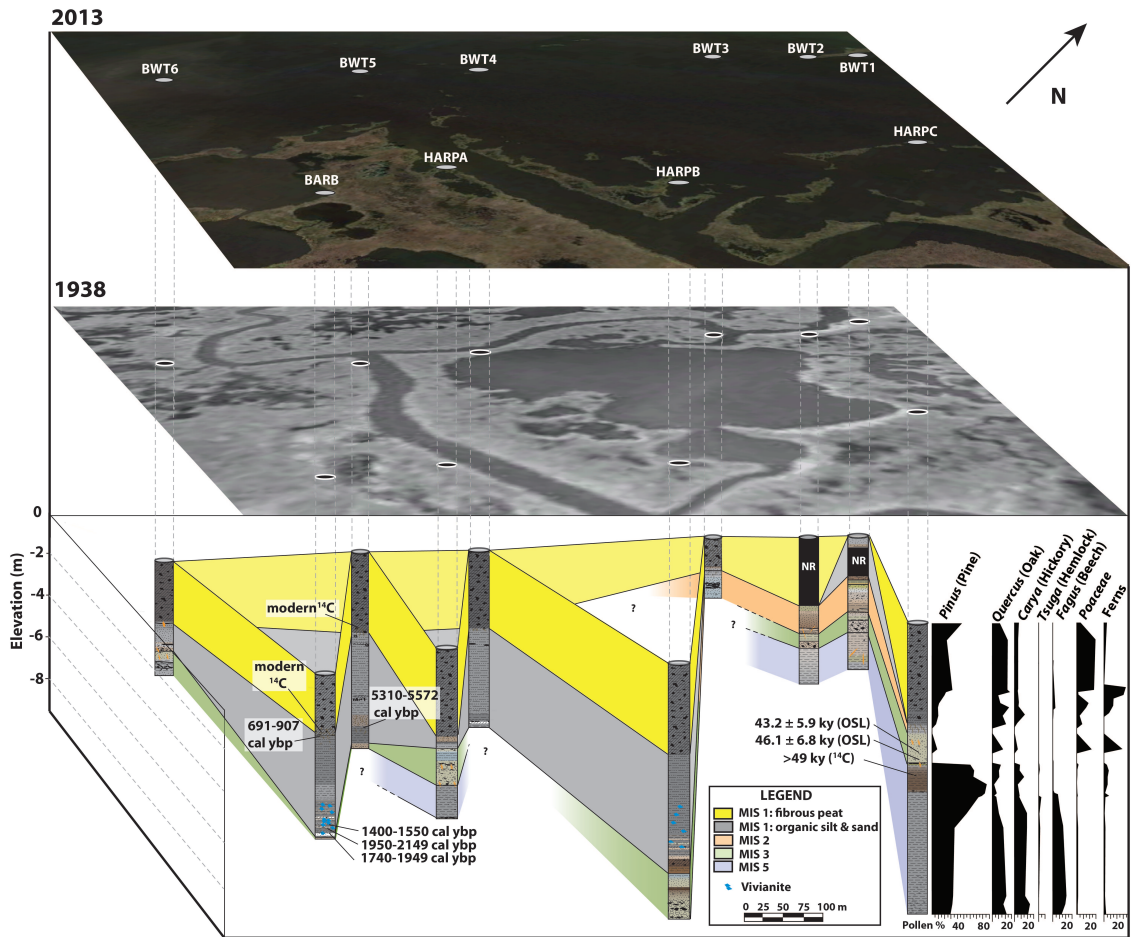


Figure 5-4 Transect across the Blackwater River valley showing the Holocene stratigraphy overlapping sediments of MIS3-2 age

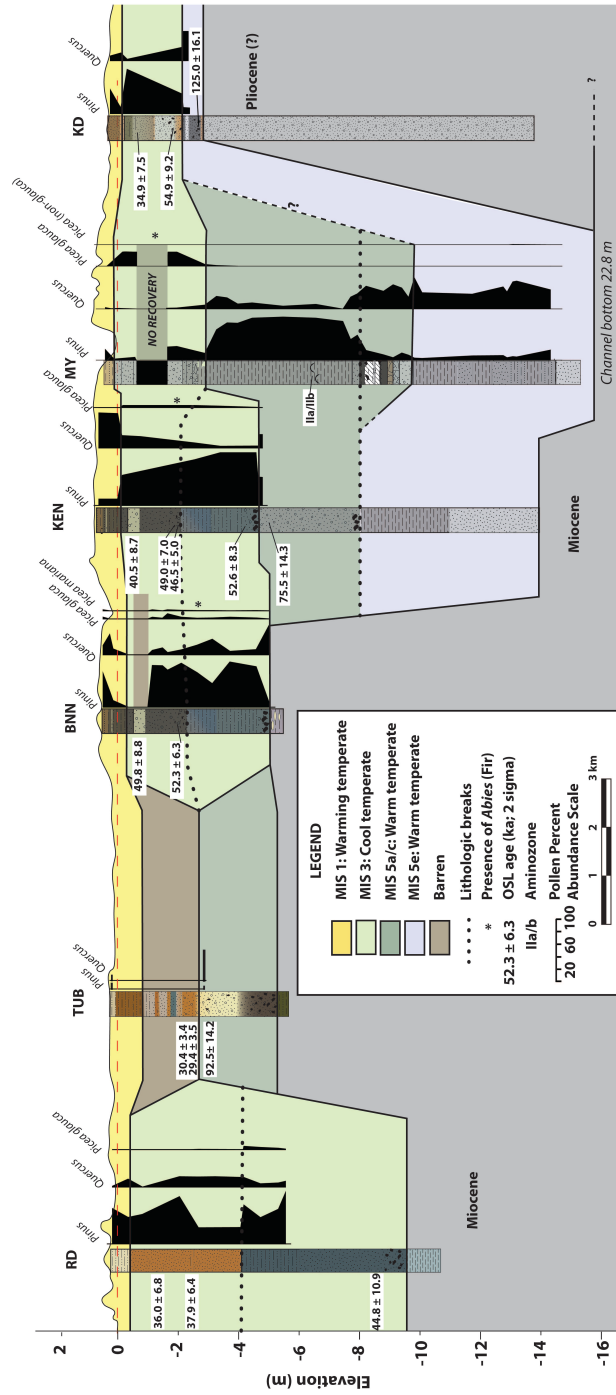


Figure 5-5 Cross-sectional diagram of pollen data indicating paleo-environmental change

5.11 Supplemental data

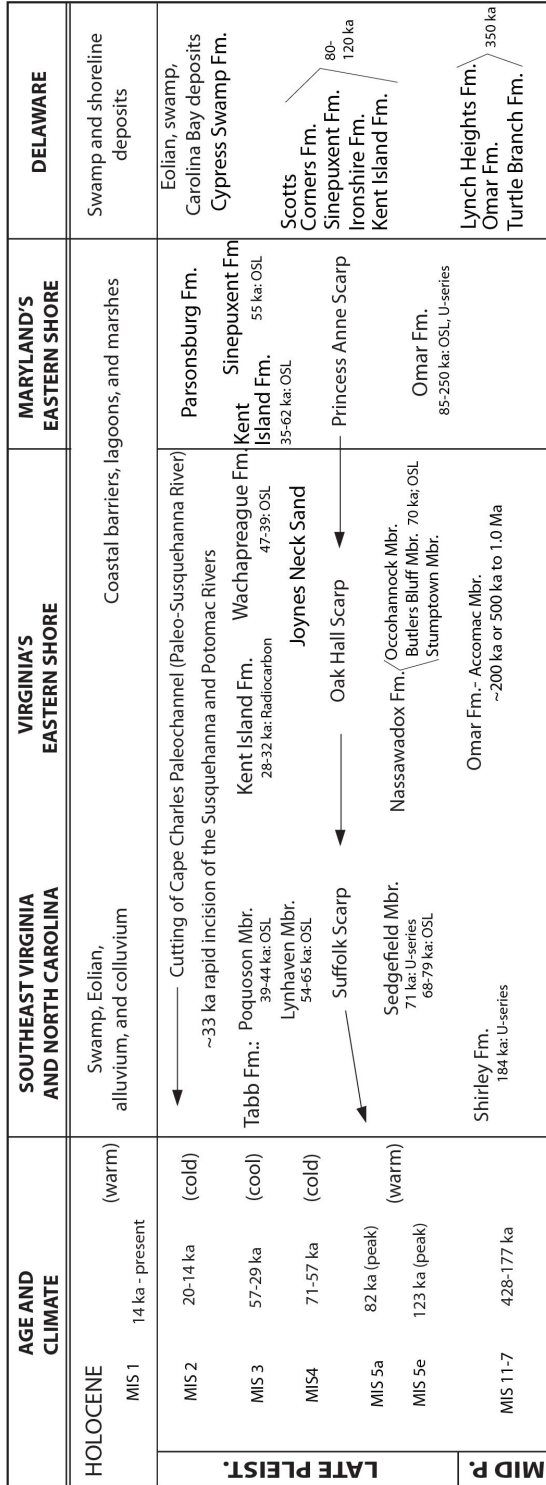


Figure 5-6 (SD1) Correlation chart of Middle to Late Pleistocene stratigraphic units across the Coastal Plain of Virginia, Maryland and Delaware. Names and ages compiled from Mixon, 1985; Mixon et al., 1989; Colman et al., 1990; Powars et al., 1992; and Johnson, 1976; Mallinson et al., 2008; Scott et al., 2010 for VA; Owens and Denny, 1978; Denny and Owens, 1979; DeJong et al., in press for MD.; Wehmiller et al., 2004; Pavich et al., 2006, personal communication for MD and VA; Groot, et al., 1990; and Ramsey, 2010 for Delaware. River incision at ~33 ka from Reusser and others, 2004

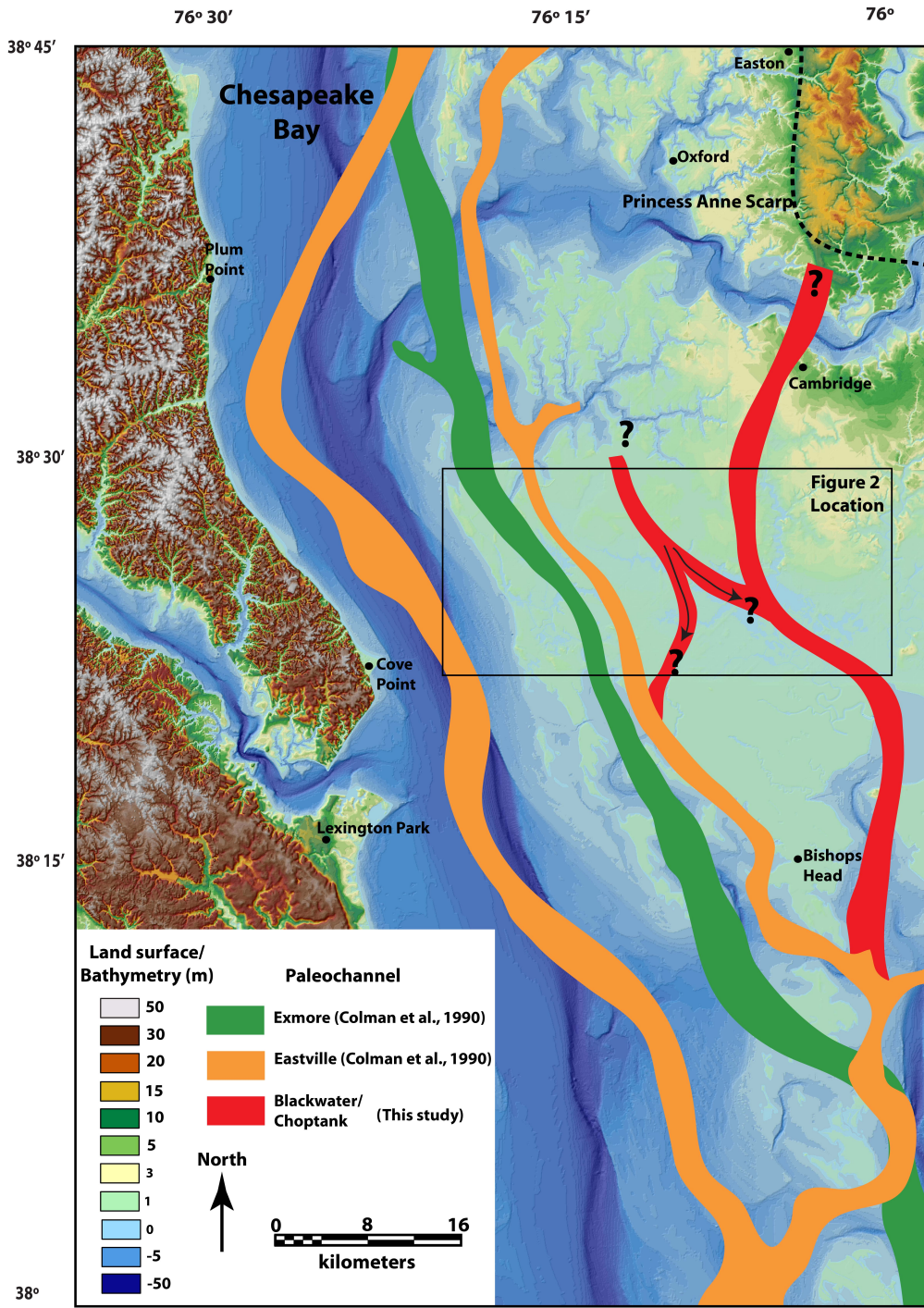
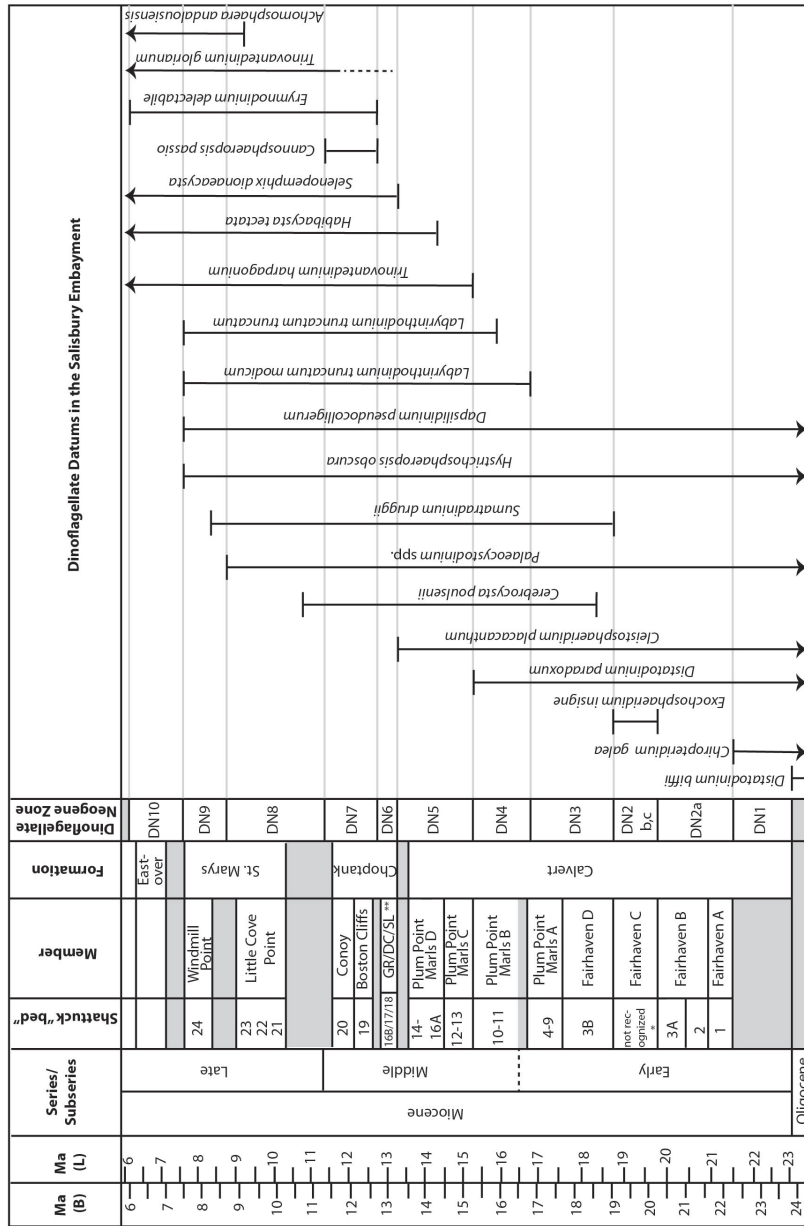


Figure 5-7 (SD2) North-south tracks of major paleochannels encountered under the field area



*Popes Creek Sand equivalent
 **Governors Run, Drumcliff, St. Leonard Members

Figure 5-8 (SD3) Chronostratigraphic and biostratigraphic context of the Miocene units under the BNWR. Species list to the right indicates upper and lower limits in the stratigraphic record. Modified from de Verteuil and Norris (1996); Shattuck “beds” defined in Shattuck (1904); B is the timescale of Berggren et al. (1995), L is the timescale of Lourens et al. (2004).

Table 5-1 (SD1) All age data associated with Quaternary deposits at the BNWR

Table SD1. All age data associated with deposits at the BNWR

CORE NAME	SAMPLE NAME	LATITUDE	LONGITUDE	CORE DEPTH	AGE	METHOD	REFERENCE
Tubman (TD)	USU-1201	38°25'5.32"N	76°11'55.96"W	2.59-2.62	30.4 ± 3.4 ka	OSL	DeJong et al., in press
Tubman (TD)	USU-1202	38°25'5.32"N	76°11'55.96"W	2.83-2.87	29.4 ± 3.5 ka	OSL	DeJong et al., in press
Tubman (TD)	USU-1203	38°25'5.32"N	76°11'55.96"W	3.35-3.38	92.5 ± 14.2 ka	OSL	DeJong et al., in press
Russel Swamp (RS)	USU-1204	38°25'10.21"N	76°14'14.48"W	4.39-4.42	58.7 ± 12.4 ka	OSL	DeJong et al., in press
Russel Swamp (RS)	USU-1205	38°25'10.21"N	76°14'14.48"W	8.56-8.59	40.7 ± 4.2 ka	OSL	DeJong et al., in press
Russel Swamp (RS)	USU-1206	38°25'10.21"N	76°14'14.48"W	8.90-8.93	70.2 ± 12.8 ka	OSL	DeJong et al., in press
Moneystamp (MD)	USU-1207	38°26'0.33"N	76°13'45.90"W	2.50-2.53	25.8 ± 4.7 ka	OSL	DeJong et al., in press
Moneystamp (MD)	USU-1208	38°26'0.33"N	76°13'45.90"W	2.77-2.80	62.0 ± 10.8 ka	OSL	DeJong et al., in press
Parsons (PD)	USU-1209	38°28'5.60"N	76°15'46.91"W	2.68-2.71	44.7 ± 7.9 ka	OSL	DeJong et al., in press
Parsons (PD)	USU-1210	38°28'5.60"N	76°15'46.91"W	4.42-4.36	45.5 ± 6.5 ka	OSL	DeJong et al., in press
Reber (RD)	USU-1211	38°22'56.65"N	76°14'27.74"W	1.46-1.50	36.0 ± 6.8 ka	OSL	DeJong et al., in press
Reber (RD)	USU-1212	38°22'56.65"N	76°14'27.74"W	2.47-2.50	37.9 ± 6.4 ka	OSL	DeJong et al., in press
Reber (RD)	USU-1213	38°22'56.65"N	76°14'27.74"W	8.66-8.67	44.8 ± 10.9 ka	OSL	DeJong et al., in press
Robbins (ROB)	USU-1221	38°22'45.64"N	76°4'35.72"W	280-2.83	68.7 ± 15.2 ka	OSL	DeJong et al., in press
Maple Dam Road (MDRN)	USU-1215	38°25'0.24"N	76°3'14.22"W	1.65-1.68	37.4 ± 5.6 ka	OSL	DeJong et al., in press
Maple Dam Road (MDRN)	USU-1216	38°25'0.24"N	76°3'14.22"W	2.04-2.07	55.1 ± 8.6 ka	OSL	DeJong et al., in press
Kuehnle (KD)	USU-1218	38°25'41.57"N	76°2'41.53"W	1.13-1.16	34.9 ± 7.5 ka	OSL	DeJong et al., in press
Kuehnle (KD)	USU-1219	38°25'41.57"N	76°2'41.53"W	1.98-2.01	54.9 ± 9.2 ka	OSL	DeJong et al., in press
Kuehnle (KD)	USU-1220	38°25'41.57"N	76°2'41.53"W	2.32-2.35	125.0 ± 16.1 ka	OSL	DeJong et al., in press
Harpers C (HC)	USU-266	38°24'54.63"N	76°4'57.31"W	4.29-4.31	43.2 ± 5.9 ka	OSL	DeJong et al., in press
Harpers C (HC)	USU-265	38°24'54.63"N	76°4'57.31"W	4.59-5.61	46.1 ± 6.8 ka	OSL	DeJong et al., in press
Kentuck (KEN)	USU-1222	38°27'18.03"N	76°6'19.98"W	1.92-1.95	40.5 ± 8.7 ka	OSL	DeJong et al., in press
Kentuck (KEN)	USU-1228	38°27'18.03"N	76°6'19.98"W	3.22-3.23	49.0 ± 7.0 ka	OSL	DeJong et al., in press
Kentuck (KEN)	USU-1223	38°27'18.03"N	76°6'19.98"W	3.29-3.32	46.5 ± 5.0 ka	OSL	DeJong et al., in press
Kentuck (KEN)	USU-1224	38°27'18.03"N	76°6'19.98"W	5.43-5.46	52.6 ± 8.3 ka	OSL	DeJong et al., in press
Kentuck (KEN)	USU-1225	38°27'18.03"N	76°6'19.98"W	5.70-5.73	75.5 ± 14.3 ka	OSL	DeJong et al., in press
Buttons Neck (BNN)	USU-1226	38°27'52.42"N	76°10'20.37"W	1.22-1.25	49.8 ± 8.8 ka	OSL	DeJong et al., in press
Buttons Neck (BNN)	USU-1227	38°27'52.42"N	76°10'20.37"W	2.35-2.38	52.3 ± 6.3 ka	OSL	DeJong et al., in press
Barbadoes Island (BI)	WW6532	38°24'45.98"N	76°10'46.60"W	3.7	Modern	¹⁴ C	DeJong et al., in press
Barbadoes Island (BI)	WW6533	38°24'45.98"N	76°5'16.85"W	3.8	691-907 cal ybp	¹⁴ C	DeJong et al., in press
Barbadoes Island (BI)	WW6535	38°24'45.98"N	76°5'16.85"W	7.8	1400-1550 cal ybp	¹⁴ C	DeJong et al., in press
Barbadoes Island (BI)	WW6536	38°24'45.98"N	76°5'16.85"W	8.0	1950-2149 cal ybp	¹⁴ C	DeJong et al., in press
Barbadoes Island (BI)	WW6537	38°24'45.98"N	76°5'16.85"W	8.3	1740-1949 cal ybp	¹⁴ C	DeJong et al., in press
BW Transect 5 (BWT5)	WW6539	38°25'12.60"N	76°5'49.78"W	3.9	Modern	¹⁴ C	DeJong et al., in press
BW Transect 5 (BWT5)	WW6540 ^c	38°25'12.60"N	76°5'49.78"W	8.4	8-277 cal ybp	¹⁴ C	DeJong et al., in press
BW Transect 5 (BWT5)	WW6541	38°25'12.60"N	76°5'49.78"W	8.6	5310-5572 cal ybp	¹⁴ C	DeJong et al., in press
Buttonso Neck Middle	BNM85	38°27'36.33"N	76°10'46.60"W	25.9	1.57 ± 0.36 Ma	CRN	DeJong et al., submitted
Hog Range	HOG17	38.448609°N	76.143293°W	5.2	0.67 ± 0.04 Ma	CRN	DeJong et al., submitted
Kentuck West	KENW53.5	38°26'52.97"N	76°7'26.47"W	16.3	2.06 ± 0.14 Ma	CRN	DeJong et al., in review
Moneystamp P.L.	MSPL37	38°26'5.85"N	76°13'30.53"W	11.3	0.66 ± 0.14 Ma	CRN	DeJong et al., submitted
Moneystamp (MD)	MD50	38°26'0.33"N	76°13'45.90"W	15.2	1.70 ± 0.08 Ma	CRN	DeJong et al., submitted
Buttons Neck (BNN)	BNN18	38°27'52.42"N	76°10'20.37"W	5.5	1.20 ± 0.18 Ma	CRN	DeJong et al., submitted
Kentuck South	KENS59	38°27'8.21"N	76°6'53.75"W	18.0	0.28 ± 0.10 Ma	CRN	DeJong et al., submitted
Madison Timberlands	MT39.5	38°29'44.51"N	76°14'13.36"W	12.0	0.91 ± 0.18 Ma	CRN	DeJong et al., in review
Oldfield	OF28.5	38°29'2.40"N	76°7'49.86"W	8.7	1.65 ± 0.14 Ma	CRN	DeJong et al., submitted
Buttonso Neck Middle	BNM	38°27'36.33"N	76.179611°W	3.4 to -7.8	MIS 5 (?)	AAR	DeJong et al., submitted
Maintenance Yard	MY	38°26'56.34"N	76°5'30.27"W	6.3	MIS 5 (?)	AAR	DeJong et al., submitted
Kentuck South	KENS	38°27'8.21"N	76°6'53.75"W	2.4	MIS 7-9	AAR	DeJong et al., submitted
Moneystamp (MD)	MD33 ^c	38°26'0.33"N	76°13'45.90"W	9.5	MIS 17-21 (?)	AAR	DeJong et al., submitted
Jacobs core	DCMD ^d	38°28'39.00"N	76°16'40.44"W	9.1	MIS 17-21	AAR	DeJong et al., submitted
Buttons Neck (BNN)	BNN	38°27'52.42"N	76°10'20.37"W	15.3	Pre-Pleistocene	AAR	DeJong et al., submitted
Moneystamp South	Golden Hill/MSS	38°25'29.76"N	76°12'22.82"W	6.9	Pre-Pleistocene	AAR	DeJong et al., submitted

Table 5-2 (SD2) Dinoflagellate species list for Miocene units under BNWR

SAMPLE	CORE	DEPTH (m)	EASTING	UTM NORTHING	UTM NORTHING
R6722A	Buttons Neck North	16.46	397724	4258012	
R6722B	Buttons Neck North	14.79	397724	4258012	
R6722C	Buttons Neck North	13.11	397724	4258012	
R6722D	Buttons Neck North	8.23	397724	4258012	
R6724A	Longfield 2	26.52	410508	4254514	
R6724B	Longfield 2	11.89	410508	4254514	
R6723B	Green Brn North	11.86	407375	4256661	
R6741A	Gum Swamp	10.66	396815	4255015	
R6741B	Gum Swamp	10.06	396815	4255015	
R6741C	Gum Swamp	7.32	396815	4255015	
R6741D	Gum Swamp	5.49	396815	4255015	
R6759	Dracon N	6.71	403511	4250758	
R6785 A	Hog West	21.04	399570	4256507	
R6785 B	Hog West	19.51	399570	4256507	
R6785 C	Hog West	17.99	399570	4256507	
R6756	Moneysump Dune	21.34	392697	4254622	
R6727	Buttons Neck Middle	28.20	397082	4257524	
R6786 B	Longfield W	17.38	409513	4254598	
R6796 A	Ball Point	11.89	397651	4253711	
R6796 B	Ball Point	11.59	397651	4253711	
R6811	Poverty Point	40.53	389333	4261485	
R6795	Old Field	10.67	401398	4260123	
R6787 B	Wild Drive	17.99	402033	4255318	
R6787 A	Wild Drive	21.04	402033	4255318	
R6786 A	Longfield W	10.36	409513	4254598	
R6808	Harrison Rd north	29.57	396268	4258567	
R6809	China Island	13.11	388662	4249428	
R6810	Floopers Neck E	19.21	386718	4261632	
R6826	HE-13	53.96	383888	4261250	
R6851	Wedge Farm	17.07	385380	4258613	
R6852	Ball Tanks N Middle	13.14	397644	4254767	
R6853	Rob Neck Preserve	16.46	386030	4254869	

*Organism-valued microfossil of unknown affinity
Pre-treatment date

References (Supplement)

- Berggren, W. A., Kent, D. V., Swisher, C. C., III, and Aubry, M. P., 1995, A revised Cenozoic geochronology and chronostratigraphy, *in* Berggren, W. A., Kent, D. V., Aubry, M.-P., and Hardenbol, J., eds., Geochronology, time scales and global stratigraphic correlation: SEPM (Society for Sedimentary Geology) Special Publication, Volume 54, p. 129–212.
- Colman, S. M., Halka, J. P., Hobbs III, C. H., Mixon, R. B., and Foster, D. S., 1990, Ancient channels of the Susquehanna River beneath Chesapeake Bay and the Delmarva Peninsula: Geological Society of America Bulletin, v. 102, p. 1268-1279.
- DeJong, B. D., Bierman, P. R., Newell, W. L., Rittenour, T. M., Mahan, S. A., Balco, G., and Rood, D. H., In press, Pleistocene relative sea levels in the Chesapeake Bay region and their implications for the next century: GSA Today.
- Denny, C. S., Owens, J. P., Sirkin, L. A., and Rubin, M., 1979, The Parsonsburg Sand in the Central Delmarva Peninsula, Maryland and Delaware, USGS Professional Paper 1067-B, p. B1-B16.
- de Verteuil, L., and Norris, G., 1996, Dinoflagellate cyst zonation and allostratigraphy of the Chesapeake Group: Micropaleontology v. 42 Supplement, p. 172 p., 118 plates.
- Groot, J. J., Ramsey, K. W., and Wehmiller, J. F., 1990, Ages of the Bethany, Beaverdam, and Omar Formations of southern Delaware: Delaware Geological

Survey Report of Investigations No. 47, 19 p.

Johnson, G. H., 1976, Geology of the Mulberry Island, Newport News North, and Hampton Quadrangles, Virginia: Virginia Division of Natural Resources Report of Investigations, v. 41, p. 72.

Lourens, L. J., Hilgen, F. J., Laskar, J., Shackleton, N. J., and Wilson, D., 2004, The Neogene period *in* Gradstein, F., Ogg, J., and Smith, A., eds., A geological Timescale.

Mallinson, D., Burdette, K., Mahan, S., and Brook, G., 2008, Optically stimulated luminescence age controls on late Pleistocene and Holocene coastal lithosomes, North Carolina, USA: *Quaternary Research*, v. 69, no. 1, p. 97-109.

Mixon, R. B., 1985, Stratigraphic and Geomorphic Framework of Uppermost Cenozoic Deposits in the Southern Delmarva Peninsula, Virginia and Maryland, USGS Professional Paper 1067-G: Reston, VA, p. 53 pp.

Mixon, R. B., Berquist, C. R., Newell, W. L., and Johnson, G. H., 1989, Geologic map and generalized cross sections of the coastal plain and adjacent parts of the piedmont, Virginia.

Owens, J. P., and Denny, C. S., 1979, Upper Cenozoic deposits of the Central Delmarva Peninsula, Maryland and Delaware, USGS Professional Paper 1067-A: Washington, DC, p. 1-27.

Ramsey, K. W., 2010, Stratigraphy, correlation, and depositional environments of the middle to late Pleistocene interglacial deposits of southern Delaware, Delaware

- Geological Survey Report of Investigations 76, Newark, Delaware, p. 43.
- Reusser, L. J., Bierman, P. R., Pavich, M. J., Zen, E.-a., Larsen, J., and Finkel, R. C., 2004, Rapid Late Pleistocene Incision of Atlantic Passive-Margin River Gorges: *Science*, v. 305, p. 499-502.
- Scott, T. W., Swift, D. J. P., Whittecar, G. R., and Brook, G. A., 2010, Glacioisostatic influences on Virginia's late Pleistocene coastal plain deposits: *Geomorphology*, v. 116, no. 1-2, p. 175-188.
- Shattuck, G. B., 1904, The Miocene deposits of Maryland; Geological and paleontological relations, with a review of earlier investigations Systematic paleontology of the Miocene deposits of Maryland: Maryland Geological Survey, p. xxxiii–cxxxvii.
- Wehmiller, J. F., Simmons, K. R., Cheng, H., Edwards, L. R., Martin-McNaughton, J., York, L. L., Krantz, D. E., and Shen, C.-C., 2004, Uranium-series coral ages from the US Atlantic Coastal Plain—the “80ka problem” revisited: *Quaternary International*, v. 120, no. 1, p. 3-14.

CHAPTER 6: CONCLUSIONS AND FUTURE RESEARCH

6.1. Summary of Findings

By defining the geologic framework underlying east-central Chesapeake Bay and sampling for a variety of age and climate proxies, I have provided information that informs resource managers as they plan for adaptation to future sea-level rise. The >28,000 acre Blackwater National Wildlife Refuge (BNWR) was established with the goal of maintaining and enhancing productive habitat for a healthy diversity of wildlife species. This goal remains, even in the face of accelerated sea level rise in the Chesapeake Bay region (Snay et al., 2007; Boon et al., 2010). My research suggests that the BNWR and the tens of thousands of acres of adjacent protected lands occupy a geomorphic surface that derives from a paleo-estuarine environment that existed during marine isotope stage 3. The implications of this age, spelled out in Chapter 2, indicate continued subsidence of the land surface for the foreseeable future, regardless of any climate amelioration strategies put into action by policy-makers and legislators.

How then, in that light, should coastal resources in the BNWR and neighboring lands be managed? The range of potential sea level rise outlined in Chapter 2 indicates rates of sea level rise that outpace rates of marsh accretion (Cahoon and Guntenspergen, 2010). As for anywhere else, the two major responses that can be implemented at the BNWR are mitigation and adaptation, or most effectively a combination of the two. Mitigation is possible at global to regional scales, with global options including the reduction of greenhouse gas emissions via climate policy (IPCC, 2013). While these

reductions would not stabilize the sea level itself, they can stabilize the rate at which sea level rises and potentially reduce it (Nicholls, 2010). This is especially pertinent to regions like the BNWR because wetland loss is driven more by the *rate* of sea-level rise than the *amount* of rise itself. Much of the marsh in the BNWR appears to have surface elevation below their ideal growing conditions, which means rapid conversion of marsh to open water can be expected to continue without reduction in greenhouse gas emission (Kirwan and Guntenspergen, 2012).

Local-to-regional mitigation is less straight-forward. Geo-engineering proposals have been offered by the U.S. Army Corps of Engineers to artificially build up portions of marsh in the BNWR using dredge spoil to force marshes to accrete more quickly than the sea is rising. This technique has been tested at Poplar Island, north of the study site (http://www.mgs.md.gov/coastal_geology/pierp.html), and to a lesser extent in 3 small areas within the BNWR. Though there were signs of improvement, they were localized and vastly out of scale with the regional challenges and associated budgets of scaling up to the Blackwater NWR and beyond.

Given that the changes to the climate already put into motion cannot be reversed in the near future (Zickfield et al., 2013) and the suggestion in Chapter 2 that land subsidence is projected to continue long into the future due to the effects of GIA, adaptation remains the best proactive alternative for managers at the BNWR. Managers are currently developing adaptation plans using green infrastructure in the form of inland migration corridors for the persistence of key habitat. This requires careful planning that

takes many different inter-related variables into account such as habitat requirements of endangered species, locations of road networks, land use/land cover of potential marsh locations, and soils suitability to wetland establishment. In addition, it takes coordination between state and federal agencies and the cooperation of neighboring entities that may not share the same vision of preservation. To date, there is no directional bias in corridor planning, and plans currently consider acquisition of several tracts of land near the southern end of the refuge where elevations are not as suitable to long-term habitat persistence. Based on sea level inundation models (Larsen et al., 2004), any marsh that migrates to these fragmented areas will be highly susceptible to storm surges, which are projected to increase along US coasts (Tebaldi et al., 2012). My recommendation is thus to continue with migration corridor planning, but to focus efforts on the region north of the current footprint of the refuge, particularly above the scarp that I identified in Chapter 2, where migration has the most successful outlook beyond 2100 when sea level is likely to be ~0.5 to 1.0 m higher than today.

Several important findings from this research were made possible through the application of geochronology to a well-defined geologic framework:

- Optically stimulated luminescence methods significantly improve understanding of the Late Pleistocene stratigraphy and geologic evolution of the field area. By developing a system for sampling from sediment cores collected from a hollow-stem auger rig system, I had the unique opportunity to constrain ages of the surficial geology in 3

dimensions with much higher resolution than has ever been done in the mid-Atlantic coastal plain setting. The results challenge long-held assumptions regarding relative sea-level history of the region and imply continued subsidence of the land surface from glacio-isostatic adjustment in the coming centuries.

- My use of cosmogenic nuclide burial dating similarly challenges old assumptions regarding the development of the Delmarva Peninsula landscape. Previously, the only methods available for dating major paleochannel fill deposits were uranium-series, applied to shell-encrusting corals, and amino acid racemization techniques applied to well-preserved shells. Corals are very rare in the Chesapeake Bay stratigraphy, and amino acid racemization techniques, while providing relative chronologies, remain poorly calibrated and depend on quantifying environmental parameters like thermal history that are extremely difficult to constrain (Wehmiller, 2013). The isochron burial ages presented in chapters 2, 3, 4 and 5 thus represent a significant improvement over previous understanding of ages of major paleochannels, and help contextualize major fill units in the Chesapeake Bay and Delmarva Peninsula subsurface with the Pliocene gravels that form the spine of the Delmarva Peninsula.
- From cosmogenic burial ages, we can calculate the concentrations of

^{10}Be present in sediment source areas at the time sediment was deposited in the BNWR. This provides a measure of relative landscape stability through time, as more stable landscapes accumulate higher concentrations of ^{10}Be , whereas ^{10}Be is stripped more readily and frequently from less stable landscapes. The ages and concentrations presented in chapter 4 suggest that denudation in the Susquehanna River watershed doubled when glacial-interglacial climate fluctuations were established, and remained relatively stable since then.

- My application of radiocarbon dating to the Holocene stratigraphy at the Blackwater NWR improves understanding of the development of tidal marsh that is the focus of preservation efforts today. Two major lithologies are present in the Holocene stratigraphy, a lower, massive silt sequence, and an upper fibrous peat. The peat represents accreted marsh deposits, which apparently began to accumulate during the last millennium, based on a limiting age at the top of the silt sequence. Radiocarbon ages produced from within the peat indicate modern ages, suggesting that the marsh is a very young feature.
- The pollen analyses that I accomplished for the upper portion of the Blackwater NWR provides additional criteria for correlation of subsurface depositional units and a robust proxy for climate through time. This analysis shows that the latest Pleistocene estuarine deposits,

dated to marine isotope stage 3, were indeed deposited when climate was cooler than present. This finding supports the interpretation that relative sea level was much higher than previously thought during this time due to significant land motion driven by glacio-isostatic adjustment.

6.2. Suggestions for future research

Reliable geochronology is central to the findings in this dissertation, and wider application of the methods herein to the coastal plain setting will improve our understanding of the timing and nature of Pleistocene cut-fill sequences that characterize Chesapeake Bay evolution. Specifically, my work reveals opportunities for wider application of OSL and cosmogenic nuclides that could significantly improve correlation of Pleistocene sequences along the western and eastern shorelines of the Delmarva Peninsula, the western shore and tributaries of Chesapeake Bay, and North Carolina coastal areas.

My application of OSL dating techniques to surficial deposits in the study area provide important constraints on the landscape evolution, as it has in similar settings in North Carolina (Parham et al., 2013) and Virginia (Scott et al., 2010), but the perception of OSL methods in the research community would benefit from additional cross-calibration with other dating methods. Recent attempts to verify OSL results against other dating methods, such as amino acid racemization and u-series, were successful in the

mid-Atlantic coastal plain (Parham et al., 2013). But in some instances, the methods disagree (J. Wehmiller, pers. commun.), leaving skeptics within the research community of OSL applications in the coastal plain. Similar responses resulted from previous advancements in geochronology; disagreement between uranium-series and amino-acid racemization dating methods spurred considerable argument for decades (e.g. Cronin et al., 1981; Mixon et al., 1982; Szabo, 1985; Wehmiller et al., 1988). This was resolved by carefully re-evaluating existing data, producing new samples for cross-calibration, and ultimately erecting a new interpretation of the relative sea-level history of the region (Wehmiller et al., 2004). So too must OSL be systematically checked against other methods, not only to test results of the method but also to improve understanding of the problems that OSL geochronology addresses, which often have societal implications (see Chapter 2).

Additionally, the OSL ages produced in this study and their implications regarding the glacial forebulge dynamics in the mid-Atlantic could be further tested by completing transects up and down the western and eastern coasts of the Delmarva Peninsula. Not only could this help validate existing OSL chronologies in the region, but it could also reveal any spatial patterns in age-elevation relationships of correlated surfaces to verify whether OSL-dated deposits conform to the shape of the forebulge determined by both radiocarbon-dated Holocene deposits and by tide gauge observations (Engelhart et al., 2009). As yet, there are not enough regional OSL ages to test spatial trends in the elevation of MIS 3-aged deposits. Such a study could significantly improve

our understanding of the magnitude of relative sea level change at the local and regional scales.

Furthermore, the stratigraphy beneath Chesapeake Bay and the Delmarva Peninsula present an unprecedented opportunity to redefine Plio-Pleistocene landscape evolution using cosmogenic nuclides in ways that have never before been possible. The uplands both west of the Chesapeake Bay and on the Delmarva Peninsula include major Plio-Pleistocene gravel sheets of the paleo-Potomac, Susquehanna, and Hudson-Delaware drainage systems (Hack, 1955; Schlee, 1957; Owens and Denny, 1979; Owens and Minard, 1979). These gravels make up the northern spine of the Delmarva Peninsula, and thus the earliest closure of the Chesapeake Bay, so dating these gravels using isochron burial techniques could definitively constrain the earliest evolution of this landscape and provide important information on paleo-Hudson-Delaware river system and source area.

The logical next step, then, would be to apply isochron dating methods to progressively younger, well-known Susquehanna River paleochannels that are spatially constrained by the aforementioned gravel sheets. I already show here that the range of ^{26}Al and ^{10}Be isotope concentrations in Susquehanna River gravels are appropriate for isochron dating, and the method is ideal for dating several other channels whose locations are well constrained both via seismic studies (e.g. Colman and Mixon, 1988; Colman et al., 1990; Oertel and Foyle, 1995) and by scores of borehole data. This work could:

- Systematically reconstruct cycles of cutting and filling of the

Susquehanna River, building upon the work I completed in Chapter 4, to provide detailed information on the response of the largest estuary in North America to major cycles of sea level change.

- Provide the framework from which to construct very long paleoclimate records for the mid-Atlantic region via pollen analyses on materials overlying dated gravels. This could potentially extend the largest existing paleoclimate record for the region, which at present does not exceed ~115 ka (Litwin et al., 2013).
- Allow for significantly improved correlation between channel deposits in the Chesapeake stratigraphy and their onshore counterparts. Previous correlation between these deposits (Pazzaglia and Gardner, 1993) has been used in part to argue against long-held geomorphic models pertaining to landscape evolution in the region (Davis, 1899) and identify physical evidence for flexural uplift. More precisely constraining relative ages of channel deposits and their correlative fluvial terraces may improve estimates of flexural uplift rates for a better parsing out of vertical land surface motion active on the landscapes both west and east of Chesapeake Bay.
- Provide unparalleled means of documenting changes in landscape processes that occurred at the Plio-Pleistocene transition via analysis of cosmogenic nuclide concentrations. Recent attempts to infer these

changes (e.g. Hidy et al., 2014) lack the long, complete records of Pliocene and Pleistocene sections that are widely available near the surface in the mid-Atlantic coastal plain.

In addition to isochrons, which strictly use *in situ* ^{10}Be , I also see great utility in applying meteoric ^{10}Be in the field area and beyond. My research shows that mid-Atlantic marshes are relatively young features of the landscape, being established within the past millennium. Research in northern Atlantic marshes suggests that these features are merely relicts from colonial (Thorson et al., 1998) to 18th century (Kirwan et al., 2011) land use practices, and that high sediment yields from land clearing enabled rapid marsh accretion. This research suggests that as marshes degrade in locations such as these today, they are actually returning to a natural state, so attempts to “restore” them are feeble attempts at fighting nature. While the story is likely more complex in expansive mid-Atlantic marshes, they record very similar Holocene stratigraphic sequences, and meteoric ^{10}Be profiles produced near the mouths of 3 Chesapeake Bay tributaries indeed show a clear spike from land clearance, or “legacy sediments” (Valette-Silver et al., 1986). Presumably, these ^{10}Be -enriched sediments stripped from the landscape were distributed into Chesapeake Bay marshes. I suggest producing meteoric ^{10}Be profiles on select sites within the Chesapeake Marshlands Wildlife Refuge Complex to see where the ^{10}Be spike is located in the marsh profile. If it is near the base of the fibrous, peaty unit that forms a continuum with active marsh, it may suggest that marsh establishment benefited greatly from anthropogenic sediment inputs that have

significantly diminished since that time. Because so much work is focused on the health of Chesapeake Bay and its marshes, it is prudent to ensure that we are indeed protecting a natural landscape feature and not a relict of up-catchment anthropogenic land use.

The work completed in this dissertation, and the research proposed in this chapter, as well as many other geologic research efforts in the region would also benefit greatly from a resurgence in land-based seismic studies. In 1994, Genau and others ran a short seismic line in the northwestern portion of my field area and uncovered important details about major Susquehanna River paleochannels that significantly guided my work. While seismic reflection and refraction studies have been used more recently to address much older and deeper questions pertaining to the Chesapeake Bay Impact Crater (Catching et al., 2008), to my knowledge no such work has been completed to improve mapping and correlation of more recent map units. Drilling has nearly exclusively been the means of accessing the subsurface for Delmarva research in recent years. While it is common procedure to accompany geophysical profiling with borehole data for ground-truthing, the inverse should also be true to some extent, because drilling alone is too costly and drill sites are geographically isolated.

Finally, the research presented in the previous chapters and the suggestions offered in this chapter highlight the potential of the Chesapeake Bay stratigraphy to help understand details of landscape evolution at a variety of timescales, but Chesapeake Bay is but one of several major coastal plain estuaries with great potential. Because all coastal plain estuaries are geologically young features that all originated during the sea-

level rise that has continued since the last glacial retreat, other major coastal plain estuaries such as the Thames River estuary in England, Ems River estuary in Germany, the Seine River estuary in France, the Si-Kiang River estuary in Hong Kong, and the Murray River estuary in Australia among others could provide an excellent opportunity to compare the response of landscapes to Pleistocene climate forcing. While these estuaries share general geomorphic domains (drowned river valleys crossing low-relief coastal plain; Bokuniewicz, 1995), they represent a gradient of climatic and tectonic conditions and a broad range in proximity to formerly active ice sheets, and could provide grounds for comparing relative sea-level forcing over long timescales if their preserved sediments were constrained in space and time. Using Chesapeake Bay as a reference, these coastal features potentially preserve multi-million year, direct records of terrestrial and near-shore processes at a range of timescales. Such analysis offers a unique opportunity to address Plio-Pleistocene, terrestrial and marine landscape evolution around the globe.

COMPREHENSIVE BIBLIOGRAPHY

- Aitken, M.J. 1998: An Introduction to Optical Dating: The dating of Quaternary sediments by the use of photon-stimulated luminescence. New York, Oxford University Press, 267 pp.
- Allen, J. R. L., 2000, Morphodynamics of Holocene salt marshes: a review sketch from the Atlantic and Southern North Sea coasts of Europe: *Quaternary Science Reviews*, v. 19, p. 1155-1231.
- Argento, D. C., Reedy, R. C., and Stone, J. O., 2013, Modeling the earth's cosmic radiation *Nuclear Instruments and Methods in Physics Research, Section B, Beam Interactions with Materials and Atoms*, v. 294, p. 464–469.
- Ayyub, B. M., Braileanu, H. G., and Qureshi, N., 2012, Prediction and impact of sea level rise on properties and infrastructure of Washington, DC: *Risk Anal*, v. 32, no. 11, p. 1901-1918.
- Balco, G., and Rovey, C. W., 2008, An isochron method for cosmogenic-nuclide dating of buried soils and sediments: *American Journal of Science*, v. 308, no. 10, p. 1083-1114.
- Balco, G., and Rovey, C. W., 2010, Absolute chronology for major Pleistocene advances of the Laurentide Ice Sheet: *Geology*, v. 38, no. 9, p. 795-798.
- Balco, G., Soreghan, G. S., Sweet, D. E., Marra, K. R., and Bierman, P. R., 2013, Cosmogenic-nuclide burial ages for Pleistocene sedimentary fill in Unaweep Canyon, Colorado, USA: *Quaternary Geochronology*, v. 18, p. 149-157.

- Barbosa, S. M., and Silva, M. E., 2009, Low-frequency sea-level change in Chesapeake Bay: Changing seasonality and long-term trends: *Estuarine, Coastal and Shelf Science*, v. 83, no. 1, p. 30-38.
- Berggren, W. A., Kent, D. V., Swisher, C. C., III, and Aubry, M. P., 1995, A revised Cenozoic geochronology and chronostratigraphy, *in* Berggren, W. A., Kent, D. V., Aubry, M.-P., and Hardenbol, J., eds., *Geochronology, time scales and global stratigraphic correlation: SEPM (Society for Sedimentary Geology) Special Publication, Volume 54*, p. 129–212.
- Bierman, P. R., and Steig, E. J., 1996, Estimating rates of denudation using cosmogenic isotope abundances in sediment: *Earth Surface Processes and Landforms*, v. 21, p. 125-139.
- Bokuniewicz, 1995, Sedimentary systems of coastal-plain estuaries, *in* Perillo, G. M. E., ed., *Geomorphology and Sedimentology of Estuaries: Amsterdam, Elsevier*, p. 49-67.
- Boon, J. D., 2012, Evidence of Sea Level Acceleration at U.S. and Canadian Tide Stations, Atlantic Coast, North America: *Journal of Coastal Research*, v. 285, p. 1437-1445.
- Boon, J. D., Brubaker, J. M., and Forrest, D. R., 2010, Chesapeake Bay land subsidence and sea level change: An evaluation of past and present trends and future outlook, Special Report No. 425 in *Applied Marine Science and Ocean Engineering to the U.S. Army Corps of Engineers Norfolk District. Virginia Institute of Marine*

Science. Gloucester Point, Virginia..

Bricker, O. P., Newell, W. L., and Simon, N. S., 2003, Bog Iron Formation in the Nassawango Watershed, Maryland: USGS Open File Report 2003-346.

Brown, E., Stallard, R. F., Larsen, M. C., Raisbeck, G. M., and Yiou, F., 1995, Denudation rates determined from the accumulation of in situ-produced ^{10}Be in the Luquillo Experimental Forest, Puerto Rico: *Earth and Planetary Science Letters*, v. 129, p. 193–202.

Cabioch, G., and Ayliffe, L. K., 2001, Raised Coral Terraces at Malakula, Vanuatu, Southwest Pacific, Indicate High Sea Level During Marine Isotope Stage 3: *Quaternary Research*, v. 56, no. 3, p. 357-365.

Cahoon, D. R., Guntnerspergen, G., Baird, S., Nagel, J., Hensel, P., Lynch, J., Bishara, D., Brennand, P., Jones, J., and Otto, C., 2010, Do annual prescribed fires enhance or slow the loss of coastal marsh habitat at Blackwater National Wildlife Refuge? Final Project Report Volume JFSP Beltsville, MD.

Cahoon, D. R., Lynch, J. C., Perez, B. C., Segura, B., Holland, R. D., Stelly, C., Stephenson, G., and Hensel, P., 2002, High-precision measurements of wetland sediment elevation: Ii. The rod surface elevation table: *Journal of Sedimentary Research*, v. 72, no. 5, p. 734-739.

Catchings, R. D., Powars, D. S., Gohn, G. S., Horton, J. W., Goldman, M. R., and Hole, J. A., 2008, Anatomy of the Chesapeake Bay impact structure revealed by seismic imaging, Delmarva Peninsula, Virginia, USA: *Journal of Geophysical Research*:

- Solid Earth, v. 113, no. B8, p. 1-23.
- Clark, P. U., Dyke, A. S., Shakun, J. D., Carlson, A. E., Clark, J., Wohlfarth, B., Mitrovica, J. X., Hostetler, S. W., and McCabe, A. M., 2009, The Last Glacial Maximum: *Science*, v. 325, no. 5941, p. 710-714.
- Colman, S. M., Baucom, P. C., Bratton, J. F., Cronin, T. M., McGeehin, J. P., Willard, D., Zimmerman, A. R., and Vogt, P. R., 2002, Radiocarbon Dating, Chronologic Framework, and Changes in Accumulation Rates of Holocene Estuarine Sediments from Chesapeake Bay: *Quaternary Research*, v. 57, no. 1, p. 58-70.
- Colman, S. M., Halka, J. P., Hobbs III, C. H., Mixon, R. B., and Foster, D. S., 1990, Ancient channels of the Susquehanna River beneath Chesapeake Bay and the Delmarva Peninsula: *Geological Society of America Bulletin*, v. 102, p. 1268-1279.
- Colman, S. M., and Mixon, R. B., 1988, The record of major Quaternary sea-level changes in a large coastal plain estuary, Chesapeake Bay, Eastern United States: *Palaeogeography, Palaeoclimatology, Palaeoecology*, v. 68, p. 99-116.
- Colman, S. M., Mixon, R. B., Rubin, M., Bloom, A. L., and Johnson, G. H., 1989, Comments and Reply on "Late Pleistocene barrier-island sequence along the southern Delmarva Peninsula: Implications for middle Wisconsin sea levels": *Geology*, v. 17, no. 1, p. 84.
- Cooke, C. W., 1930, Correlation of Coastal Terraces: *The Journal of Geology*, v. 38, p. 577-589.

- Cooke, C. W., 1958, Pleistocene shorelines in Maryland: Geological Society of America Bulletin, v. 69, no. 9, p. 1187-1190.
- Corbett, L. B., Young, N. E., Bierman, P. R., Briner, J. P., Neumann, T. A., Rood, D. H., and Graly, J. A., 2011, Paired bedrock and boulder ^{10}Be concentrations resulting from early Holocene ice retreat near Jakobshavn Isfjord, western Greenland: Quaternary Science Reviews, v. 30, no. 13-14, p. 1739-1749.
- Cronin, T. M., 1981, Rates and possible causes of neotectonic vertical crustal movements of the emerged southeastern United States Atlantic Coastal Plain: Geological Society of America Bulletin, v. 92, no. 11, p. 812-833.
- Cronin, T. M., 2012, Rapid sea-level rise: Quaternary Science Reviews, v. 56, p. 11-30.
- Cronin, T. M., Bybell, L. M., Poor, R. Z., Blackwelder, B. W., Liddicoat, J. C., and Hazel, J. E., 1984, Age and correlation of emerged Pliocene and Pleistocene deposits, U.S. Atlantic coastal plain: Pelogeography, Palaeoclimatology, Palaeoecology, v. 47, p. 21-51.
- Cronin, T. M., Szabo, B. J., Ager, T. A., Hazel, J. E., and Owens, J. P., 1981, Quaternary Climates and Sea Levels of the U.S. Atlantic Coastal Plain: Science, v. 211, no. 4479, p. 233-240.
- Dalrymple, R. W., Zaitlin, B. A., and Boyd, R., 1992, Estuarine facies models: conceptual basis and stratigraphic implications: Journal of sedimentary petrology, v. 62, p. 1130-1146.
- Davis, J. L., and Mitrovica, J. X., 1996, Glacial isostatic adjustment and the anomalous

- tide gauge record of eastern North America: *Nature*, v. 379, p. 331-333.
- DeJong, B. D., Bierman, P. R., Newell, W. L., Rittenour, T. M., Mahan, S. A., Balco, G., and Rood, D. H., In press, Pleistocene relative sea levels in the Chesapeake Bay region and their implications for the next century: *GSA Today*.
- Denny, C. S., and Owens, J. P., 1979, Sand Dunes on the Central Delmarva Peninsula, Maryland and Delaware, USGS Professional Paper 1067-C, p. 1-15.
- Denny, C. S., Owens, J. P., Sirkin, L. A., and Rubin, M., 1979, The Parsonsburg Sand in the Central Delmarva Peninsula, Maryland and Delaware, USGS Professional Paper 1067-B, p. 1-16.
- de Verteuil, L., and Norris, G., 1996, Dinoflagellate cyst zonation and allostratigraphy of the Chesapeake Group: *Micropaleontology* v. 42 Supplement, p. 172 p., 118 plates.
- Eggleston, J. E., and Pope, J., 2013, Land Subsidence and Relative Sea-Level Rise in the Southern Chesapeake Bay Region, *in* Interior, D. o. t., ed., Volume USGS Circular: Reston, VA, p. 30 pp.
- Engelhart, S. E., Horton, B. P., Douglas, B. C., Peltier, W. R., and Tornqvist, T. E., 2009, Spatial variability of late Holocene and 20th century sea-level rise along the Atlantic coast of the United States: *Geology*, v. 37, no. 12, p. 1115-1118.
- Erlanger, E. D., Granger, D. E., and Gibbon, R. J., 2012, Rock uplift rates in South Africa from isochron burial dating of fluvial and marine terraces: *Geology*, v. 40, no. 11, p. 1019-1022.

- Ezer, T., and Corlett, W. B., 2012, Is sea level rise accelerating in the Chesapeake Bay? A demonstration of a novel new approach for analyzing sea level data: *Geophysical Research Letters*, v. 39, no. 19, p. n/a-n/a.
- Finkelstein, K. F., and Kearney, M. S., 1988, Late Pleistocene barrier-island sequence along the southern Delmarva Peninsula: Implications for middle Wisconsin sea levels: *Geology*, v. 16, p. 41-45.
- Fleming, B. J., DeJong, Benjamin D., Phelan, Daniel J., 2011, Geology, Hydrology, and Water Quality of the Little Blackwater River Watershed, Dorchester County, Maryland, 2006-2009, *in* Survey, U. S. G., ed., p. 1-27.
- Forman, S. L., Pierson, J., and Lepper, K., 2000, Luminescence geochronology, *in* Noller, J. S., Sowers, J. M., and Lettis, W. R., eds., *Quaternary Geochronology: Methods and Applications*: Washington D.C., Wiley, p. 157-176.
- Foss, J. E., Fanning, D. S., Miller, F. P., and Wagner, D. P., 1978, Loess deposits of the Eastern Shore of Maryland: *Soil Science Society of America Journal*, v. 42, no. 2, p. 329-334.
- Galbraith, R.F., Roberts, R.G., Laslett, G.M., Yoshida, H., Oleey, J.M., 1999. Optical dating of single and multiple grains of quartz from Jinmium Rock Shelter, northern Australia: Part I, Experimental design and statistical models: *Archaeometry*, v. 41, p. 339-364.
- Gao, C., 2014, Relict Thermal-contraction-crack Polygons and Past Permafrost South of the Late Wisconsinan Glacial Limit in the Mid-Atlantic Coastal Plain, USA:

- Permafrost and Periglacial Processes, p. 144-149.
- Genau, R. B., Madsen, J. A., McGeary, S., and Wehmiller, J. F., 1994, Seismic-Reflection Identification of Susquehanna River Paleochannels on the Mid-Atlantic Coastal Plain: *Quaternary Research*, v. 42, p. 166-174.
- Gibbons, S. J. A., and Nicholls, R. J., 2006, Island abandonment and sea-level rise: An historical analog from the Chesapeake Bay, USA: *Global Environmental Change*, v. 16, no. 1, p. 40-47.
- Gosse, J. C., and Phillips, F. M., 2001, Terrestrial in situ cosmogenic nuclides; Theory and application: *Quaternary Science Reviews*, v. 20, no. 14, p. 1475-1560.
- Granger, D. E., 2006, A review of burial dating methods using ^{26}Al and ^{10}Be , in Siame, I. L., Bourlies, D. L., and Brown, E. T., eds., *In Situ-Produced Cosmogenic Nuclides and Quantification of Geological Processes: Geological Society of America Special Paper 415*, Volume 415, p. 1-16.
- Granger, D. E., 2014, Cosmogenic Nuclide Burial Dating in Archaeology and Paleoanthropology: *Treatise on Geochemistry*, v. 14, p. 81-97.
- Granger, D. E., Kirchner, J. W., and Finkel, R., 1996, Spatially averaged long-term erosion rates measured from in-situ produced cosmogenic nuclides in alluvial sediment: *Journal of Geology*, v. 104, p. 249-257.
- Granger, D. E., Kirchner, J. W., and Finkel, R. C., 1997, Quaternary downcutting rate of the New River, Virginia, measured from differential decay of cosmogenic ^{26}Al and ^{10}Be in cave-deposited alluvium: *Geology*, v. 25, no. 2, p. 107-110.

- Granger, D. E., and Muzikar, P. F., 2001, Dating sediment burial with in situ-produced cosmogenic nuclides: theory, techniques, and limitations: *Earth and Planetary Science Letters*, v. 188, p. 269-281.
- Groot, J. J., Ramsey, K. W., and Wehmiller, J. F., 1990, Ages of the Bethany, Beaverdam, and Omar Formations of southern Delaware: Delaware Geological Survey Report of Investigations No. 47, 19 p.
- Guerin, G., Mercier, N., Adamiec, G., 2011. Dose-rate conversion factors: update: *Ancient TL*, v. 29, p. 5-8.
- Hack, J. T., 1955, Geology of the Brandywine area and origin of the upland of southern Maryland, USGS Professional Paper 267-A, p. 1-43.
- Hansen, H. J., 3rd, 1966, Pleistocene stratigraphy of the Salisbury area, Maryland, and its relationship to the lower Eastern Shore—A subsurface approach, *in* Survey, M. G., ed., Volume Report of Investigations, p. 56.
- Herman, F., Seward, D., Valla, P. G., Carter, A., Kohn, B., Willett, S. D., and Ehlers, T. A., 2013, Worldwide acceleration of mountain erosion under a cooling climate: *Nature*, v. 504, no. 423-426.
- Hidy, A. J., Gosse, J. C., Blum, M. D., and Gibling, M. R., 2014, Glacial–interglacial variation in denudation rates from interior Texas, USA, established with cosmogenic nuclides: *Earth and Planetary Science Letters*, v. 390, p. 209-221.
- Hidy, A. J., Gosse, J. C., Froese, D. G., Bond, J. D., and Rood, D. H., 2013, A latest Pliocene age for the earliest and most extensive Cordilleran Ice Sheet in

- northwestern Canada: *Quaternary Science Reviews*, v. 61, p. 77-84.
- Hobbs III, C. H., 2004, Geological history of Chesapeake Bay, USA: *Quaternary Science Reviews*, v. 23, no. 5-6, p. 641-661.
- IPCC, 2013, *Climate change 2013: The physical science basis. Contribution of the Working Group 1 to the Fifth Assessment report of the Intergovernmental Panel on Climate Change.*, Cambridge, UK, Cambridge Univ. Press.
- Jacobs, J. M., 1980, Stratigraphy and lithology of Quaternary landforms on the eastern coast of the Chesapeake Bay [MS thesis]: University of Delaware, 81 p.
- Johnson, G. H., 1976, Geology of the Mulberry Island, Newport News North, and Hampton Quadrangles, Virginia: Virginia Division of Natural Resources Report of Investigations, v. 41, p. 72.
- Joughin, I., Smith, B. E., and Medley, B., 2014, Marine ice sheet collapse potentially under way for the Thwaites Glacier Basin, West Antarctica: *Science*, v. 344, no. 6185, p. 735-738.
- Jull, A. J. T., Scott, E. M., and Bierman, P., in press, The CRONUS-Earth inter-comparison for cosmogenic isotope analysis: *Quaternary Geochronology*.
- Kaufman, D. S., and Manley, W. F., 1998, A new procedure for determining DL amino acid ratios in fossils using reverse phase liquid chromatography: *Quaternary Science Reviews (Quaternary Geochronology)*, v. 17, p. 987-1000.
- Kirwan, M. L., and Guntenspergen, G. R., 2012, Feedbacks between inundation, root production, and shoot growth in a rapidly submerging brackish marsh: *Journal of*

- Ecology, v. 100, no. 3, p. 764-770.
- Kirwan, M. L., Murray, A. B., Donnelly, J. P., and Corbett, D. R., 2011, Rapid wetland expansion during European settlement and its implication for marsh survival under modern sediment delivery rates: *Geology*, v. 39, no. 5, p. 507-510.
- Klein, J., Giegengack, R., Middleton, R., Sharma, P., Underwood, J. R., and Weeks, R. A., 1986, Revealing histories of exposure using *in situ* produced ²⁶Al and ¹⁰Be in Libyan desert glass.
- Kohl, C. P., and Nishiizumi, K., 1992, Chemical isolation of quartz for measurement of in-situ-produced cosmogenic nuclides: *Geochimica et Cosmochimica Acta*, v. 56, p. 3583-3587.
- Lal, D., and Peters, B., 1967, Cosmic ray produced radioactivity on the Earth, *in* Sitte, K., ed., *Handbuch der Physik*: New York, Springer-Verlag, p. 551-612.
- Lambeck, K., and Chappell, J., 2001, Sea level change through the last glacial cycle: *Science*, v. 292, no. 5517, p. 679-686.
- Lambeck, K., Yokoyama, Y., and Purcell, A., 2002, Into and out of the Last Glacial Maximum: sea-level change during Oxygen Isotope Stages 3 and 2: *Quaternary Science Reviews*, v. 21, p. 343-360.
- Larsen, C., Clark, I., Guntenspergen, G. R., Cahoon, D. R., Caruso, V., Hupp, C., and Yanosky, T., 2004, The Blackwater NWR Inundation Model. Rising Sea Level on a Low-lying Coast: Land Use Planning for Wetlands, USGS Open File Report 2004-1302: Reston, VA.

- Lifton, N., Sato, T., and Dunai, T. J., 2014, Scaling in situ cosmogenic nuclide production rates using analytical approximations to atmospheric cosmic-ray fluxes: *Earth and Planetary Science Letters*, v. 386, p. 149-160.
- Lisiecki, L. E., and Raymo, M. E., 2005, A Pliocene-Pleistocene stack of 57 globally distributed benthic $\delta^{18}\text{O}$ records: *Paleoceanography*, v. 20, no. 1, p. 1-17.
- Litwin, R. J., Smoot, J. P., Pavich, M. J., Markewich, H. W., Brook, G., and Durika, N. J., 2013, 100,000-year-long terrestrial record of millennial-scale linkage between eastern North American mid-latitude paleovegetation shifts and Greenland ice-core oxygen isotope trends: *Quaternary Research*, v. 80, no. 2, p. 291-315.
- Lourens, L. J., Hilgen, F. J., Laskar, J., Shackleton, N. J., and Wilson, D., 2004, The Neogene period *in* Gradstein, F., Ogg, J., and Smith, A., eds., *A geological Timescale*.
- Lowery, D. L., O'Neal, M. A., Wah, J. S., Wagner, D. P., and Stanford, D. J., 2010, Late Pleistocene upland stratigraphy of the western Delmarva Peninsula, USA: *Quaternary Science Reviews*, v. 29, no. 11–12, p. 1472-1480.
- Mallinson, D., Burdette, K., Mahan, S., and Brook, G., 2008, Optically stimulated luminescence age controls on late Pleistocene and Holocene coastal lithosomes, North Carolina, USA: *Quaternary Research*, v. 69, no. 1, p. 97-109.
- Markewich, H. W., Litwin, R. J., Pavich, M. J., and Brook, G. A., 2009, Late Pleistocene eolian features in southeastern Maryland and Chesapeake Bay region indicate strong WNW–NW winds accompanied growth of the Laurentide Ice Sheet:

- Quaternary Research, v. 71, no. 3, p. 409-425.
- Miller, K. G., and al., e., 2005, The Phanerozoic record of global sea-level change: Science, v. 310, p. 1293-1298.
- Miller, L., and Douglas, B. C., 2004, Mass and volume contributions to twentieth-century global sea level rise: Nature, v. 428, no. 6981, p. 406-409.
- Mixon, R. B., 1985, Stratigraphic and Geomorphic Framework of Uppermost Cenozoic Deposits in the Southern Delmarva Peninsula, Virginia and Maryland, USGS Professional Paper 1067-G: Reston, VA, p. 53 pp.
- Mixon, R. B., Berquist, C. R., Newell, W. L., and Johnson, G. H., 1989, Geologic map and generalized cross sections of the coastal plain and adjacent parts of the piedmont , Virginia.
- Murray, A.S., Wintle, A.G., 2000. Luminescence dating of quartz using an improved single aliquot regenerative-dose protocol: Radiation Measurements v. 32, p. 57-73.
- Murray, A.S., Wintle, A.G., 2003. The single aliquot regenerative dose protocol: potential for improvements in reliability: Radiation Measurements v. 37, p. 377-381.
- Murray-Wallace, C. V., Belperio, A. P., Gostin, V. A., and Cann, J. H., 1993, Amino acid racemization and radiocarbon dating of interstadial marine strata (oxygen isotope stage 3), Gulf St. Vincent, South Australia: Marine Geology, v. 110, p. 83–92.
- Newell, W. L., and Clark, I., 2008, Geomorphic map of Worcester County, Maryland,

- interpreted from a LiDAR-based digital elevation model, USGS Open File Report 2008-1005, p. 34.
- Newell, W. L., and DeJong, B. D., 2011, Cold-climate slope deposits and landscape modifications of the Mid-Atlantic Coastal Plain, Eastern USA: Geological Society, London, Special Publications, v. 354, no. 1, p. 259-276.
- Newell, W. L., and Queen, D. E., 2000, Hoverprobe 2000, a new tool for drilling in modern depositional environments: Drill Bits, no. 2, p. 4.
- Nishiizumi, K., Imamura, M., Caffee, M. W., Southon, J. R., Finkel, R. C., and McAninch, J., 2007, Absolute calibration of ^{10}Be AMS standards: Nuclear Instruments and Methods in Physics Research B, v. 258, no. 2, p. 403-413.
- Nishiizumi, K., Lal, D., Klein, J., Middleton, R., and Arnold, J. R., 1986, Production of ^{10}Be and ^{26}Al by cosmic rays in terrestrial quartz in situ and implications for erosion rates: Nature, v. 319, p. 134-136
- NOAA, 2003, Storm Data and Unusual Weather Phenomena, <http://www.weather.gov/media/lwx/stormdata/storm0903.pdf>
- NOAA, 2013, National Climatic Data Center; <http://www.ncdc.noaa.gov/billions/events>
- Oaks, R. A., Coch, N. K., Sanders, J. E., and Flint, R. F., 1974, Post-Miocene shorelines and sea levels, Southeastern Virginia, in Oaks, R. A., and DuBar, J. R., eds., Post-Miocene Stratigraphy Central and Southern Atlantic Coastal Plain: Logan, UT, Utah State University Press, p. 53-87.
- Oaks, R. Q., Jr., and Coch, N. K., 1963, Pleistocene Sea Levels, Southeastern Virginia:

- Science, v. 140, no. 3570, p. 979-983.
- Oertel, G. F., and Foyle, A. M., 1995, Drainage Displacement by Sea-Level Fluctuation at the Outer Margin of the Chesapeake Seaway: *Journal of Coastal Research*, v. 11, no. 3, p. 583-604.
- Olley, J. M., Caitcheon, G. G., and Murray, A. S., 1998, The distribution of apparent dose as determined by optically stimulated luminescence in small aliquots of fluvial quartz: implications for dating young sediments: *Quaternary Science Reviews*, v. 17, p. 1033-1040.
- Owens, J. P., and Denny, C. S., 1979, Upper Cenozoic deposits of the Central Delmarva Peninsula, Maryland and Delaware, USGS Professional Paper 1067-A: Washington, DC, p. 1-27.
- Owens, J. P., and Denny, C. S., 1986, Geologic Map of Dorchester County: US Geological Survey.
- Owens, J. P., and Minard, J. P., 1979, Upper Cenozoic sediments of the lower Delaware Valley and the Northern Delmarva Peninsula, New Jersey, Pennsylvania, Delaware, and Maryland, USGS Professional Paper 1067-D: Washington D.C., p. 1-47.
- Parham, P. R., Riggs, S. R., Culver, S. J., Mallinson, D. J., Jack Rink, W., and Burdette, K., 2013, Quaternary coastal lithofacies, sequence development and stratigraphy in a passive margin setting, North Carolina and Virginia, USA: *Sedimentology*, v. 60, no. 2, p. 503-547.

- Pavich, M. J., Markewich, H. W., and Brook, G. A., 2006, Significance of Kent Island Formation to geomorphic history of the Mid-Atlantic region, Geological Society of America, Volume Abstracts with programs 38, p. 226.
- Pazzaglia, F. J., 1993, Stratigraphy, petrography, and correlation of late Cenozoic middle Atlantic Coastal Plain deposits: Implications for late-stage passive-margin geologic evolution: GSA Bulletin, v. 105, p. 1617-1634.
- Pedoja, K., Husson, L., Johnson, M. E., Melnick, D., Witt, C., Pochat, S., Nexer, M., Delcaillau, B., Pinegina, T., Poprawski, Y., Authemayou, C., Elliot, M., Regard, V., and Garestier, F., 2014, Coastal staircase sequences reflecting sea-level oscillations and tectonic uplift during the Quaternary and Neogene: Earth-Science Reviews, v. 132, p. 13-38.
- Peltier, W. R., 1986, Deglaciation induced vertical motion of the North American continent and transient lower mantle rheology: Journal of Geophysical Research, v. 91, no. B8, p. 9099-9123.
- Peltier, W. R., 1996, Global sea level rise and glacial isostatic adjustment: An analysis of data from the east coast of North America: Geophysical Research Letters, v. 23, no. 7, p. 717-720.
- Peltier, W. R., 2009, Closure of the budget of global sea level rise over the GRACE era: the importance of magnitudes of the required corrections for global glacial isostatic adjustment: Quaternary Science Reviews, v. 28, p. 1658-1674.
- Perillo, G.M.E., ed., 1995, Geomorphology and Sedimentology of Estuaries, Elsevier,

Amsterdam.

- Potter, E.-K., and Lambeck, K., 2003, Reconciliation of sea-level observations in the Western North Atlantic during the last glacial cycle: *Earth and Planetary Science Letters*, v. 217, no. 1-2, p. 171-181.
- Powers, D. S., Mixon, R.B., and Bruce, S., , 1992, Uppermost Mesozoic and Cenozoic geologic cross section, outer coastal plain of Virginia, *in* Gohn, G. S., ed., *Proceedings of the 1988 U.S. Geological Survey Workshop on the Geology and Geohydrology of the Atlantic Coastal Plain*, U.S. Geological Survey Circular 1059, p. 85-101.
- Prescott, J. R., Hutton, J.T., 1994. Cosmic ray contributions to dose rates for luminescence and ESR dating: *Radiation Measurements* 23, 497-500.
- Ramsey, K. W., 2010, Stratigraphy, correlation, and depositional environments of the middle to late Pleistocene interglacial deposits of southern Delaware, *in* Survey, D. G., ed.: Newark, Delaware, p. 43.
- Reimer, P. J., Bard, E., Bayliss, A., Beck, J. W., Blackwell, P. G., Bronk Ramsey, C., Buck, C. E., Cheng, H., Edwards, R. L., Friedrich, M., Grootes, P. M., Guilderson, T. P., Hafliðason, H., Hajdas, I., Hatté, C., Heaton, T. J., Hoffmann, D. L., Hogg, A. G., Hughen, K. A., Kaiser, K. F., Kromer, B., Manning, S. W., Niu, M., Reimer, R. W., Richards, D. A., Scott, E. M., Southon, J. R., Staff, R. A., Turney, C. S. M., and van der Plicht, J., 2013, INTCAL13 and marine13 radiocarbon age calibration curves 0–50,000 years CAL BP: *Radiocarbon*, v.

55, no. 4, p. 1869-1887.

- Reusser, L. J., Bierman, P. R., Pavich, M. J., Zen, E.-a., Larsen, J., and Finkel, R. C., 2004, Rapid Late Pleistocene Incision of Atlantic Passive-Margin River Gorges: *Science*, v. 305, p. 499-502.
- Reuter, J., 2005, Erosion rates and pattern inferred from cosmogenic ^{10}Be in the Susquehanna River Basin. [MS thesis], University of Vermont, 160 p.
- Rignot, E., Mouginot, J., Morlighem, M., Seroussi, H., and Scheuchl, B., 2014, Widespread, rapid grounding line retreat of Pine Island, Thwaites, Smith, and Kohler glaciers, West Antarctica, from 1992 to 2011: *Geophysical Research Letters*, p. 1-8.
- Rittenour, T.M., Goble, R.J., Blum, M.D., 2003, An Optical Age Chronology of Fluvial Deposits in the Northern Lower Mississippi Valley: *Quaternary Science Reviews*, v. 22, p. 1105-1110.
- Rittenour, T.M., Goble, R.J., Blum, M.D., 2005, Development of an OSL chronology for late Pleistocene channel belts in the lower Mississippi valley: *Quaternary Science Reviews*, v.24, p. 2539-2554.
- Rodriguez, A. B., Anderson, J. B., Banfield, L. A., Taviani, M., Abdulah, K., and Snow, J. N., 2000, Identification of a -15 m middle Wisconsin shoreline on the Texas inner continental shelf: *Palaeogeography, Palaeoclimatology, Palaeoecology*, v. 158, p. 25-43.
- Rood, D.H., Hall, S., Guilderson, T.P., Finkel, R.C., Brown, T.A., 2010, Challenges and

- opportunities in high-precision Be-10 measurements at CAMS, Nuclear Instruments and Methods B: Beam Interactions with Materials and Atoms, v. 268, no. 7-8, p. 730-732.
- Rood, D.H., Brown, T.A., Finkel, R.C., Guilderson, T.P., 2013, Poisson and non-Poisson uncertainty estimations of $^{10}\text{Be}/^9\text{Be}$ measurements at LLNL-CAMS, Nuclear Instruments and Methods B: Beam Interactions with Materials and Atoms, v. 294, p. 426-429.
- Sallenger, A. H., Doran, K. S., and Howd, P. A., 2012, Hotspot of accelerated sea-level rise on the Atlantic coast of North America: Nature Climate Change, v. 2, p. 884-888.
- Schlee, J., 1957, Upland gravels of southern Maryland: Geological Society of America Bulletin, v. 68, p. 1371-1410.
- Schubel, J. R., and Zabawa, C. F., 1972, A Pleistocene Susquehanna River Channel Connects the Lower Reaches of the Chester, Miles, and Choptank Estuaries: Chesapeake Biological Laboratory Special Report, v. 24.
- Scott, M., McDermott, L., Silva, E., and Watson, E., 2009, Digital spatial capture of marsh extent in Blackwater National Wildlife Refuge, 1930 and 2006: Unpubl. Report. Eastern Shore GIS Cooperative, Salisbury University.
- Scott, T. W., Swift, D. J. P., Whittecar, G. R., and Brook, G. A., 2010, Glacioisostatic influences on Virginia's late Pleistocene coastal plain deposits: Geomorphology, v. 116, no. 1-2, p. 175-188.

- Sella, G. F., Stein, S., Dixon, T. H., Craymer, M., James, T. S., Mazzotti, S., and Dokka, R., 2007, Observation of glacial isostatic adjustment in “stable” North America with GPS: *Geophysical Research Letters*, v. 34.
- Shattuck, G. B., 1901, The Pleistocene problem of the North Atlantic Coastal Plain, *American Geologist*, v. 28, p. 87-107.
- Shattuck, G. B., 1902, The geology of the Coastal Plain formations, *in* The physical features of Cecil County, Maryland Geol. Survey, Cecil County [Volume], p. 149-194.
- Shattuck, G. B., 1904, The Miocene deposits of Maryland; Geo-logical and paleontological relations, with a review of earlier investigations Systematic paleontology of the Miocene deposits of Maryland: Maryland Geological Survey, p. xxxiii–cxxxvii.
- Shattuck, G.B., 1906, The Pliocene and Pleistocene deposits of Maryland: Maryland Geol. Survey, Pliocene and Pleistocene [Volume], p. 21-137.
- Siddall, M., Rohling, E. J., Thompson, W. G., and Waelbroeck, C., 2008, Marine isotope stage 3 sea level fluctuations: Data synthesis and new outlook: *Reviews of Geophysics*, v. 46, no. 4, p. 29 p.
- Silliman, B. R., Grosholz, E., and M.D., B., 2008, A synthesis of anthropogenic impacts on North American salt marshes, *in* Silliman, B. R., M.D., B., and Strong, D., eds., *Anthropogenic Modification of North American Salt Marshes*, University of California Press.

- Stauch, G., Ijmker, J., Pötsch, S., Zhao, H., Hilgers, A., Diekmann, B., Dietze, E., Hartmann, K., Opitz, S., Wünnemann, B., and Lehmkuhl, F., 2012, Aeolian sediments on the north-eastern Tibetan Plateau: *Quaternary Science Reviews*, v. 57, p. 71-84.
- Stevenson, J. C., Kearney, M. S., and Koch, E. W., 2002, Impacts of sea level rise on tidal wetlands and shallow water habitats: A case study from Chesapeake Bay: *American Fisheries Society Symposium*, v. 32, p. 23-26.
- Stevenson, J. C., Kearney, M. S., and Pendleton, E. C., 1985, Sedimentation and erosion in a Chesapeake Bay brackish marsh system: *Marine Geology*, v. 67, no. 3-4, p. 213-235.
- Susman, K. R., and Heron, S. D., 1979, Evolution of a barrier island—Shackleford Banks, Carteret County, North Carolina: *Geological Society of America Bulletin*, v. 90, p. 205-215.
- Stuiver, M., and Reimer, P. J., 1993, Extended ^{14}C database and revised CALIB radiocarbon calibration program: *Radiocarbon* v. 35, p. 215-230.
- Szabo, B. J., 1985, Uranium-series dating of fossil corals from marine sediments of southeastern United States Atlantic coastal plain: *Geological Society of America Bulletin*, v. 96, p. 398-406.
- Tebaldi, C., Strauss, B. H., and Zervas, C. E., 2012, Modelling sea level rise impacts on storm surges along US coasts: *Environmental Research Letters*, v. 7, no. 1, p. 1-11.

- Thorson, R. M., Harris, A. G., Harris, S. L., Gradle III, R., and Lefor, M. W., 1998, Colonial impacts to wetlands in Lebanon, Connecticut, A Paradox of Power: Voices of Warning and Reason in the Geosciences, Volume XII: Boulder, CO, Geological Society of America.
- Titus, J. G., Hudgens, D. E., Trescott, D. L., Craghan, M., Nuckols, W. H., Hershner, C. H., Kassakian, J. M., Linn, C. J., Merritt, P. G., McCue, T. M., O'Connell, J. F., Tanski, J., and Wang, J., 2009, State and local governments plan for development of most land vulnerable to rising sea level along the US Atlantic coast: Environmental Research Letters, v. 4, no. 4, p. 044008.
- U.S. Census Bureau American FactFinder, 2014, U.S., 2010 Census Redistricting Data Summary File (https://www.census.gov/geo/maps-data/maps/pdfs/thematic/us_popdensity_2010map.pdf)
- U.S. Geological Survey, Crapo Quadrangle, Maryland [map], 1:50,000, 15 Minute Series, Washington D.C., 1905.
- Valette-Silver, J. N., Brown, L., Pavich, M. J., Klein, J., and Middleton, R., 1986, Detection of erosion events using ^{10}Be profiles: example of the impact of agriculture on soil erosion in the Chesapeake Bay area (U.S.A.): Earth and Planetary Science Letters, v. 80, p. 82-90.
- Wehmiller, J. F., 2013, United States Quaternary coastal sequences and molluscan racemization geochronology – What have they meant for each other over the past 45 years?: Quaternary Geochronology, v. 16, p. 3-20.

- Wehmiller, J. F., Belknap, D. F., Boutin, B. S., Mirecki, J. E., Rahaim, S. D., and York, L. L., 1988, A review of the aminostratigraphy of Quaternary mollusks from United States Atlantic Coastal Plain sites: GSA Special Paper, v. 227, p. 69-110.
- Wehmiller, J. F., and Miller, G. H., 2000, Aminostratigraphic dating methods in Quaternary geology, *in* Noller, J. S., Sowers, J.M., Lettis, W.R., ed., Quaternary Geochronology, Methods and Applications, Volume 4, American Geophysical Union Reference Shelf, p. 187–222.
- Wehmiller, J. F., Simmons, K. R., Cheng, H., Edwards, L. R., Martin-McNaughton, J., York, L. L., Krantz, D. E., and Shen, C.-C., 2004, Uranium-series coral ages from the US Atlantic Coastal Plain—the “80ka problem” revisited: Quaternary International, v. 120, no. 1, p. 3-14.
- Wehmiller, J. F., Thieler, E. R., Miller, D., Pellerito, V., Bakeman Keeney, V., Riggs, S. R., Culver, S., Mallinson, D., Farrell, K. M., and York, L. L., 2010, Aminostratigraphy of surface and subsurface Quaternary sediments, North Carolina coastal plain, USA: Quaternary Geochronology, v. 5, no. 4, p. 459-492.
- Weigle, J. M., 1972, Exploration and mapping of Salisbury paleochannel, Wicomico County, Maryland: Maryland Geological Survey Bulletin, v. 31, no. 2, p. 61-123.
- Wellner, R. W., Ashley, G. M., and Sheridan, R. E., 1993, Seismic stratigraphic evidence for a submerged middle Wisconsin barrier: Implications for sea-level history: Geology, v. 21, no. 2, p. 109-112.
- Willenbring, J. K., and von Blanckenburg, F., 2010, Long-term stability of global erosion

- rates and weathering during late-Cenozoic cooling: *Nature*, v. 465, p. 211-214.
- Wintle, A.G. Murray, A.S., 2006, A review of quartz optically stimulated luminescence characteristics and their relevance in single-aliquot regenerative protocols: *Radiation Measurements*, v. 41, p. 369-391.
- Xu, S., Dougans, A. B., Freeman, S. P. H. T., Schnabel, C., and Wilcken, K. M., 2010, Improved ^{10}Be and ^{26}Al -AMS with a 5 MV spectrometer: *Nuclear Instruments and Methods in Physics Research B*, v. 268, p. 736–738.
- Xu, S., Freeman, S. P. H. T., Rood, D. H., and Shanks, R. P., 2014, ^{26}Al interferences in accelerator mass spectrometry measurements: *Nuclear Instruments and Methods in Physics Research B*, v. 333, no. 42-45.
- Yin, J., Griffies, S. M., and Stouffer, R. J., 2010, Spatial Variability of Sea Level Rise in Twenty-First Century Projections: *Journal of Climate*, v. 23, no. 17, p. 4585-4607.
- Zickfeld, K., Eby, M., Weaver, A. J., Alexander, K., Crespin, E., Edwards, N. R., Eliseev, A. V., Feulner, G., Fichefet, T., Forest, C. E., Friedlingstein, P., Goosse, H., Holden, P. B., Joos, F., Kawamiya, M., Kicklighter, D., Kienert, H., Matsumoto, K., Mokhov, I. I., Monier, E., Olsen, S. M., Pedersen, J. O. P., Perrette, M., Philippon-Berthier, G., Ridgwell, A., Schlosser, A., Schneider Von Deimling, T., Shaffer, G., Sokolov, A., Spahni, R., Steinacher, M., Tachiiri, K., Tokos, K. S., Yoshimori, M., Zeng, N., and Zhao, F., 2013, Long-Term Climate Change Commitment and Reversibility: An EMIC Intercomparison: *Journal of Climate*, v. 26, no. 16, p. 5782-5809.